

Physik und Anwendungen von weicher Röntgenstrahlung I

(Physics and applications of soft X-rays I)

Sommersemester 2015

Veranstalter :

Prof. Dr. Ulf Kleineberg (**ulf.kleineberg@physik.uni-muenchen.de**)
LMU, Physik Department
Am Coulombwall 1, 85748 Garching
(089) 289 14003

Vorlesungstermine + Ort :

3 SWS (plus 1 SWS Laborbesichtigung) 6 ECTS Punkte
LMU Garching, Coulombwall 1
Mittwochs, 13:00 – 16:00 Uhr, Seminarraum 224
(bis einschliesslich 3.6.) mündliche Abschlussprüfung

Vorlesungsinfos : www.xray.physik.uni-muenchen.de

Literatur:

Eberhard Spiller: Soft X-ray Optics / (SPIE Optical Engineering Press, Bellingham, Washington, ISBN 0-8184-1654-1)

A. Michette : X-ray Optics

D.T. Attwood: Soft X-ray and Extreme Ultraviolet Radiation (Cambridge Univ. Press, ISBN 0-521-65214-6)

Sowie aktuelle Wissenschaftspublikationen...

Begleitendes Seminar :

Studentische Vorträge zu aktuellen Forschungsarbeiten
(z.B. Röntgenmikroskopie, EUV Lithographie, Röntgenlaser, ...)
Ort und Zeit : Mittwochs 16 c.t – 18 Uhr, Seminarraum 219

Outline :

- **Basics :**

- Introduction to physics in the soft X-ray range
- Basic processes, emission and absorption
- Maxwell-equations, wave equation
- Scattering by free and bound electron
- Scattering by multiple electron atom, atomic scattering factor
- Complex refraction index, wave propagation in media

- **Thin films optics :**

- Interfaces, Fresnel-equations, total external reflection, Brewster angle
- Multilayer-Optics, basics, theory and technology

- **Sources :**

- Introduction to Synchrotron Radiation, Wigglers and Undulators
- Basics of the Free Electron Laser (FEL)
- Laser Plasma (LIP) and discharge plasma (DPP) sources
- X-ray lasers, High Harmonics

- **Nanooptics and diffractive optics**

- Diffractive optics, amplitude and phase gratings
- Zoneplates and refractive optics
- Waveguides and capillary optics

- **Detectors for soft X-rays**

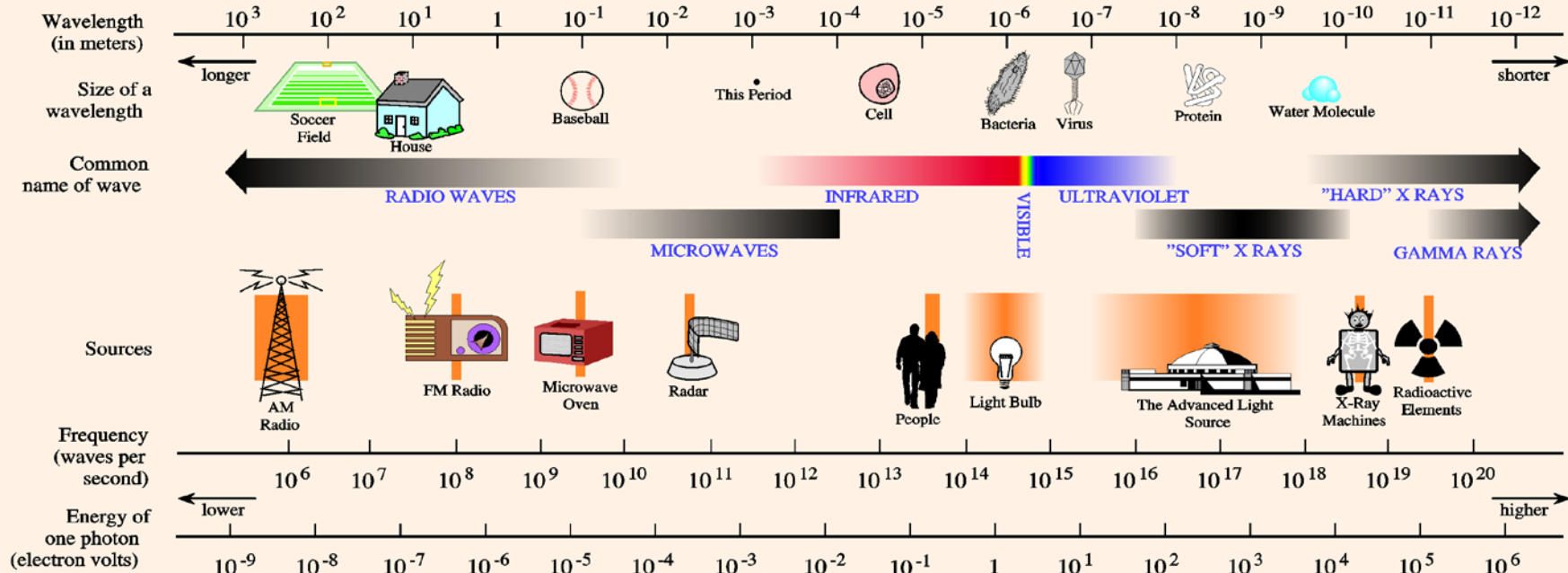
- CCD, photodiode, DLD detector

Technology and applications :

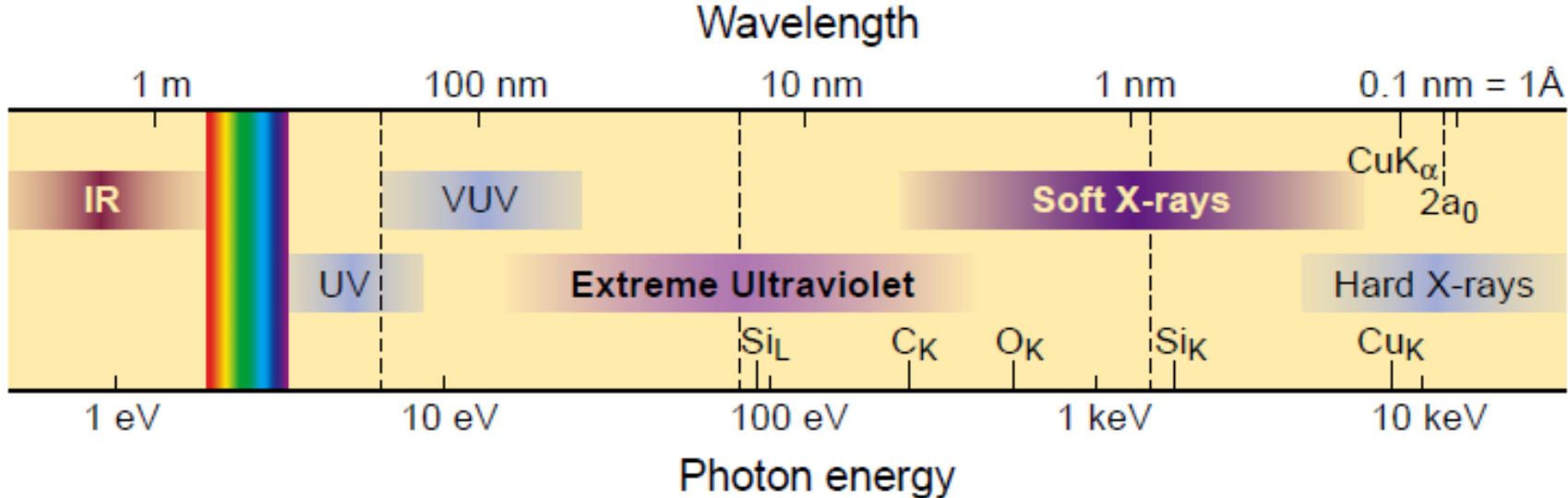
- Soft X-ray microscopy and micro-spectroscopy**
 - Diffractive Imaging and Holography**
 - Extreme Ultraviolet Lithography**
 - Attosecond electron spectroscopy and microscopy**
 - Solar astronomy**
-
-**

From radio waves to gamma rays

THE ELECTROMAGNETIC SPECTRUM



What is specific about the soft X-ray range ?

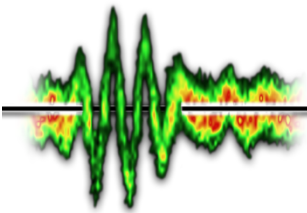


Short wavelength ~ 1 nm > see smaller features
> write smaller features

Core level electron energies > element specificity
> chemical specificity

Single cycle period sub-fsec > shortest electromagnetic pulses
> attosecond physics of e-dynamics

Resolution



How to determine the resolution of an optimal instrument / microscope ?

- Rayleigh-criterion:

$$d = \frac{0,61 * \lambda}{NA}$$

with λ = wavelength

NA = numerical Aperture

NA Animation : [NA](#)

<http://micro.magnet.fsu.edu/primer/java/nuaperture/index.html>

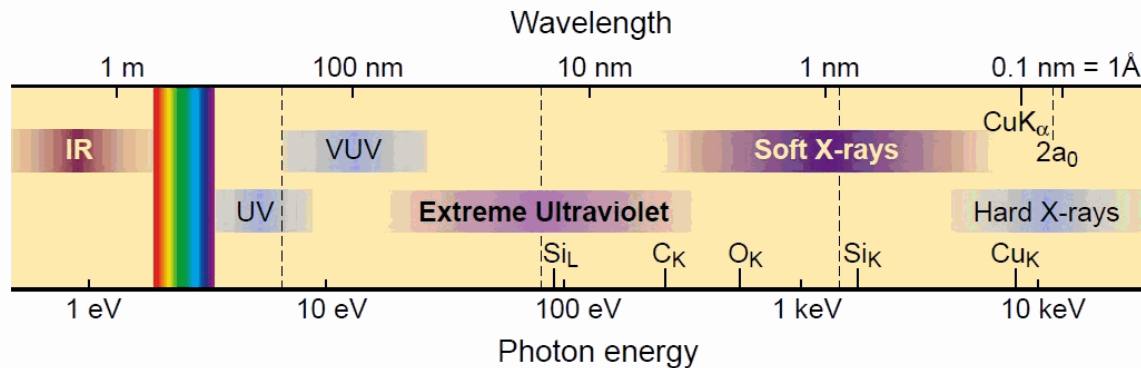
NA Immersion : [NA Immersion](#)

<http://micro.magnet.fsu.edu/primer/java/microscopy/immersion/index.html>

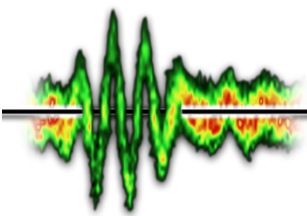
Rayleigh: [Resolution](#)

<http://micro.magnet.fsu.edu/primer/java/imageformation/rayleighdisks/index.html>

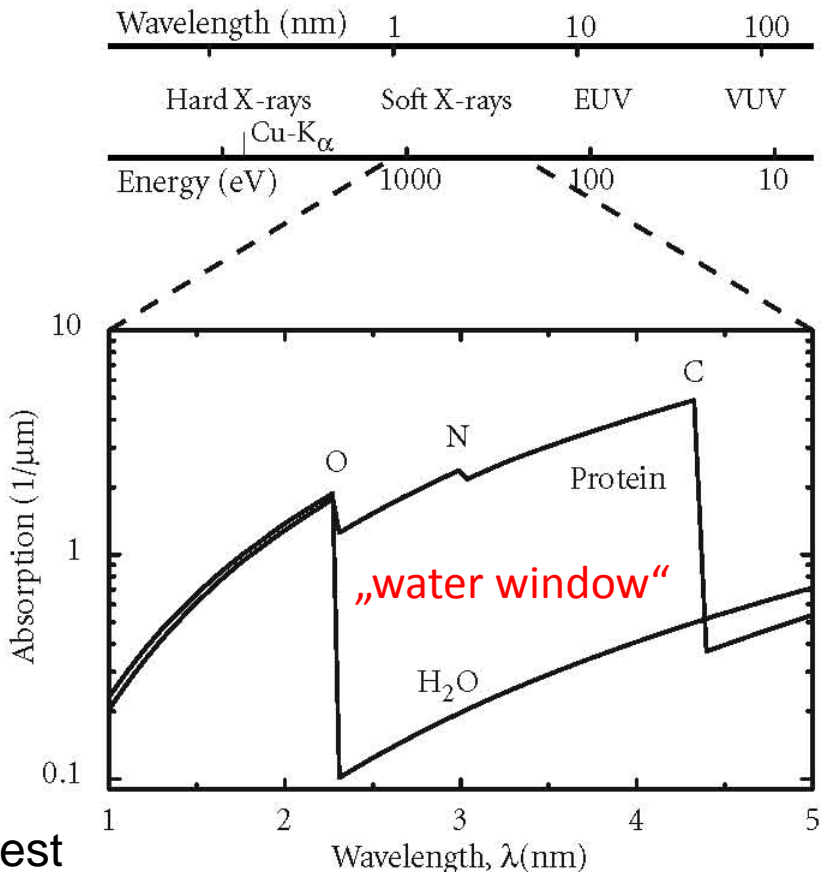
See smaller features with smaller wavelength !



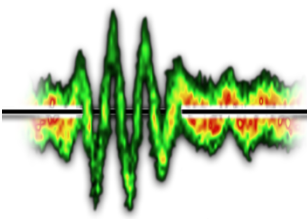
X-ray microscopy in the water window



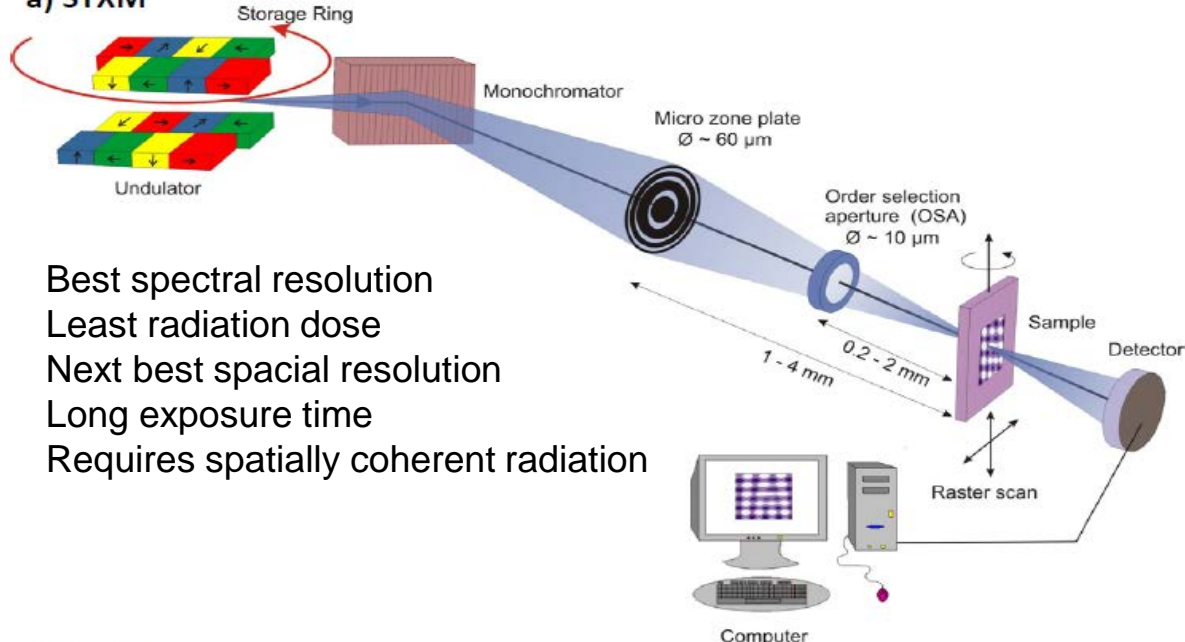
- Between the K-edge of carbon and oxygen
K-absorption edge O₂ : 2.28 nm = 543.1 eV
K-absorption edge C : 4.36 nm = 284.2 eV
- Natural contrast between materials containing carbon and water
- In-Vivo image of biological objects with high resolution
- Of high microscopic and spectroscopic interest



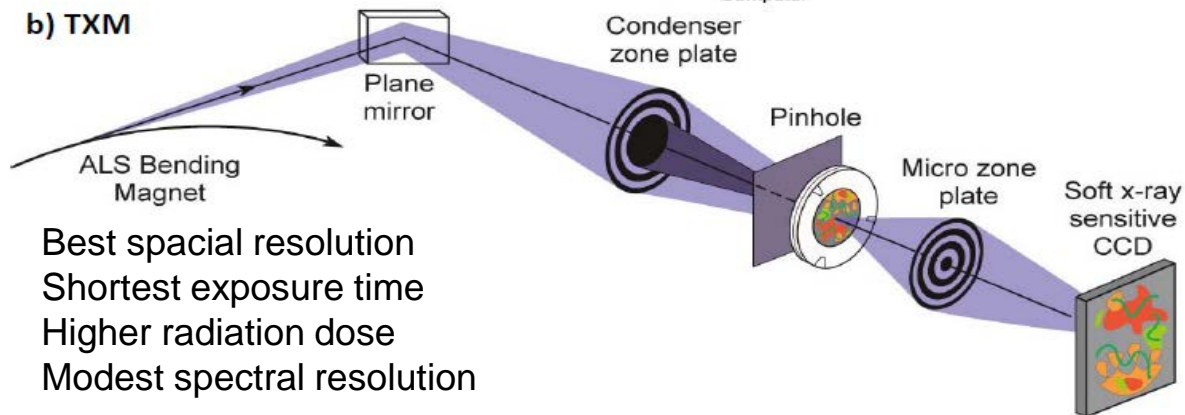
X-ray microscopy methods



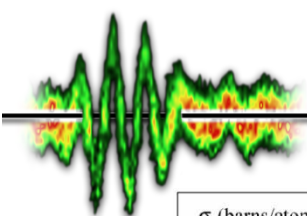
a) STXM



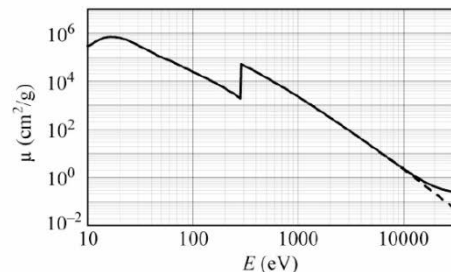
b) TXM



Refractive index, X-ray optics

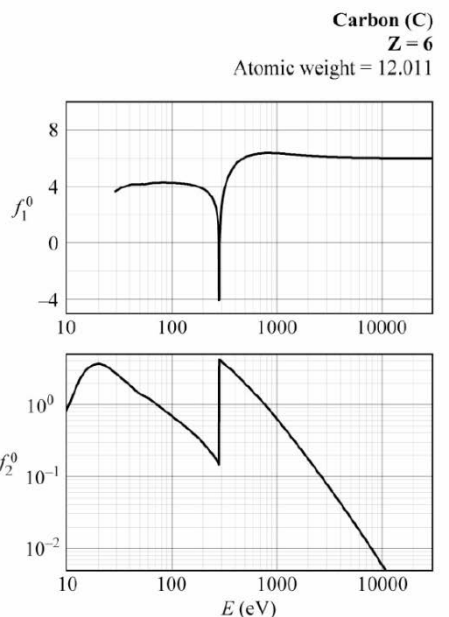


Energy (eV)	f_1^0	f_2^0	$\mu (\text{cm}^2/\text{g})$
30	3.692	2.664E+00	3.111E+05
70	4.249	1.039E+00	5.201E+04
100	4.253	6.960E-01	2.438E+04
300	2.703	3.923E+00	4.581E+04
700	6.316	1.174E+00	5.878E+03
1000	6.332	6.328E-01	2.217E+03
3000	6.097	7.745E-02	9.044E+01
7000	6.025	1.306E-02	6.536E+00
10000	6.013	5.892E-03	2.064E+00
30000	6.000	4.425E-04	5.168E-02



Edge Energies: K 284.2 eV

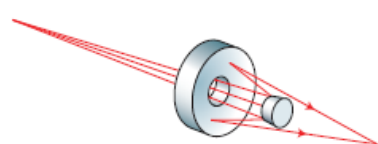
(Henke and Gullikson; www-cxro.LBL.gov)



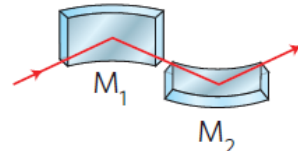
Ch02_F13VG.ai

- a) Zone plate
- b) Schwarzschild optics
- c) Kirkpatrick-Baez mirror pair
- d) Laue lens

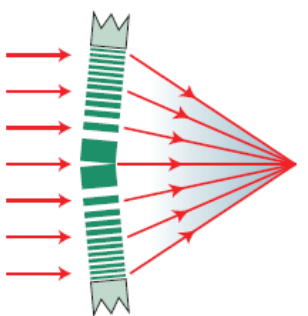
b



c

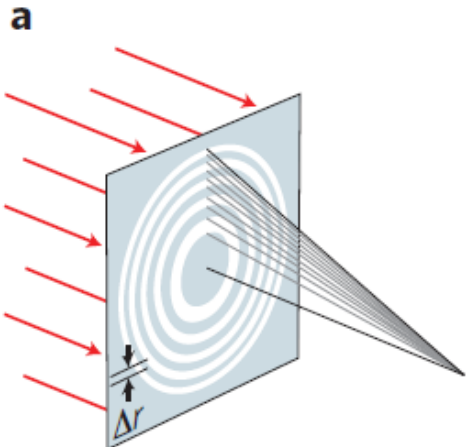


d

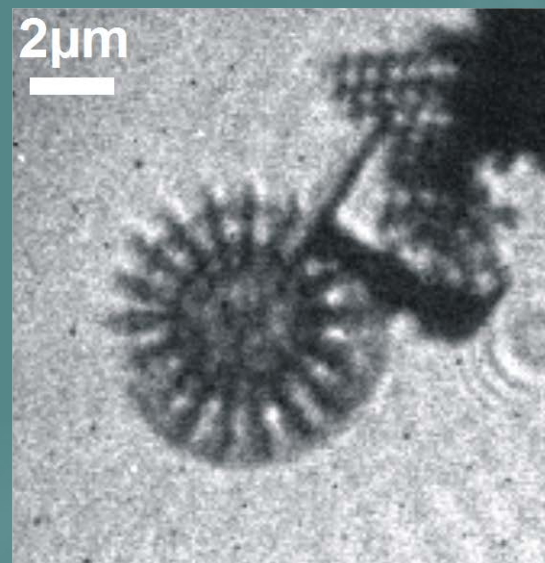
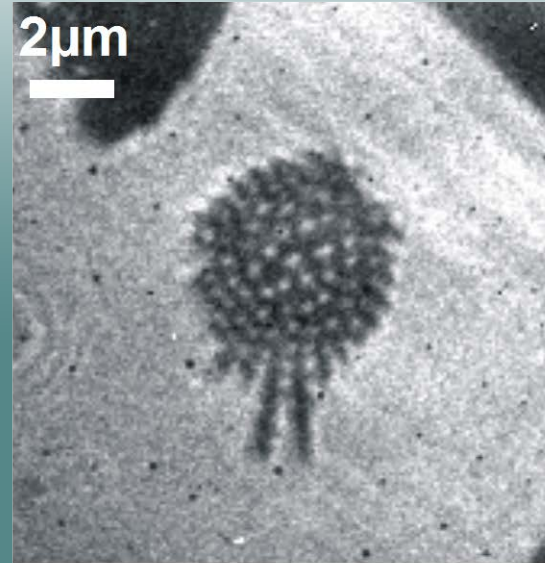
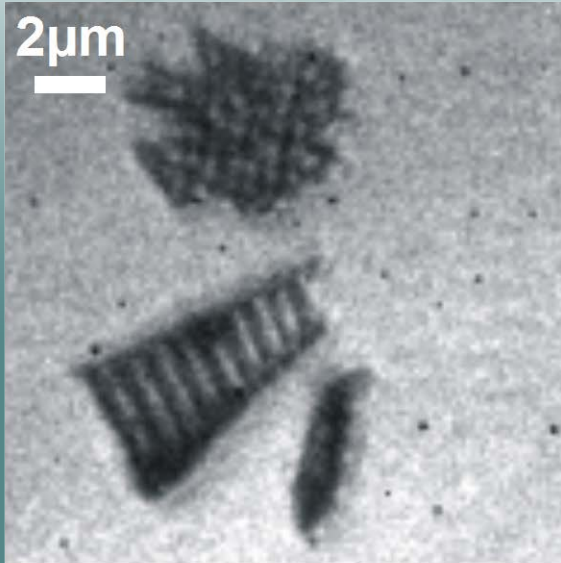


$$\theta_c = \sqrt{2\delta}$$

Four common X-ray microscopy optics:



See smaller features : soft X-ray microscopy



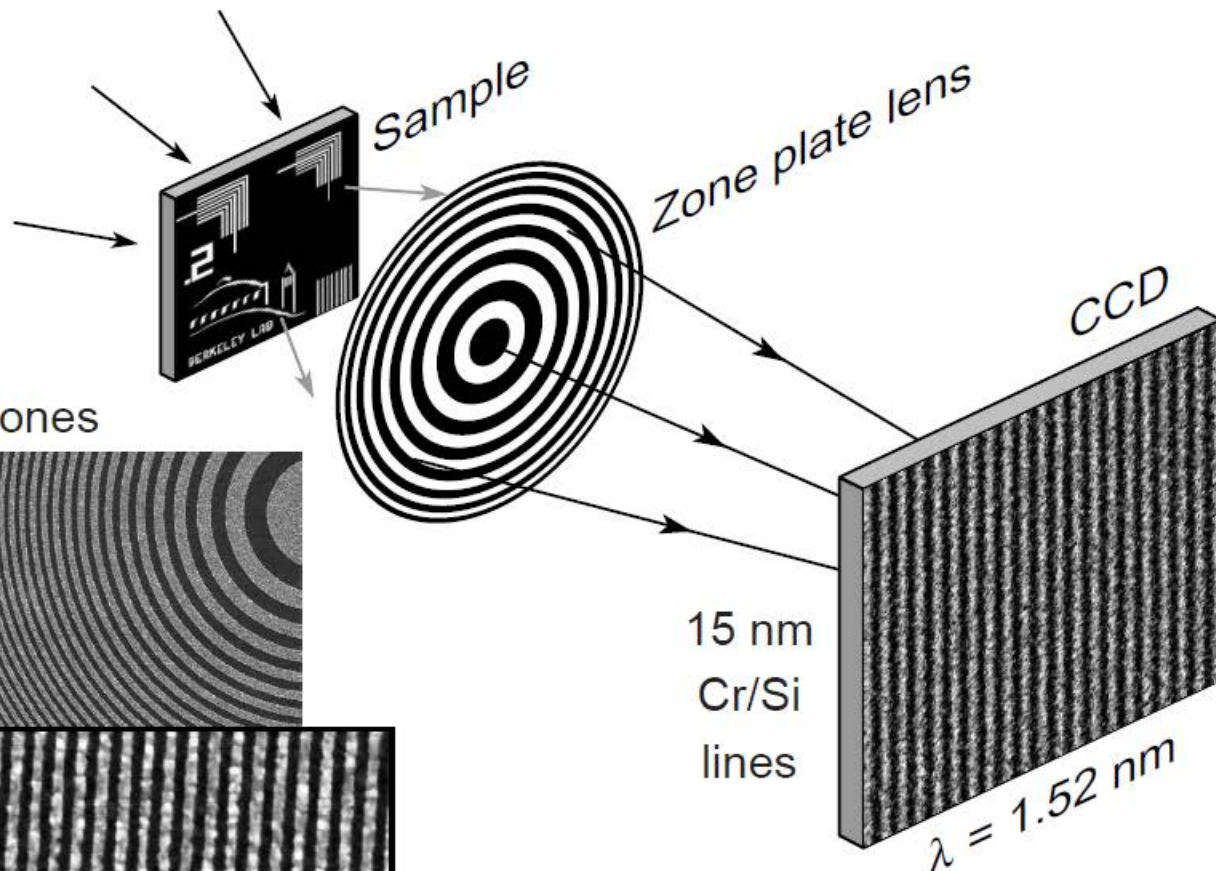
Soft X-ray microscopy
on diatoms (silica algae)

Eph = 97 eV

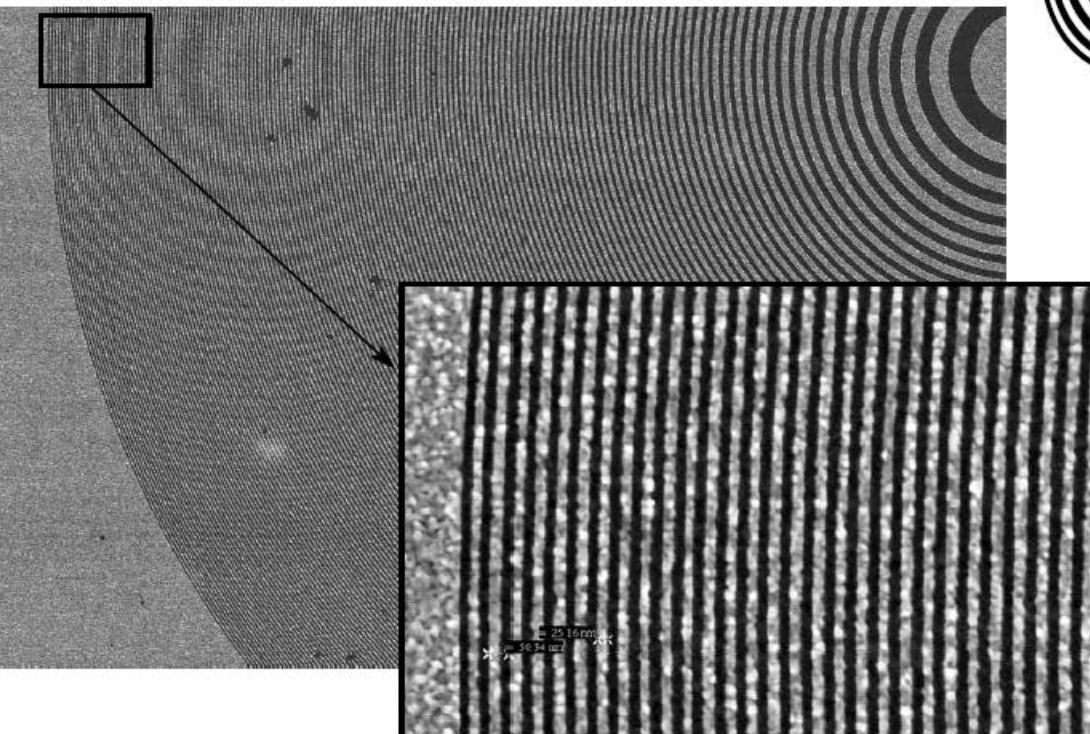
Lateral resolution :
< 200 nm



Soft X-Ray Microscopy at the ALS



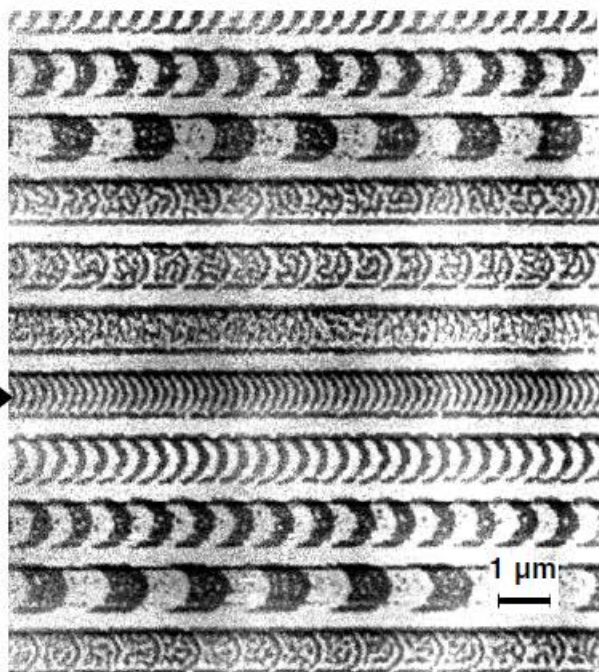
$\Delta r = 25 \text{ nm}, D = 63 \mu\text{m}, N = 618 \text{ zones}$



Courtesy of E. Anderson and W. Chao (CXRO/LBNL)



Magnetic Recording Materials

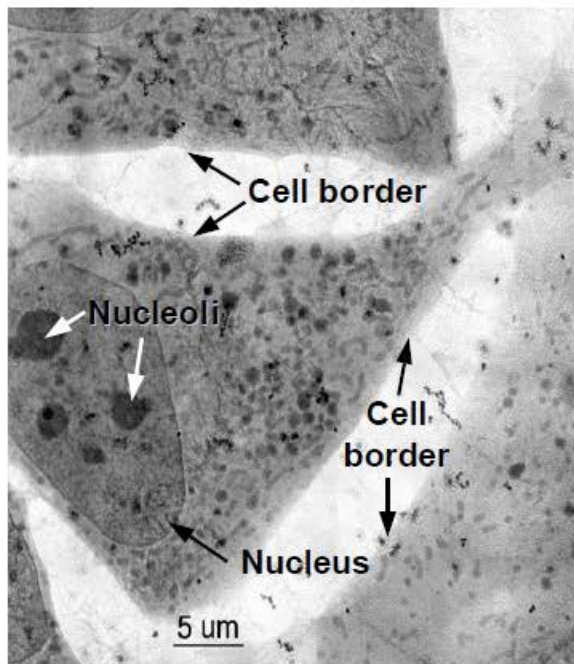


Fe L₃ @ 707.5 eV

FeTbCo Multilayer
with AL Capping Layer

Courtesy of P. Fischer, Wuerzberg
and G. Denbeaux, CXRO/LBNL

Cryo Microscopy for the Life Sciences



Cryo X-Ray Microscopy
of 3T3 Fibroblast Cells

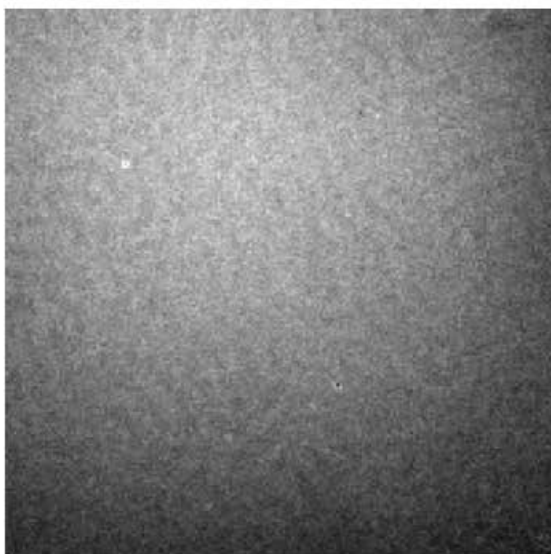
Courtesy of C. Larabell, UCSF
and W. Meyer-Ilse, CXRO/LBNL



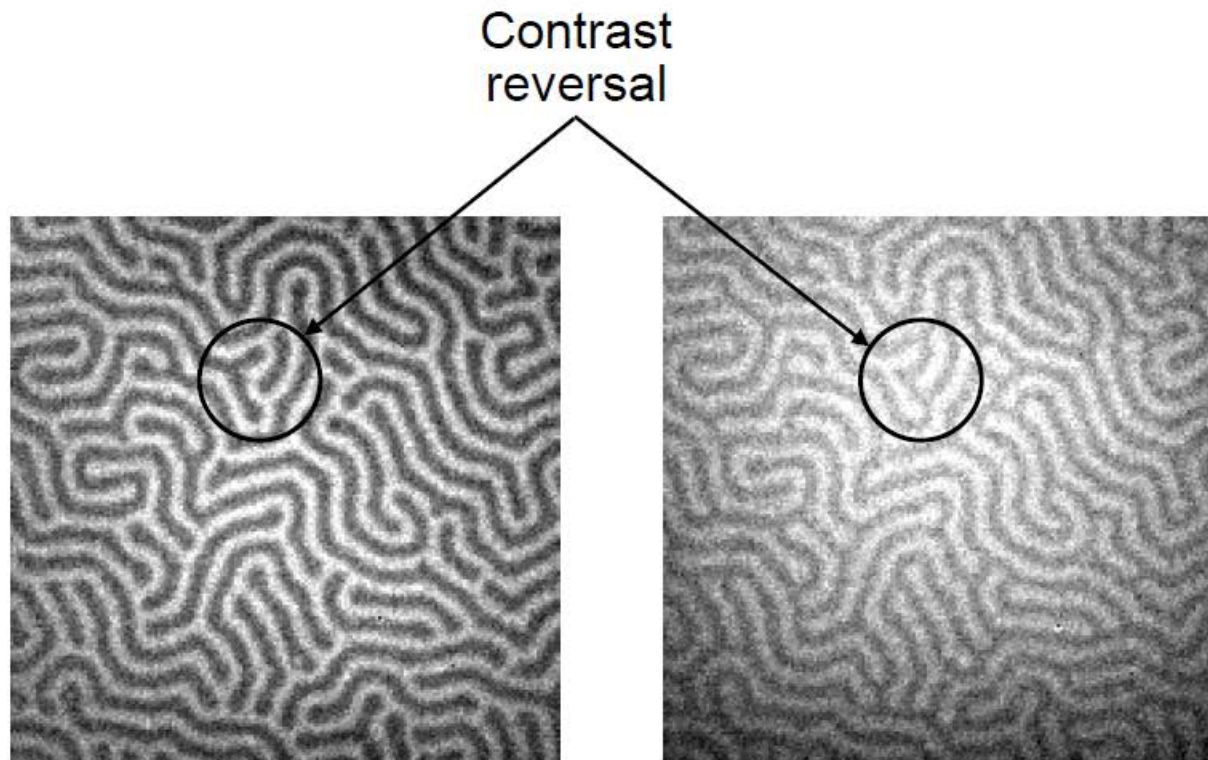


FeGd Multilayer

1 μm

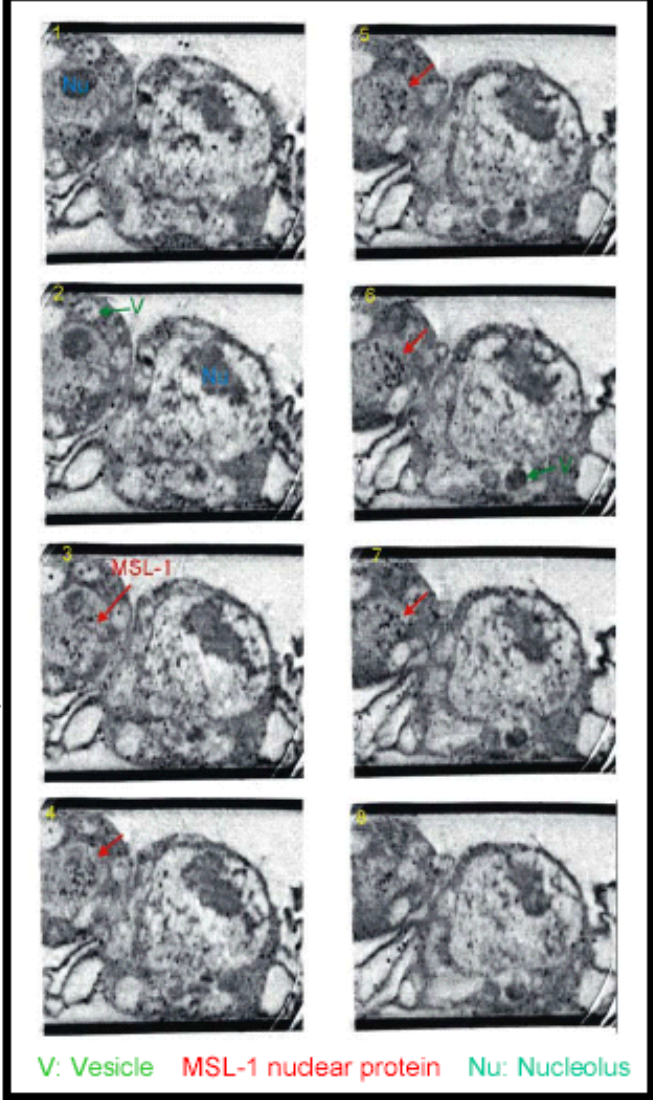
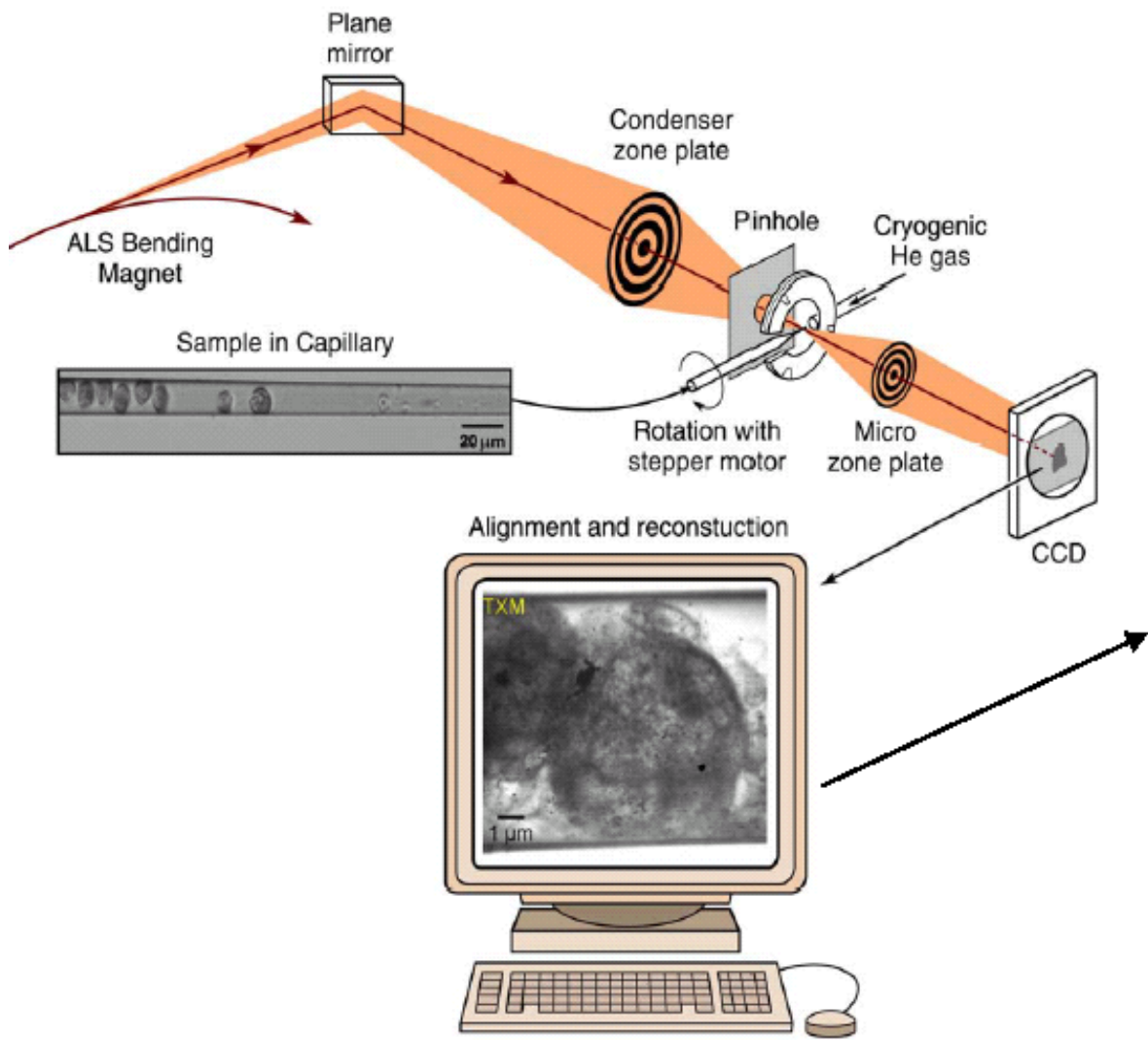


$\hbar\omega = 704 \text{ eV}$
below Fe L-edges



$\hbar\omega = 707.5 \text{ eV}$
Fe L_3 -edge

$\hbar\omega = 720.5 \text{ eV}$
Fe L_2 -edge



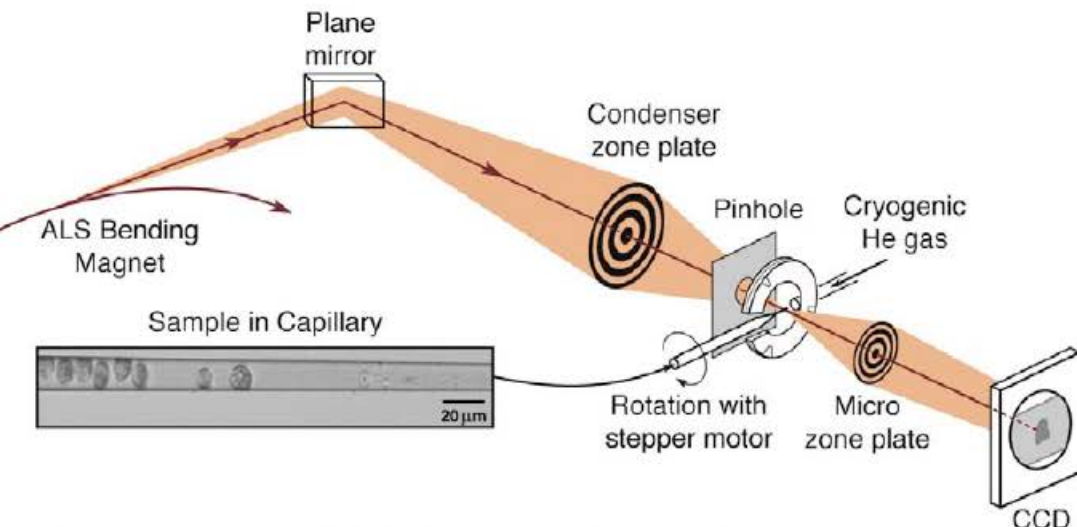
150 nm thick slices through the volume



Bio-Nanotomography for 3D Imaging of Cells

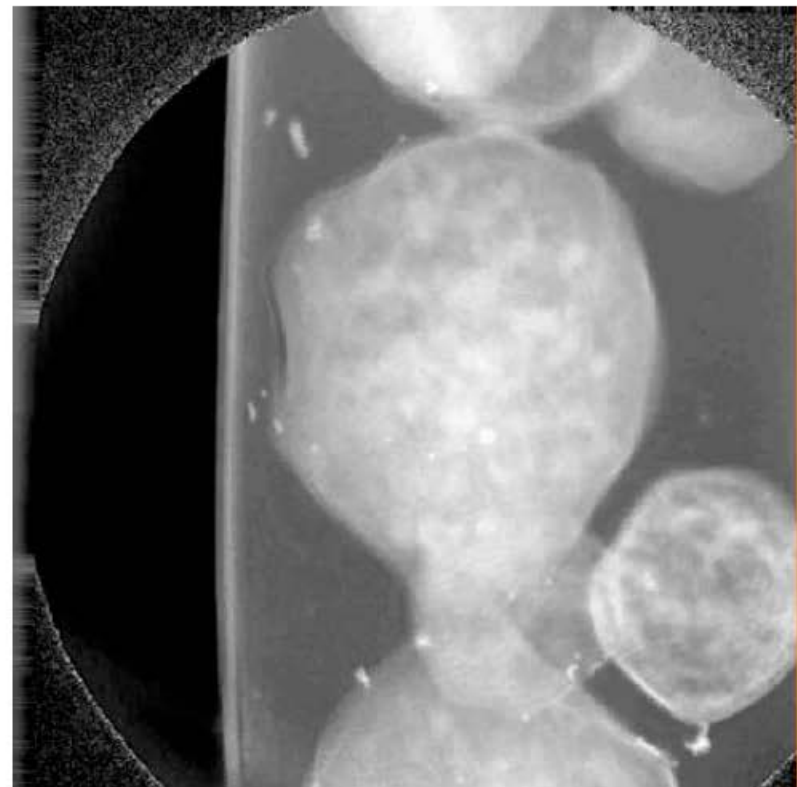


Nanotomography of Cryogenic Fixed Cells

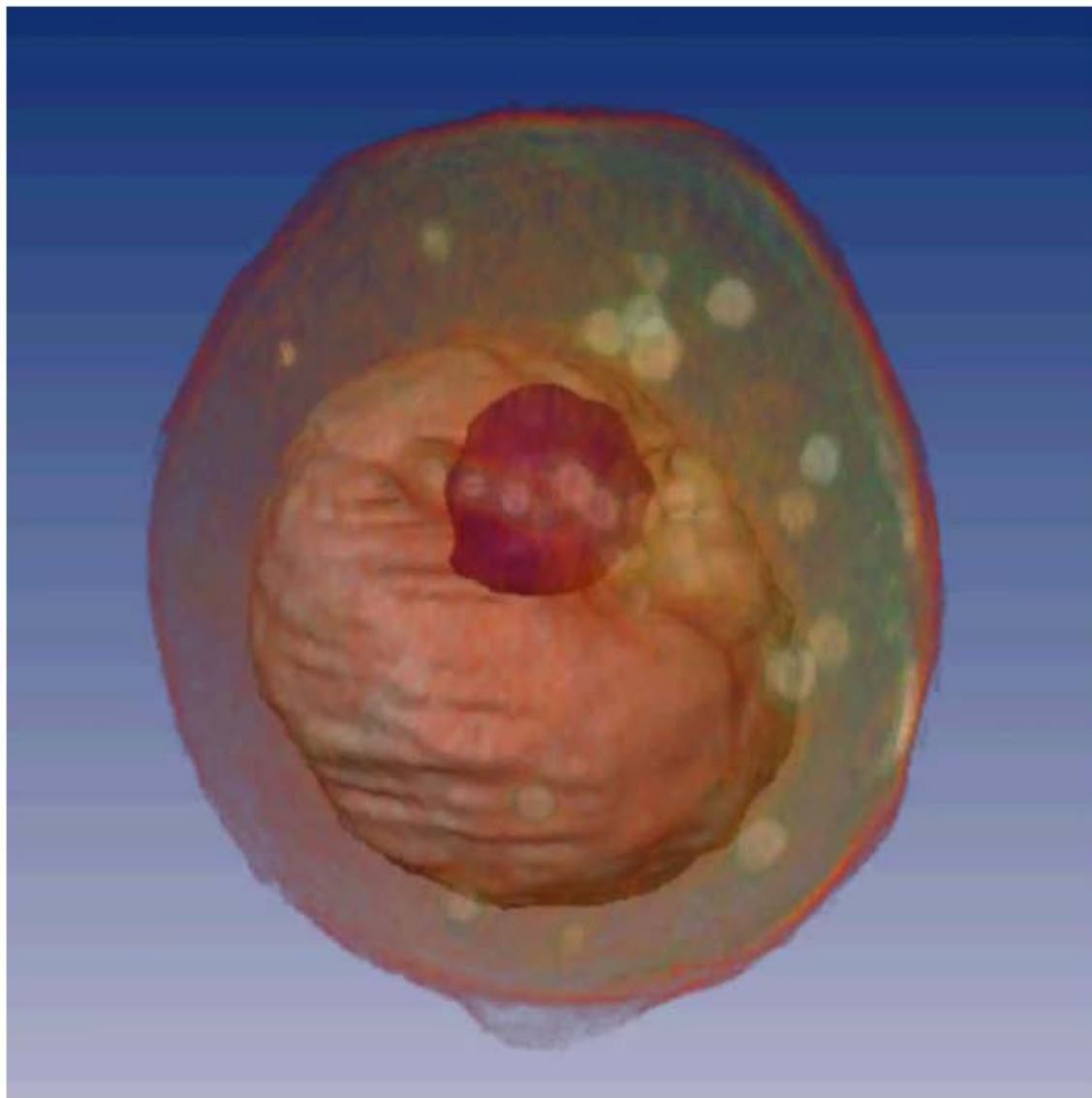


Courtesy of G. Schneider (BESSY)
Surf. Rev. Lett. 9, 177 (2002)

Soft X-Ray Nanotomography of a Yeast Cell

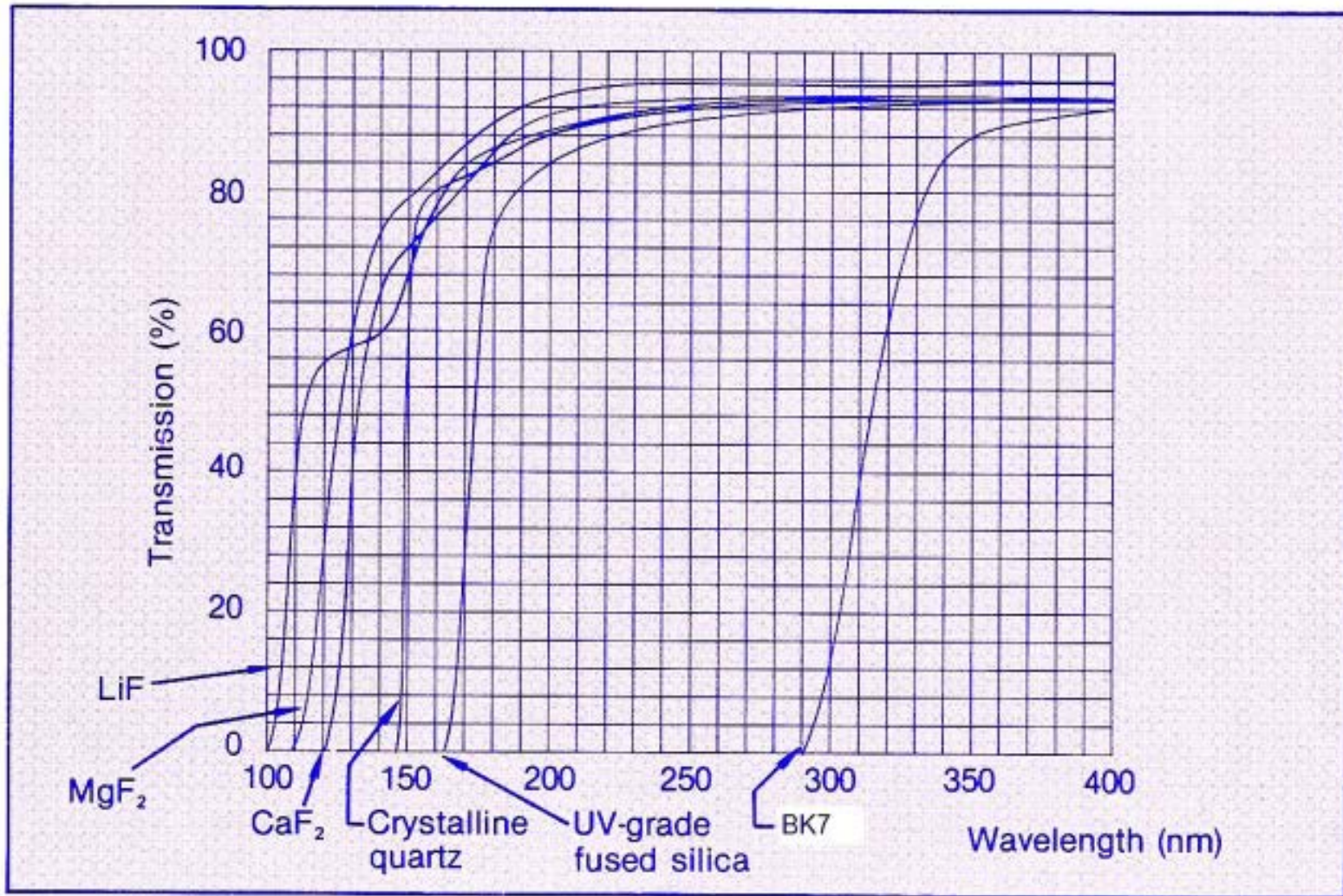


Courtesy of C. Larabell (UCSF & LBNL)
and M. LeGros (LBNL)



Courtesy of C. Larabell / UCSF & LBNL, and M. LeGros / LBNL

Transmission of fluoride materials in the DUV



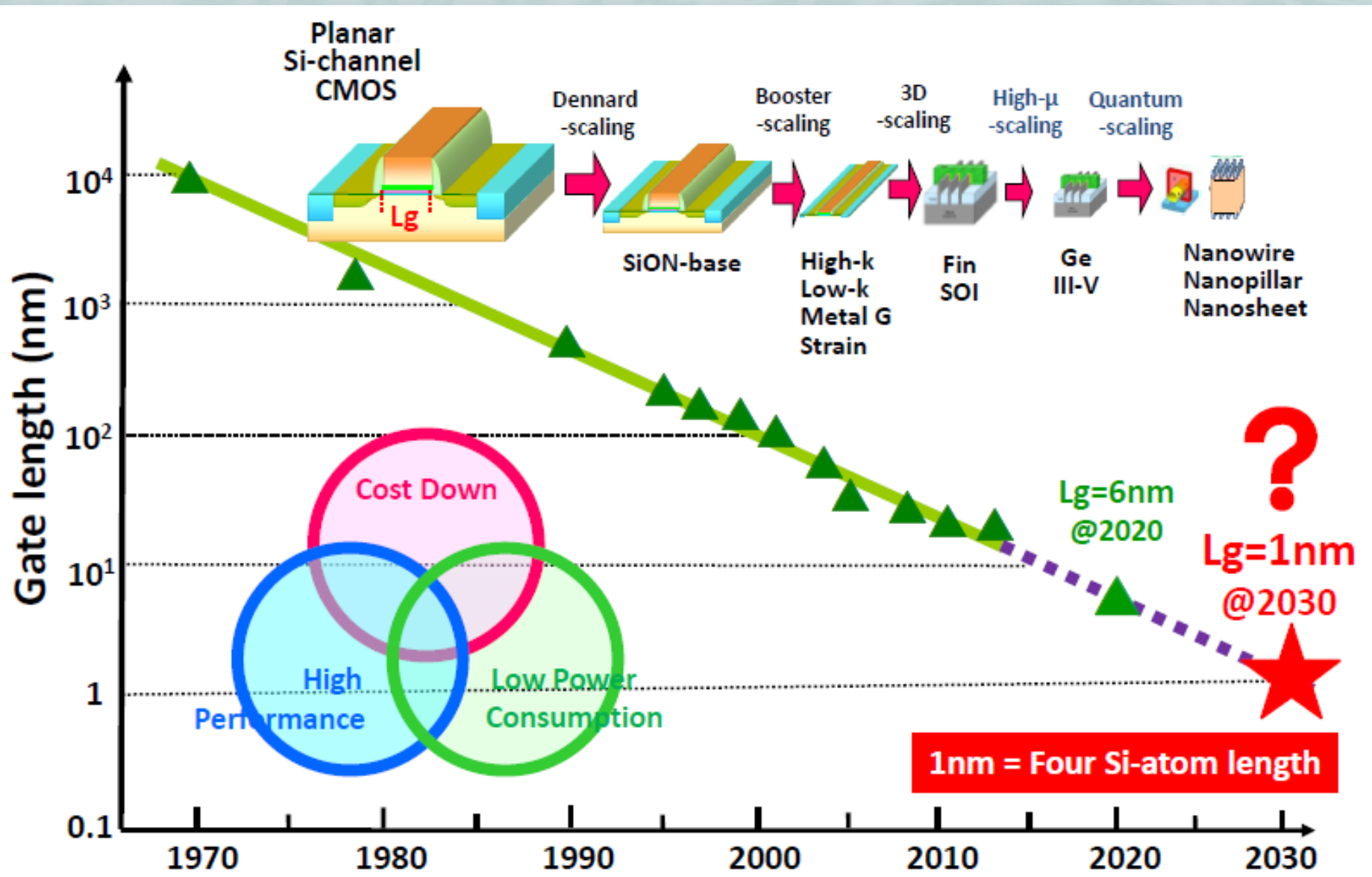
- No window materials below 110 nm wavelength
- No conventional transmission lenses possible !

193 nm DUV lithography objective (Zeiss)



> CaF aspherical lense optics

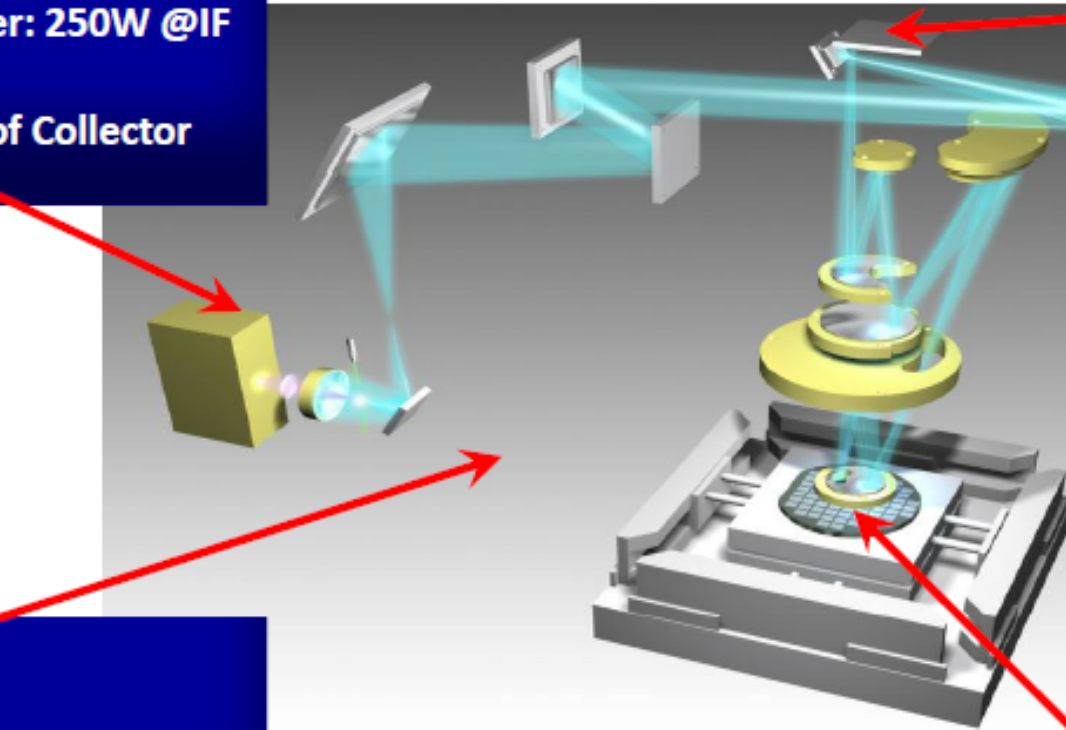
Write smaller features : Extreme Ultraviolet Lithography



Challenges of Extreme Ultraviolet Lithography

Source

- ✓ High power: 250W @IF
- ✓ Stability
- ✓ Long Life of Collector Mirror

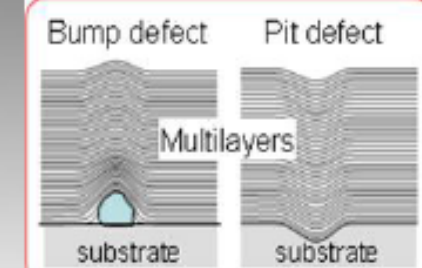


Scanner

- ✓ Field data
- ✓ Higher quality / Long lifetime of optical components

Mask

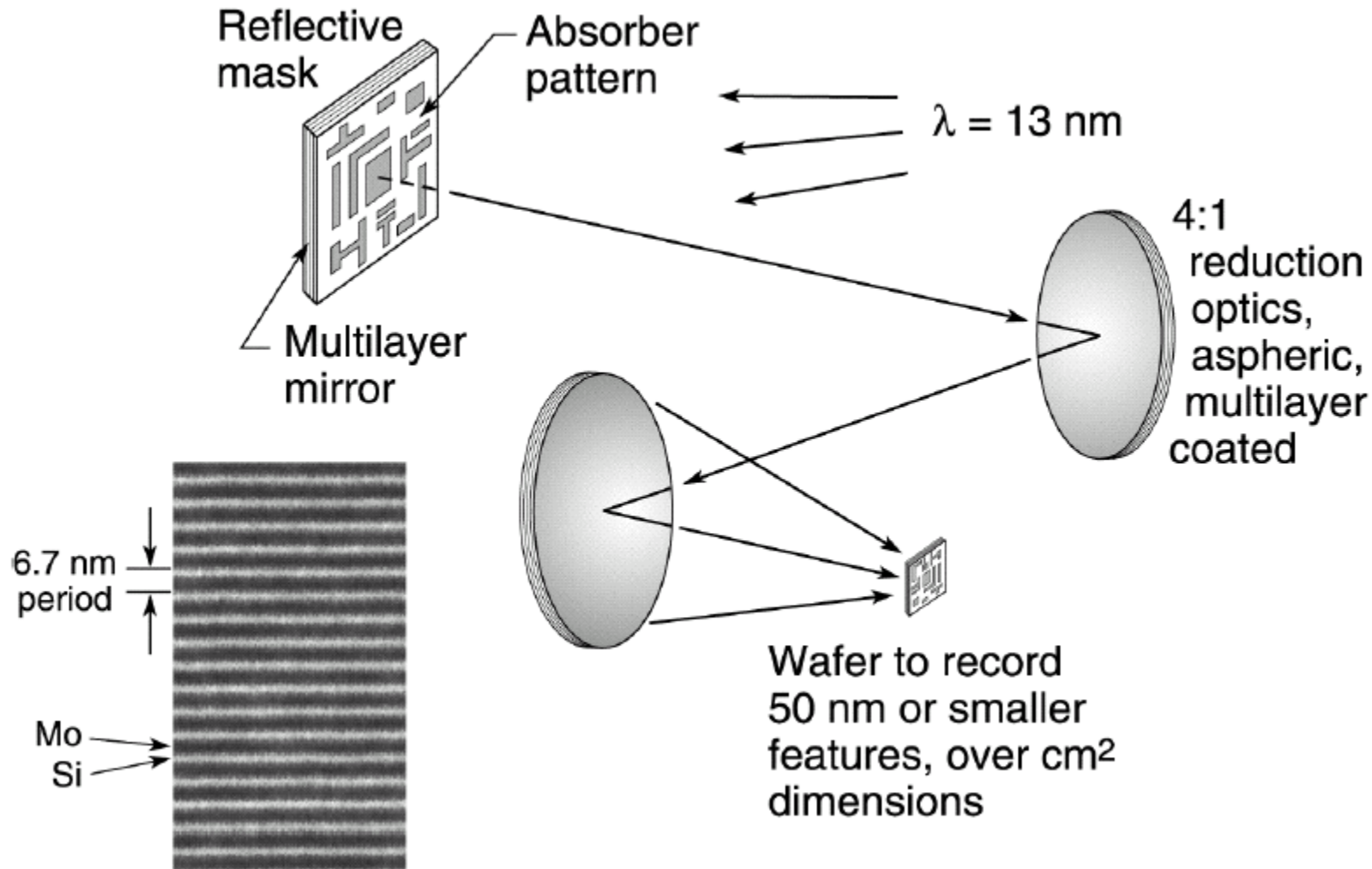
- ✓ Blank Inspection
- ✓ Patterned Mask Inspection
- ✓ Defect Review System
- ✓ Particle Free Handling

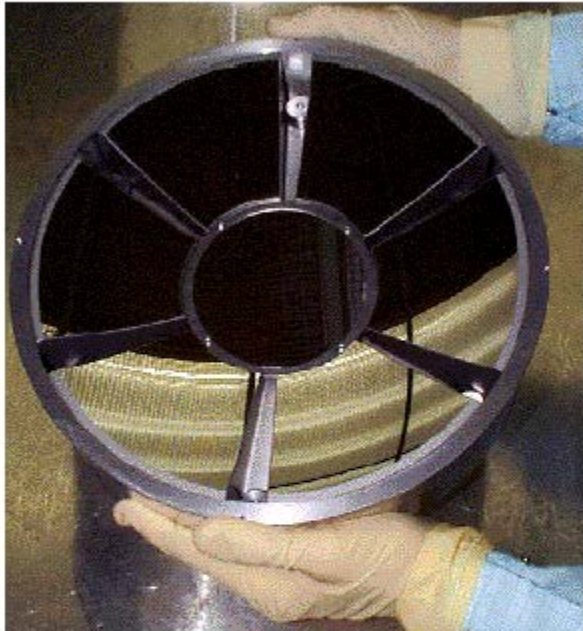


Courtesy by EUVA

Resist

- ✓ Resolution < 20nmHP
- ✓ Sensitivity < 10mJ/cm²
- ✓ LER < 2nm
- ✓ Lower outgassing



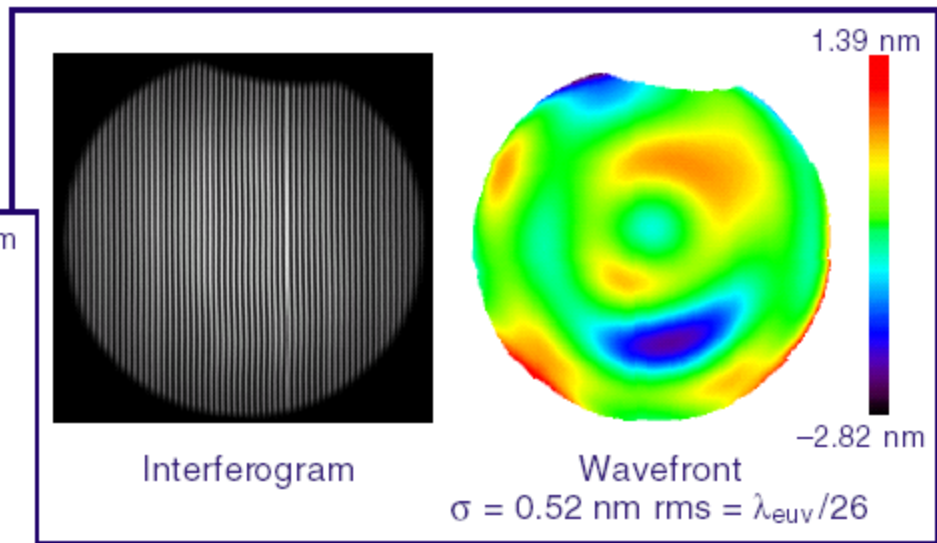
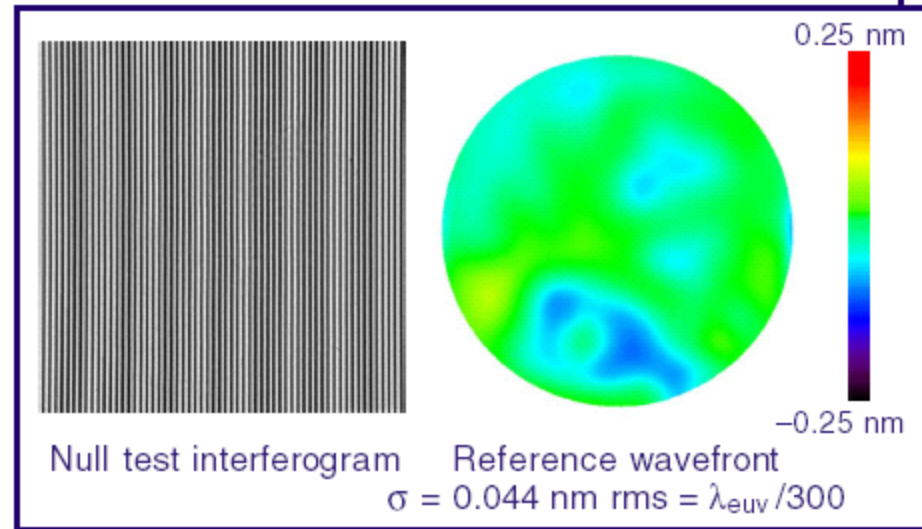
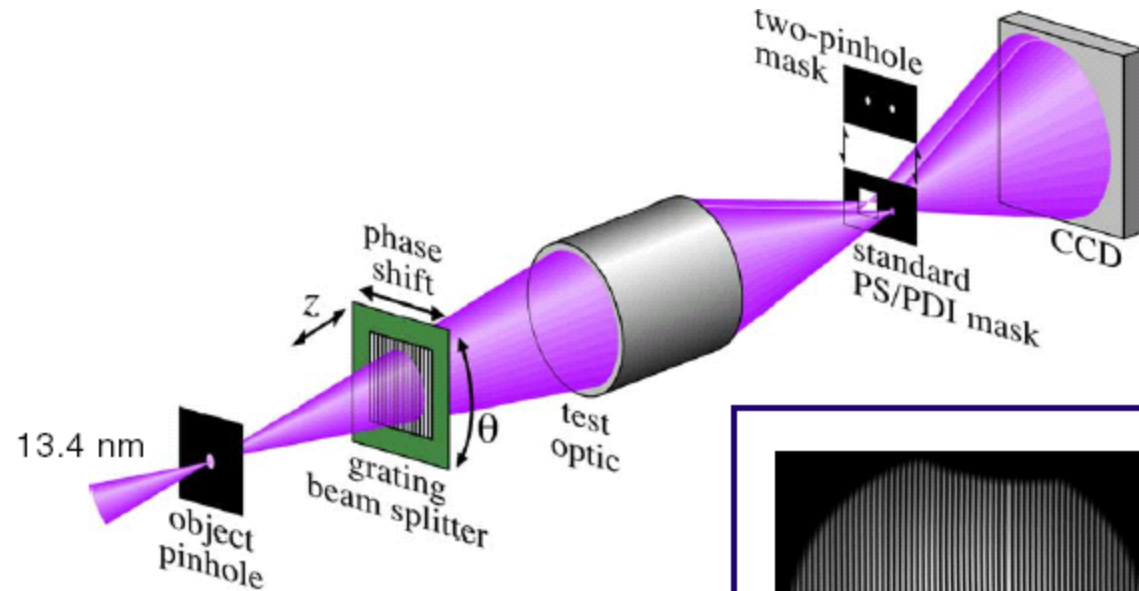


Condenser optic



Projection optic

Courtesy of J. Taylor and D. Sweeney / LLNL

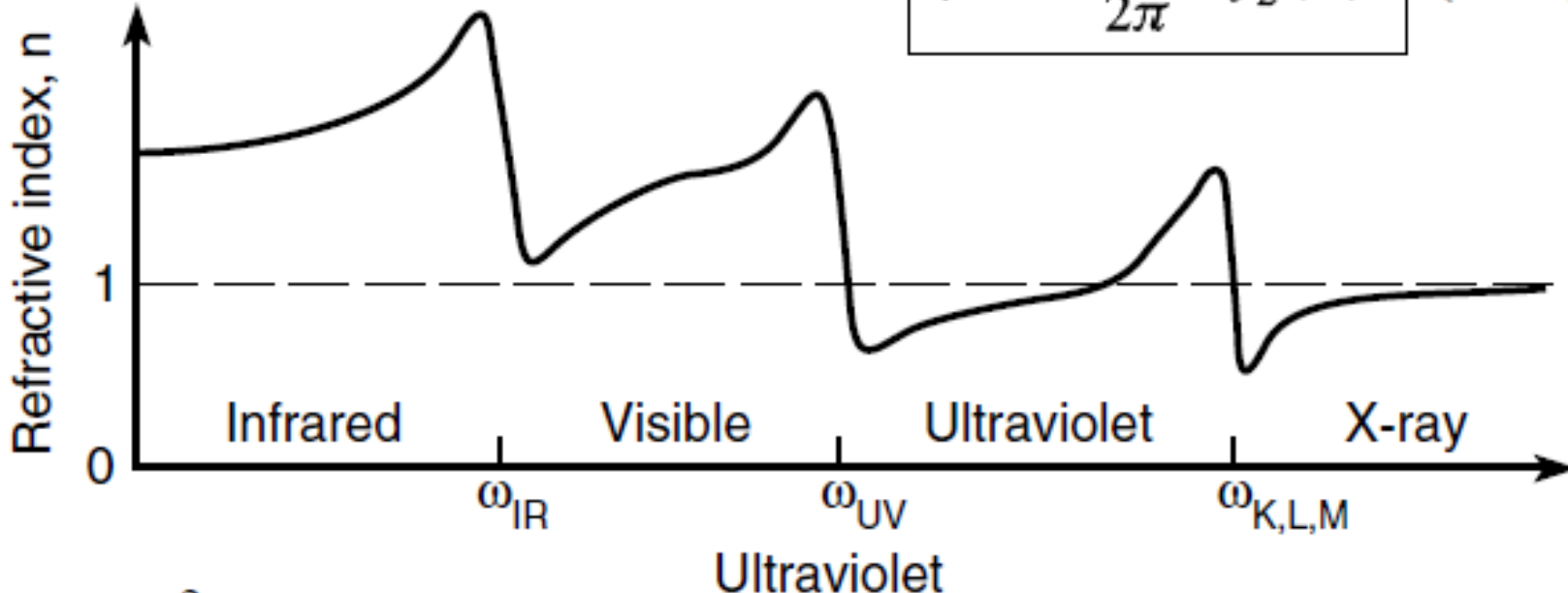


Complex index of refraction/atomic scattering factors

$$n(\omega) = 1 - \delta + i\beta \quad (3.12)$$

$$\delta = \frac{n_a r_e \lambda^2}{2\pi} f_1^0(\omega) \quad (3.13a)$$

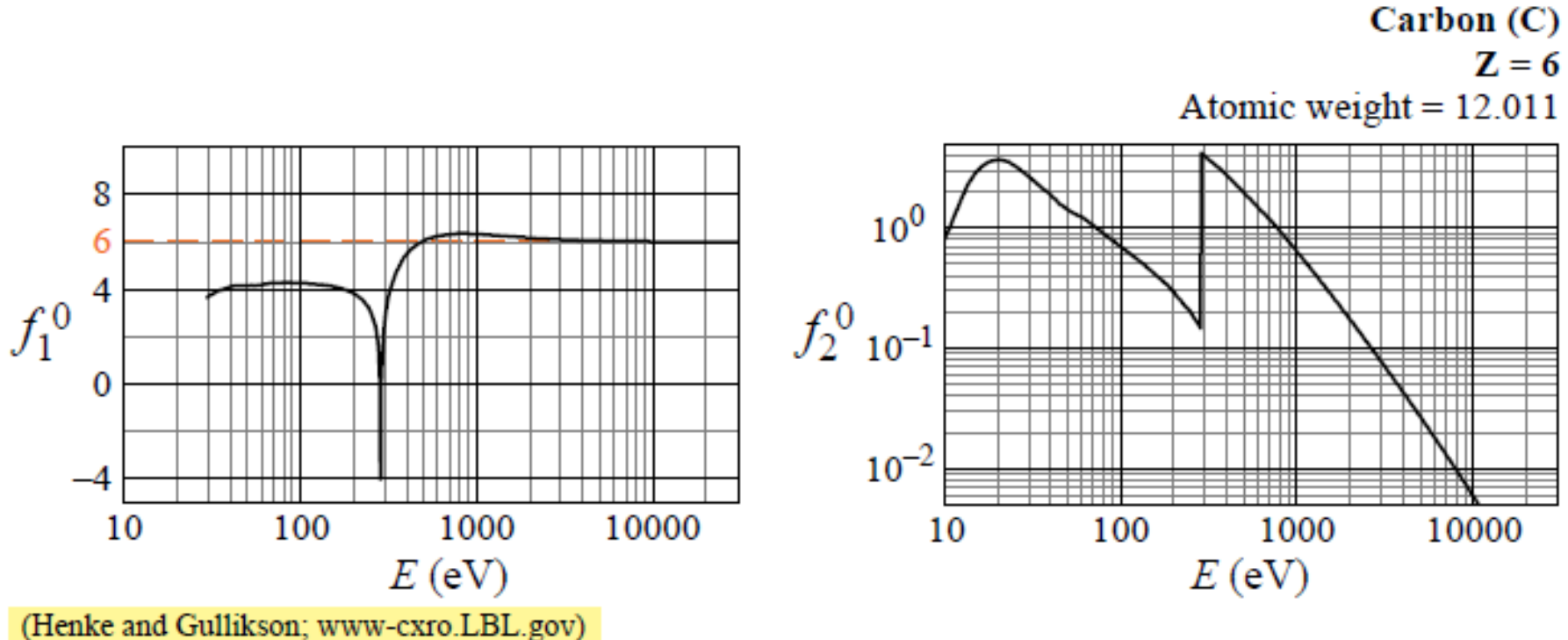
$$\beta = \frac{n_a r_e \lambda^2}{2\pi} f_2^0(\omega) \quad (3.13b)$$



- λ^2 behavior
- $\delta & \beta \ll 1$
- δ -crossover

Complex atomic scattering factors

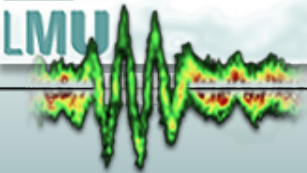
$$f^0(\omega) = f_1^0(\omega) - i f_2^0(\omega)$$



valid only for : long wavelength $\lambda \gg a_0$ (0.529 Å) or forward scattering

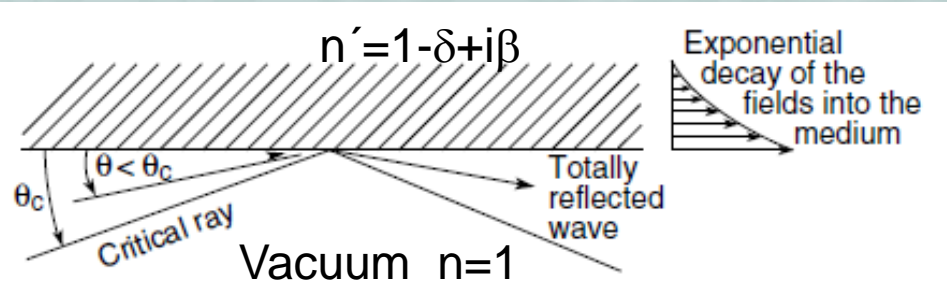
f_1 equals Z for $\omega \gg \omega_s$ all electrons scatter in phase !

Scattering cross section $\sim Z^2$



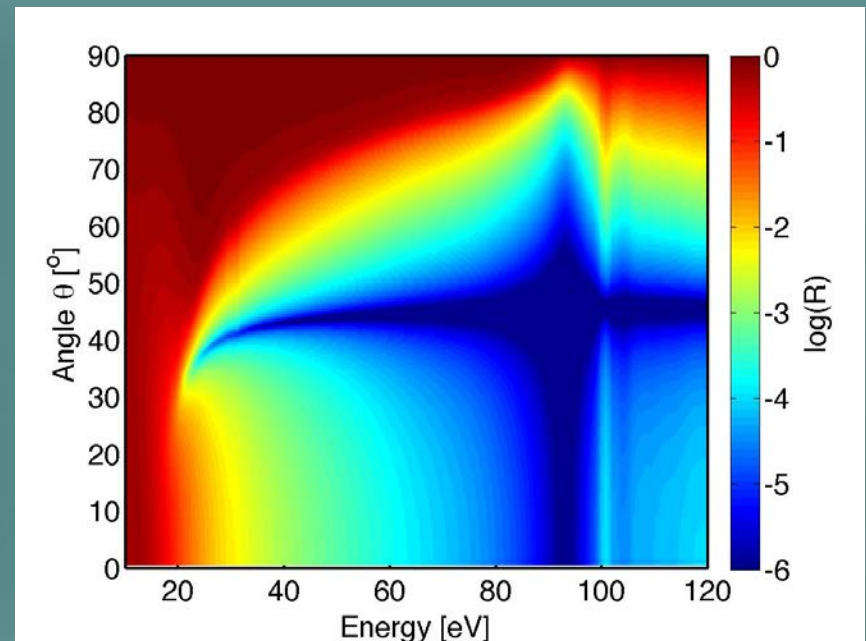
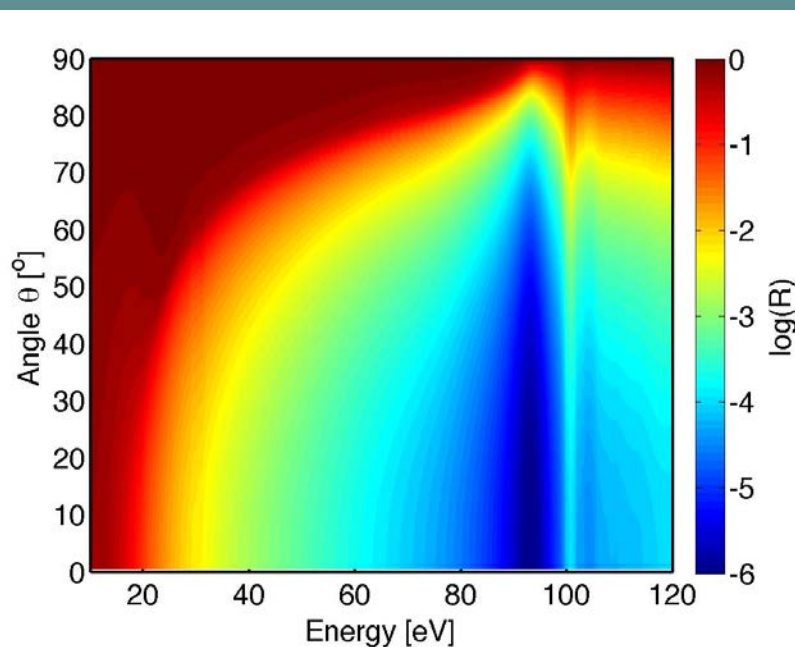
Single interface optics (example Si)

S- polarisation



Snell's law :
 $\sin \phi' = \sin \phi / n'$
 Critical angle : $\Theta_c = 2\delta^{1/2}$

P- polarisation



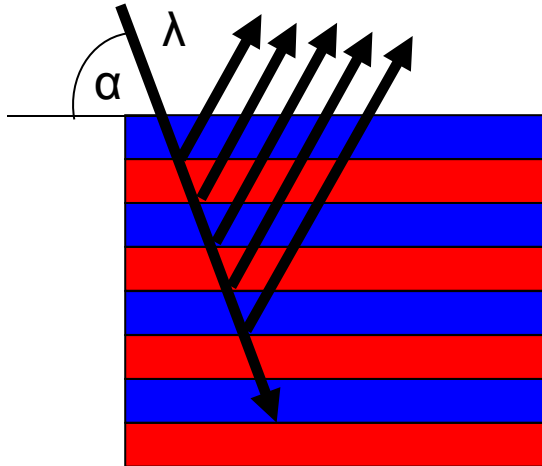
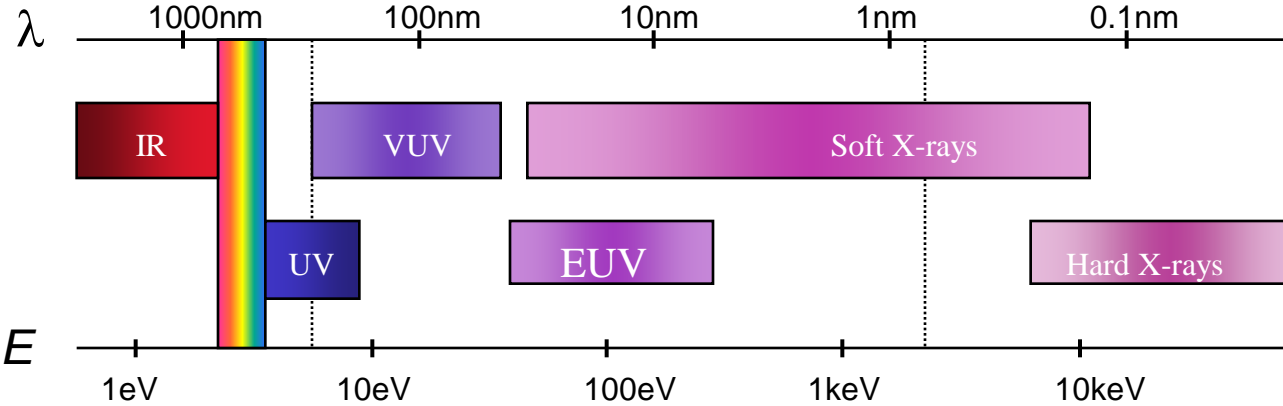
$$R_s = \frac{|\cos \phi - \sqrt{n^2 - \sin^2 \phi}|^2}{|\cos \phi + \sqrt{n^2 - \sin^2 \phi}|^2}$$

Fresnel Equations (s, p pol.)

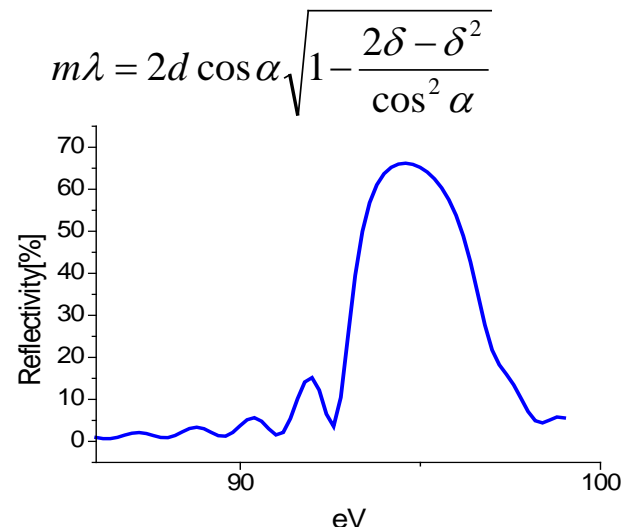
$$R_{\text{perp}} = (\delta^2 + \beta^2)/4$$

$$R_p = \left| \frac{E_0''}{E_0} \right|^2 = \frac{\left| n^2 \cos \phi - \sqrt{n^2 - \sin^2 \phi} \right|^2}{\left| n^2 \cos \phi + \sqrt{n^2 - \sin^2 \phi} \right|^2}$$

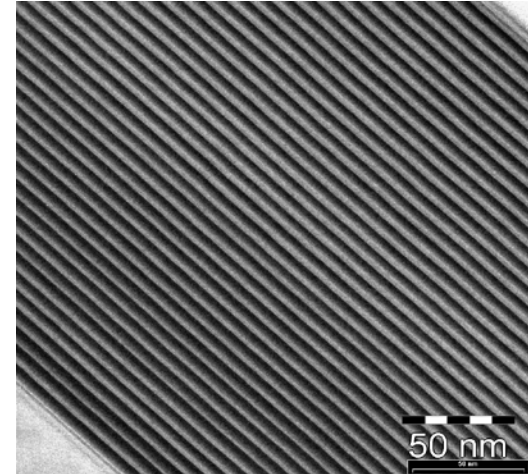
Principle of XUV multilayer mirrors at near normal incidence angles



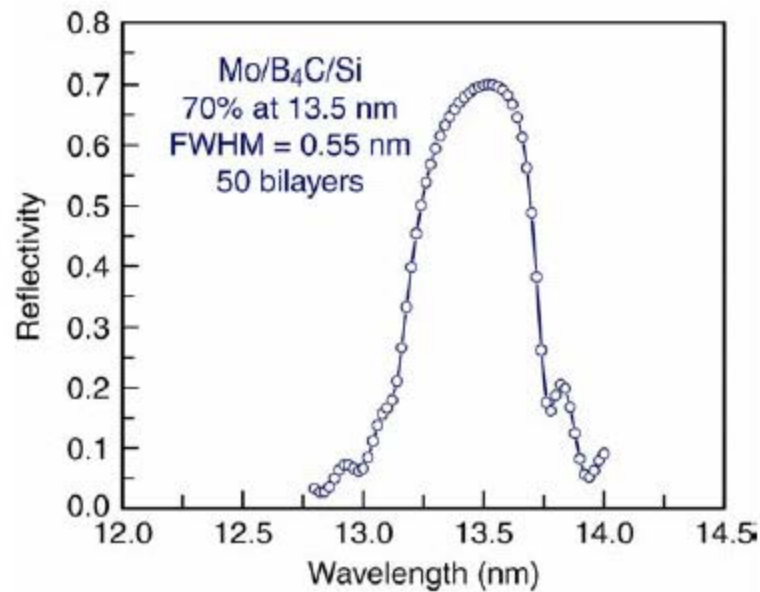
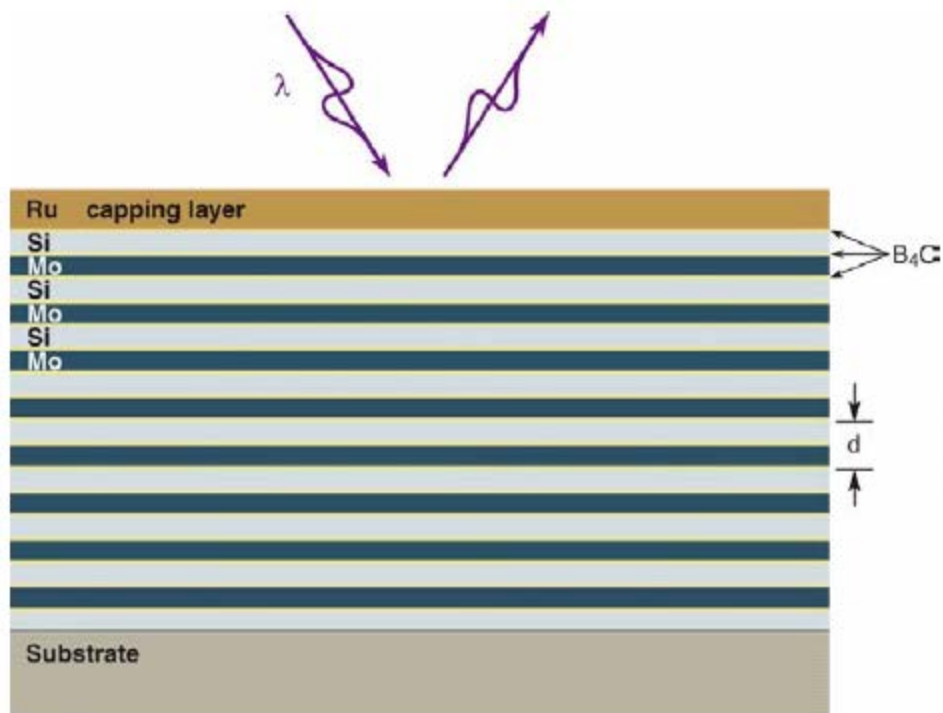
Principle of an XUV
multilayer mirror



68% measured reflectivity of a
MoSi multilayer mirror @ 93 eV



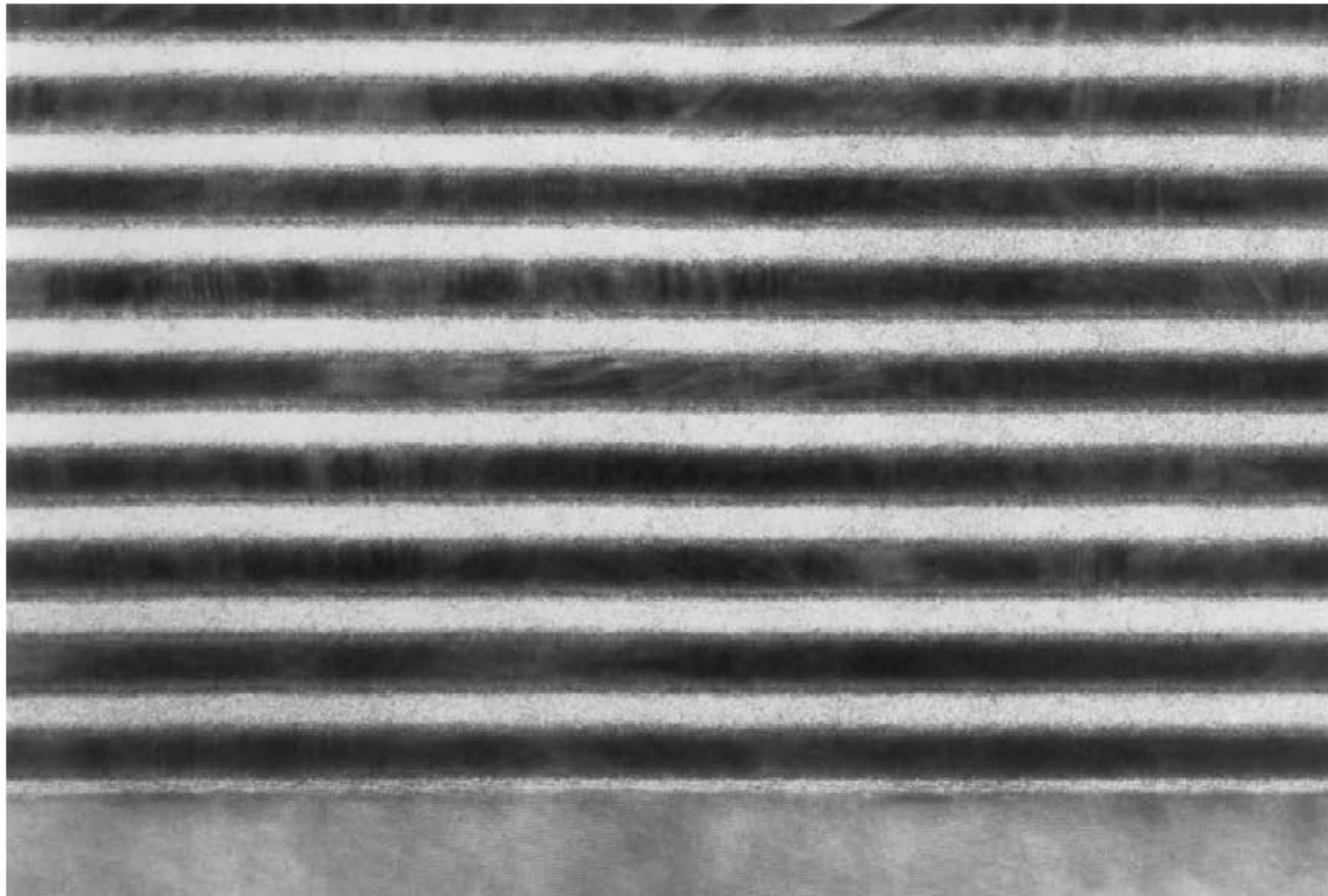
TEM image of a MoSi multilayer



Courtesy of Saša Bajt / LLNL



Mo/Si Multilayer Coating



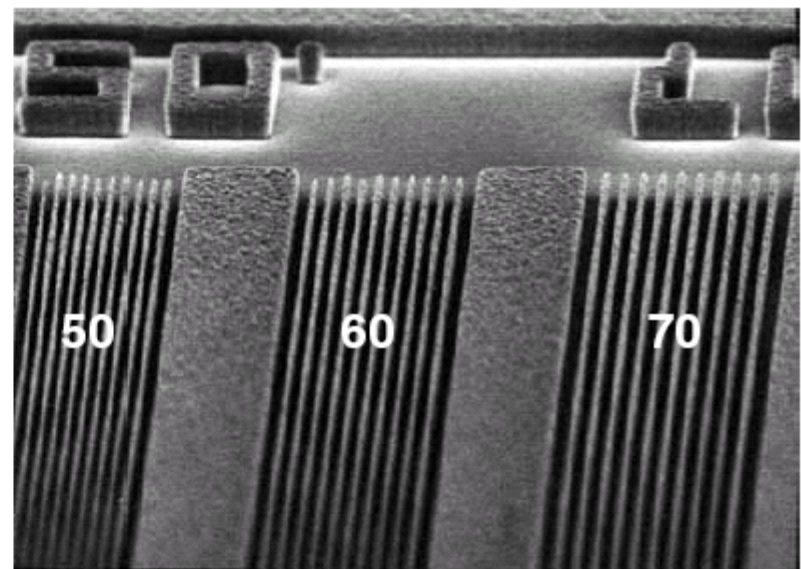
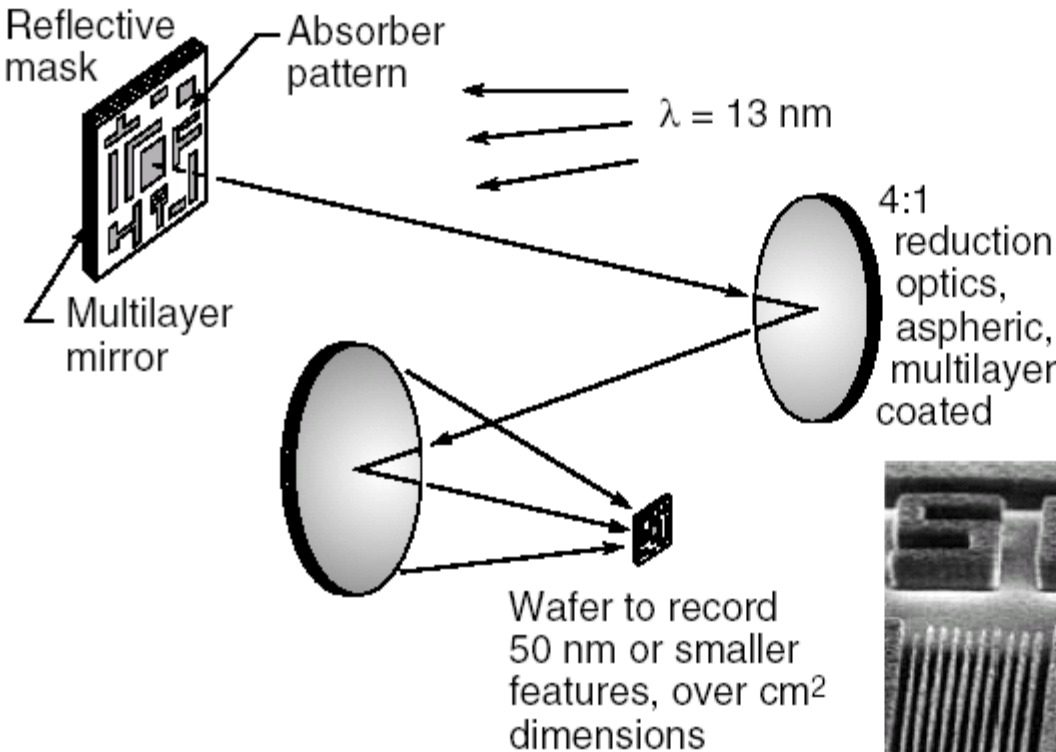
(T. Nguyen, CXRO/LBNL)

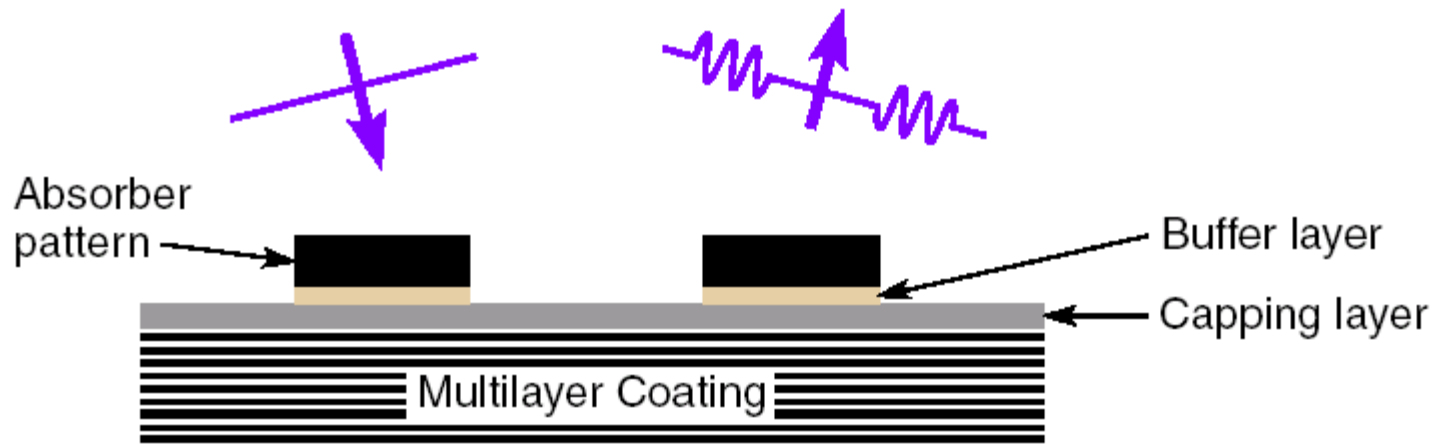
First year of volume production	2001	2003* 2004	2005* 2007	2007* 2010	2009* 2013	2011* 2016
Technology Generation (Dense lines, printed in resist)	130 nm	90 nm	65 nm	45 nm	32 nm	23 nm
Isolated Lines (in resist) [Physical gate, post-etch]	90 nm [65 nm]	53 nm [37 nm]	35 nm [25 nm]	25 nm [18 nm]	18 nm [13 nm]	13 nm [9 nm]
Chip Frequency	1.7 GHz	4.0 GHz	6.8 GHz	12 GHz	19 GHz	29 GHz
Transistors per chip (HV) (3 × for HP ; 5 × for ASICs)	100 M	190 M	390 M	780 M	1.5 B	3.1 B
DRAM Memory (bits)	510 M	1.1 G	4.3 G	8.6 G	34 G	69 G
Gate CD Control (3σ, post-etch)	5 nm	3 nm	2 nm	1.5 nm	1.1 nm	0.7 nm
Field Size (mm × mm)	25 × 32	25 × 32	22 × 26	22 × 26	22 × 26	22 × 26
Chip Size (mm) (2.2 × for HP ; to 4 × for ASIC)	140	140	140	140	140	140
Wafer Size (diameter)	300 mm	300 mm	300 mm	450 mm	450 mm	450 mm

*Semiconductor Industry Association (SIA), December 2001. *Possible 2-year cycle.



Extreme Ultraviolet (EUV) Lithography





Substrate:

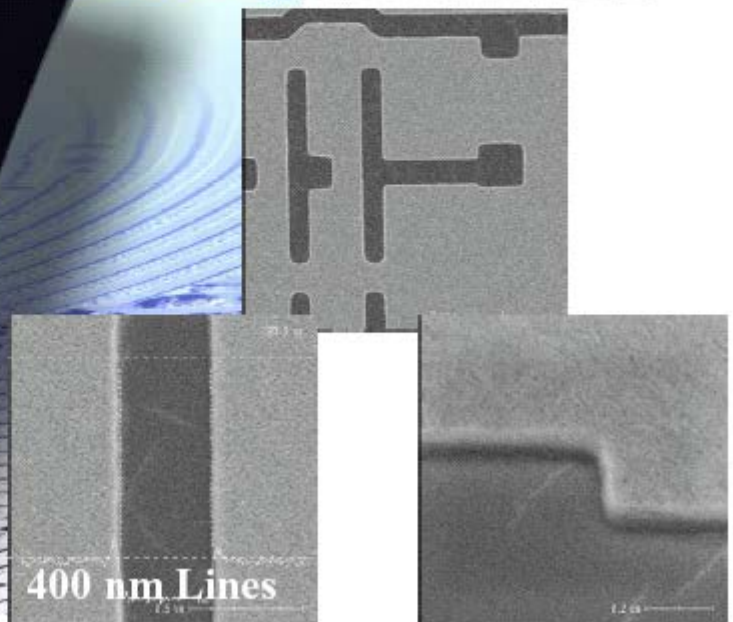
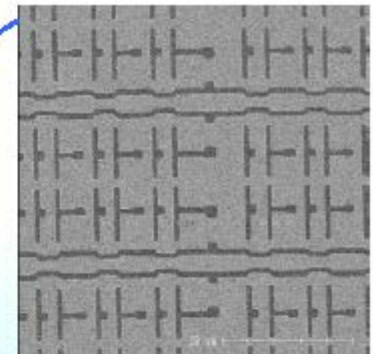
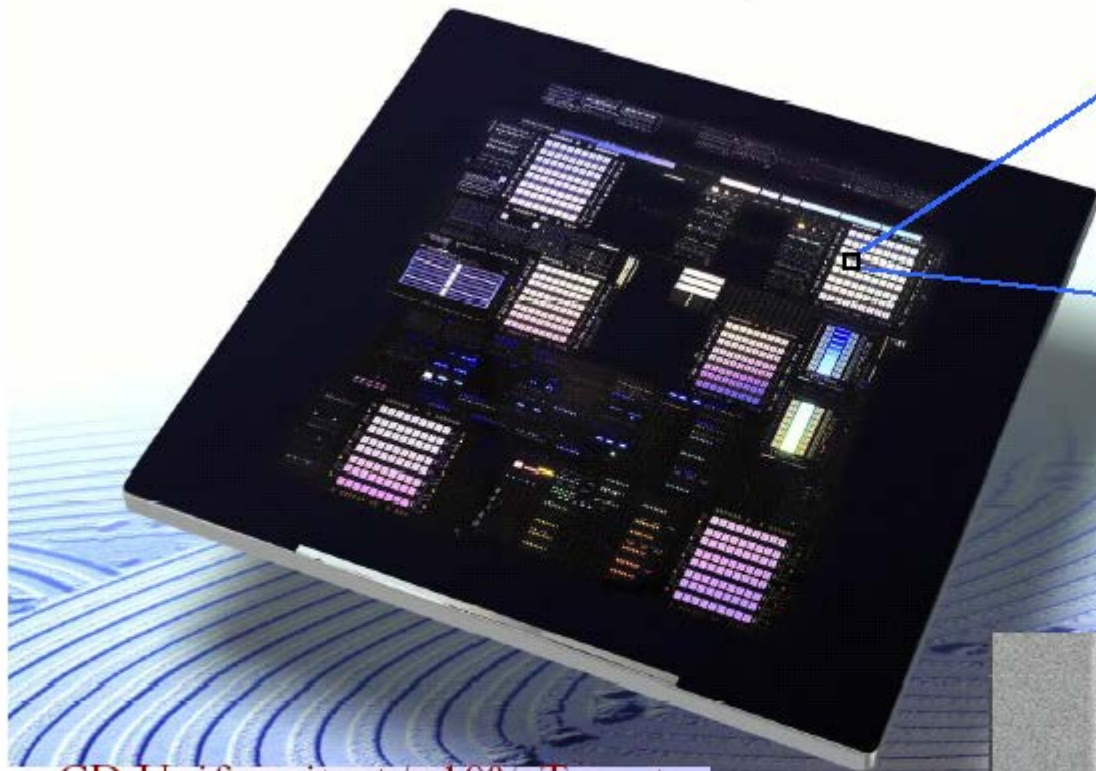
Low thermal expansion material (LTEM)
(6" square \times 1/4" thick)

Typically

Mo/Si multilayer ($d = 6.7$ nm)
with 30 nm SiO₂ capping layer
Cr or TaN absorber (~70 nm)
with 50 nm Ru Buffer layer

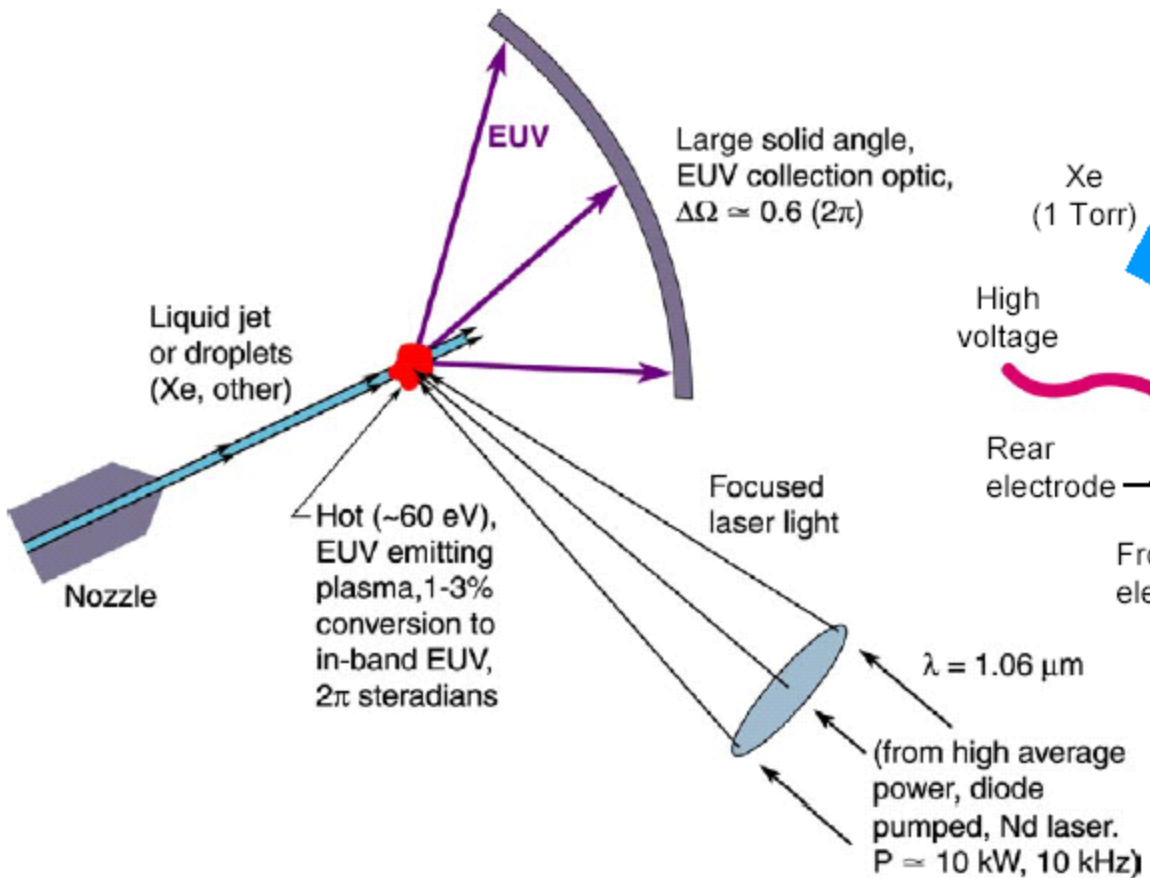
LTEM substrate
(Ti-doped fused silica)
ULE (Corning), or
Zerodur (Schott)

Stack: Cr/SiON/MoSi Multilayers

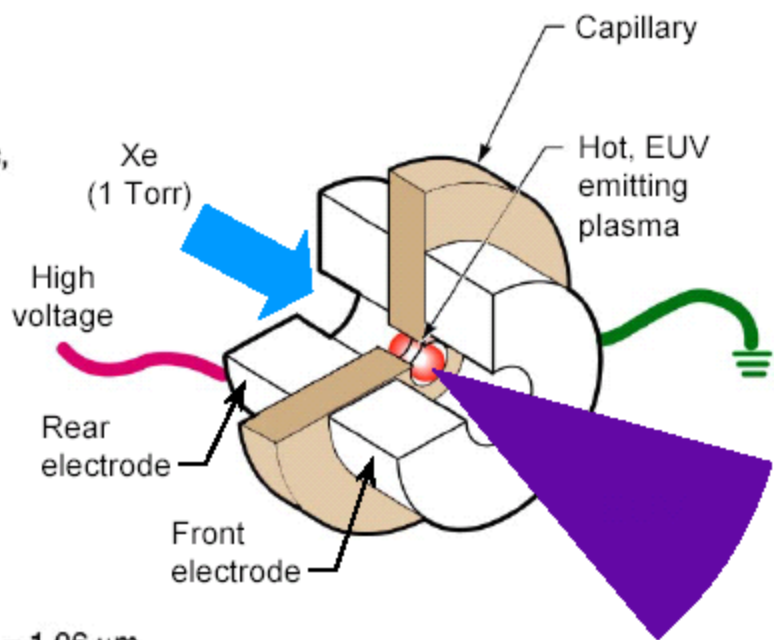


- CD Uniformity +/- 10% Target
 - Data set for 100 nm node
- Min. Resolution: 0.32 μm

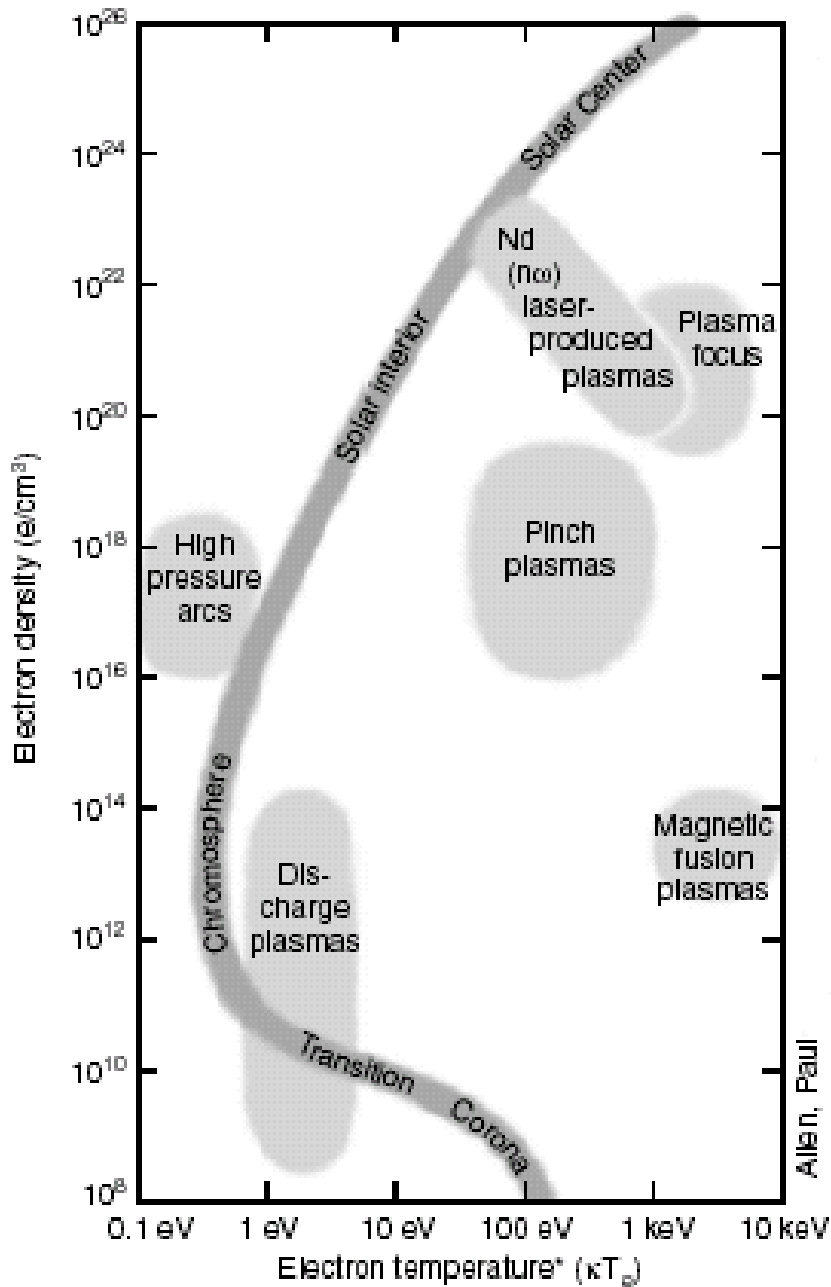
Laser Produced Plasma Source



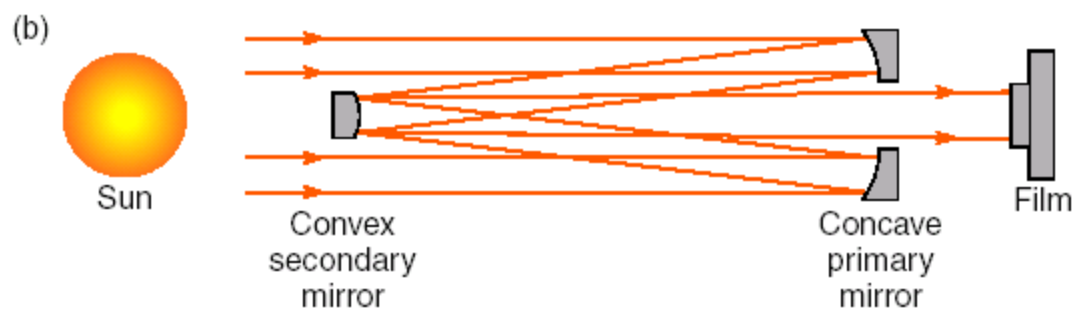
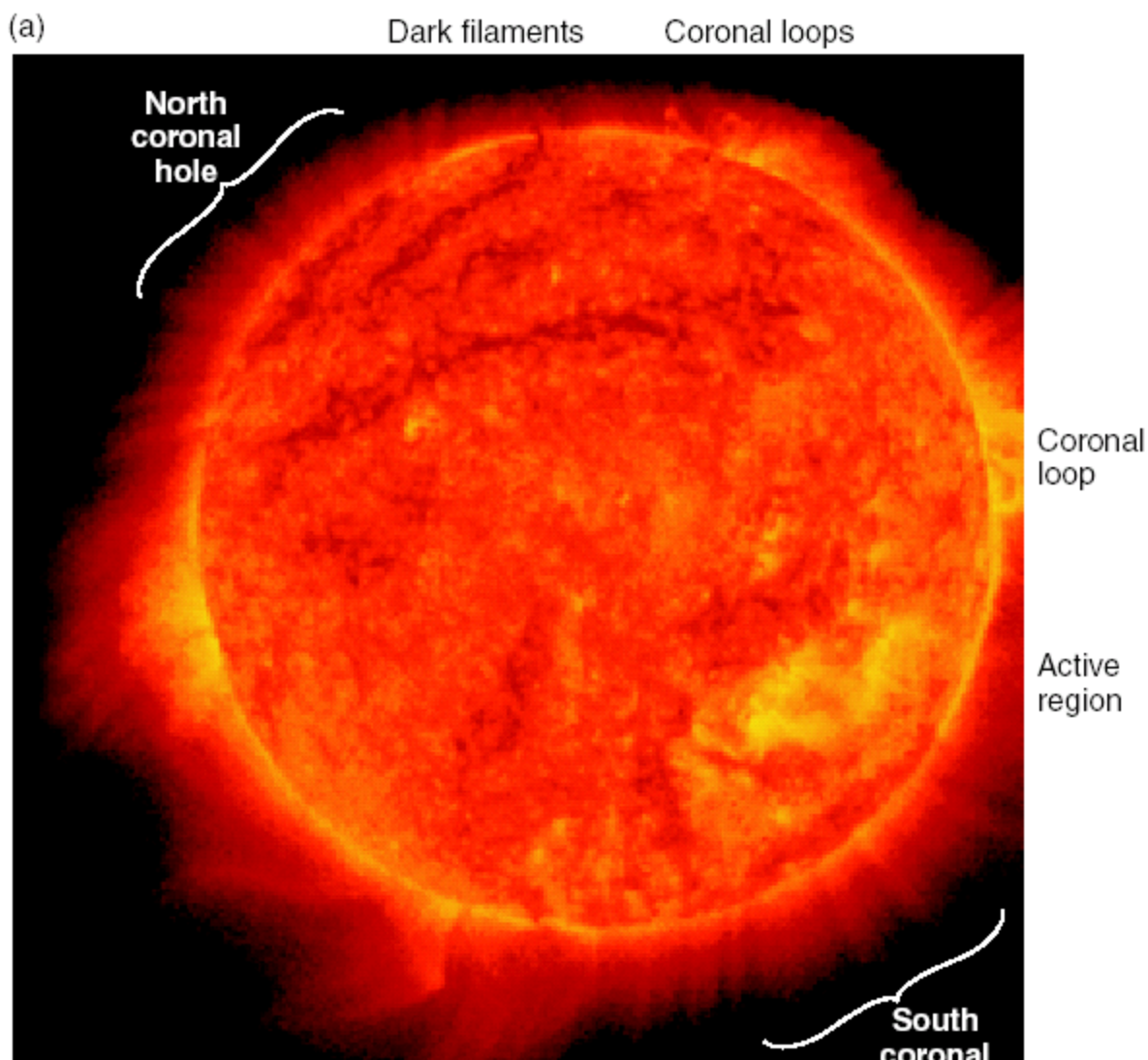
Electrical Discharge Plasma Source

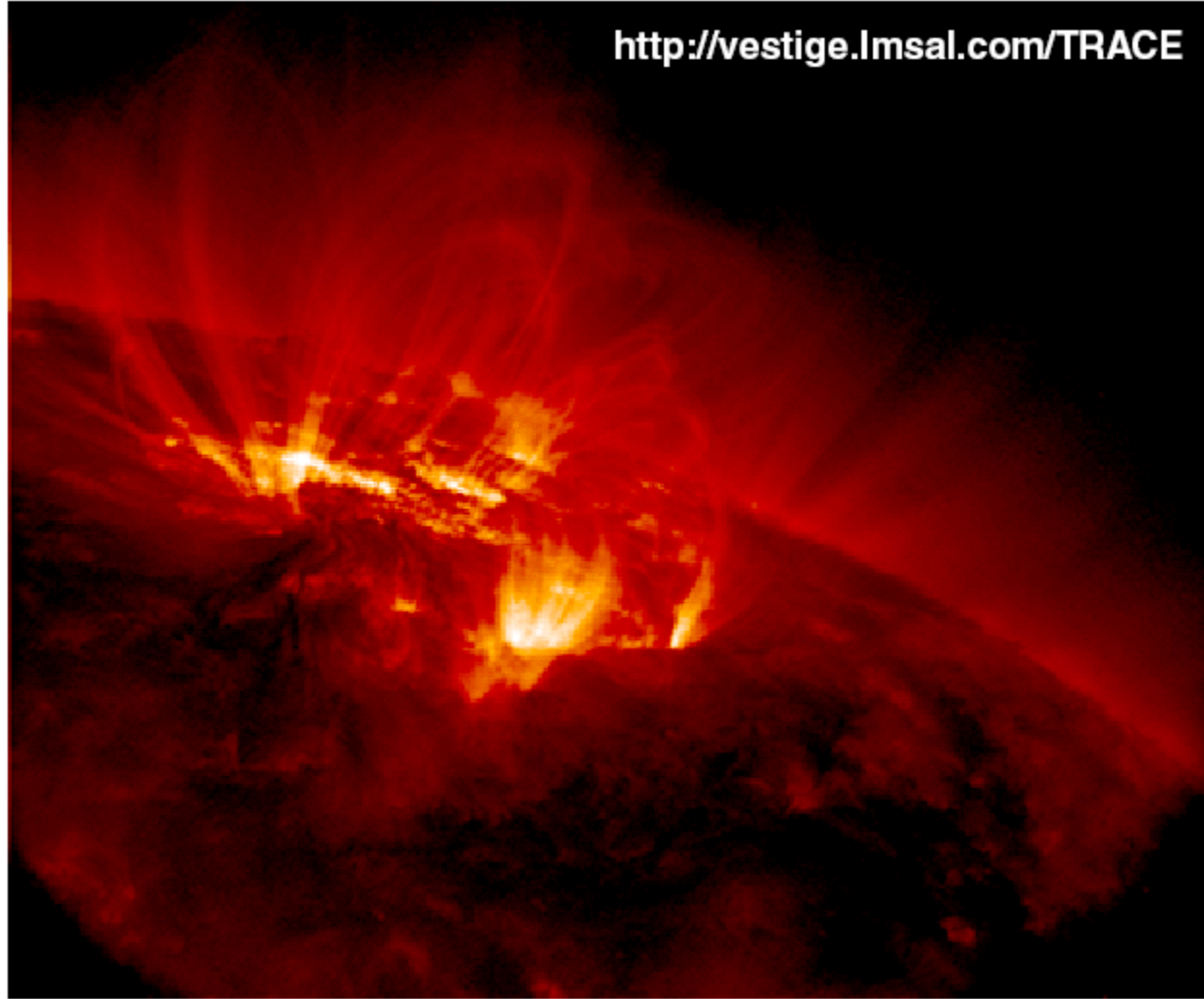


Courtesy of Neil Fornaciari
and Glenn Kubiak, Sandia.



EIT telescope SOHO mission

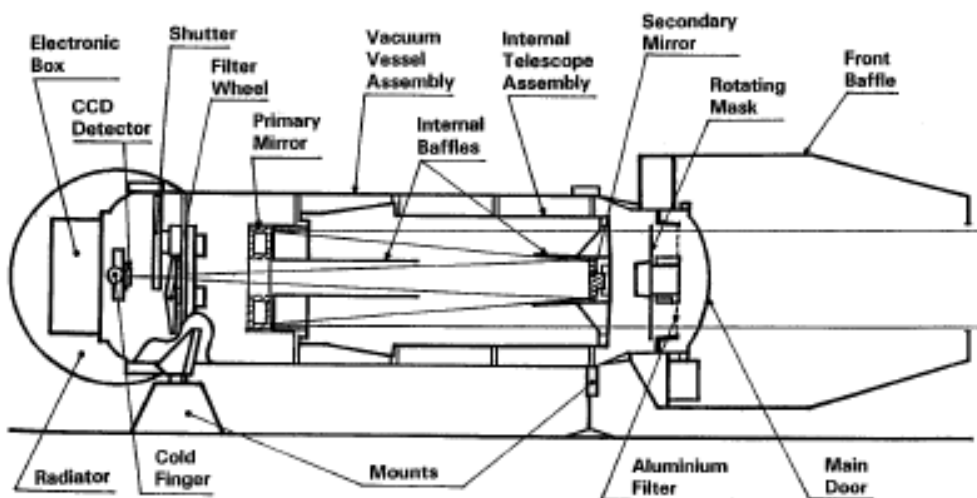
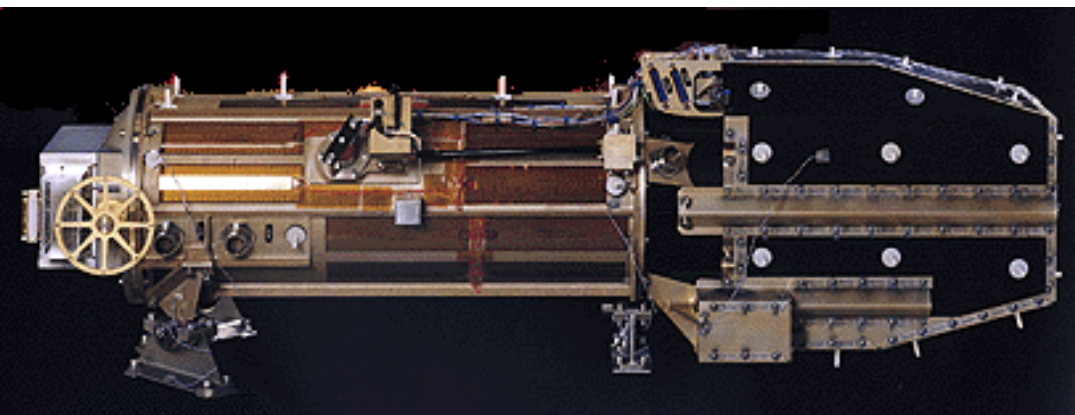




<http://vestige.lmsal.com/TRACE>

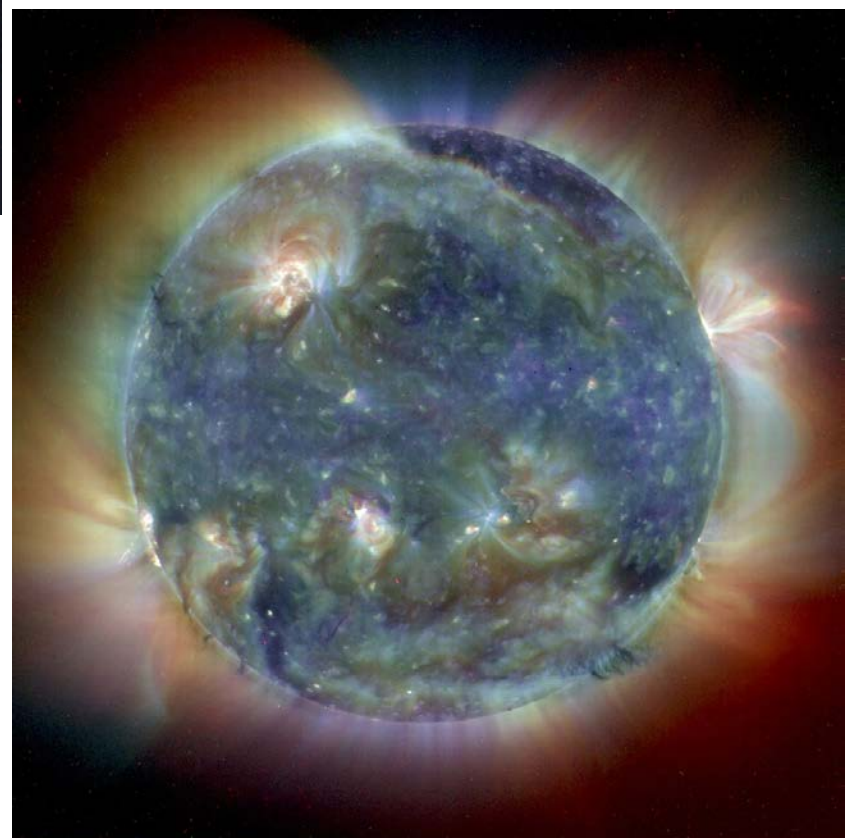
(Courtesy of L.Golub, Harvard-Smithsonian and T. Barbee, LLNL)

The Extreme Ultraviolet Imaging Telescope (EIT)



Multilayer coated normal incidence cassegrain objective

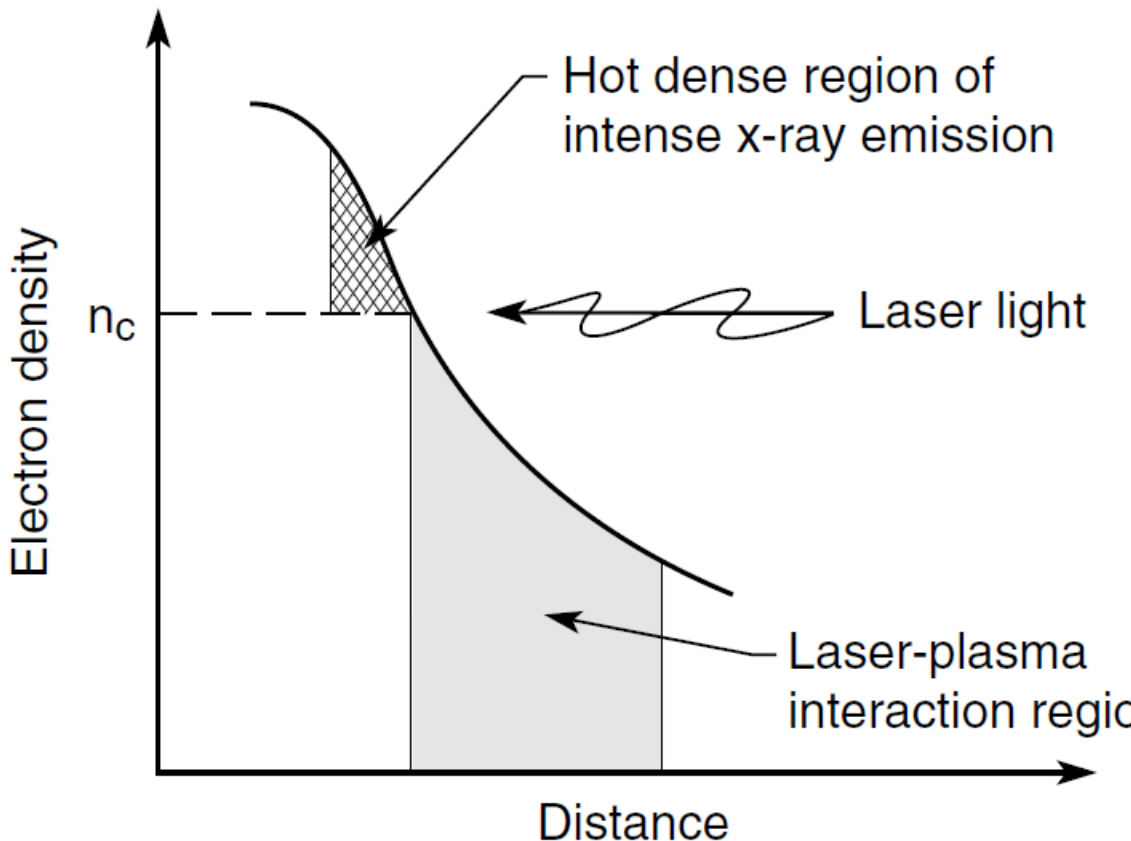
EIT composite image



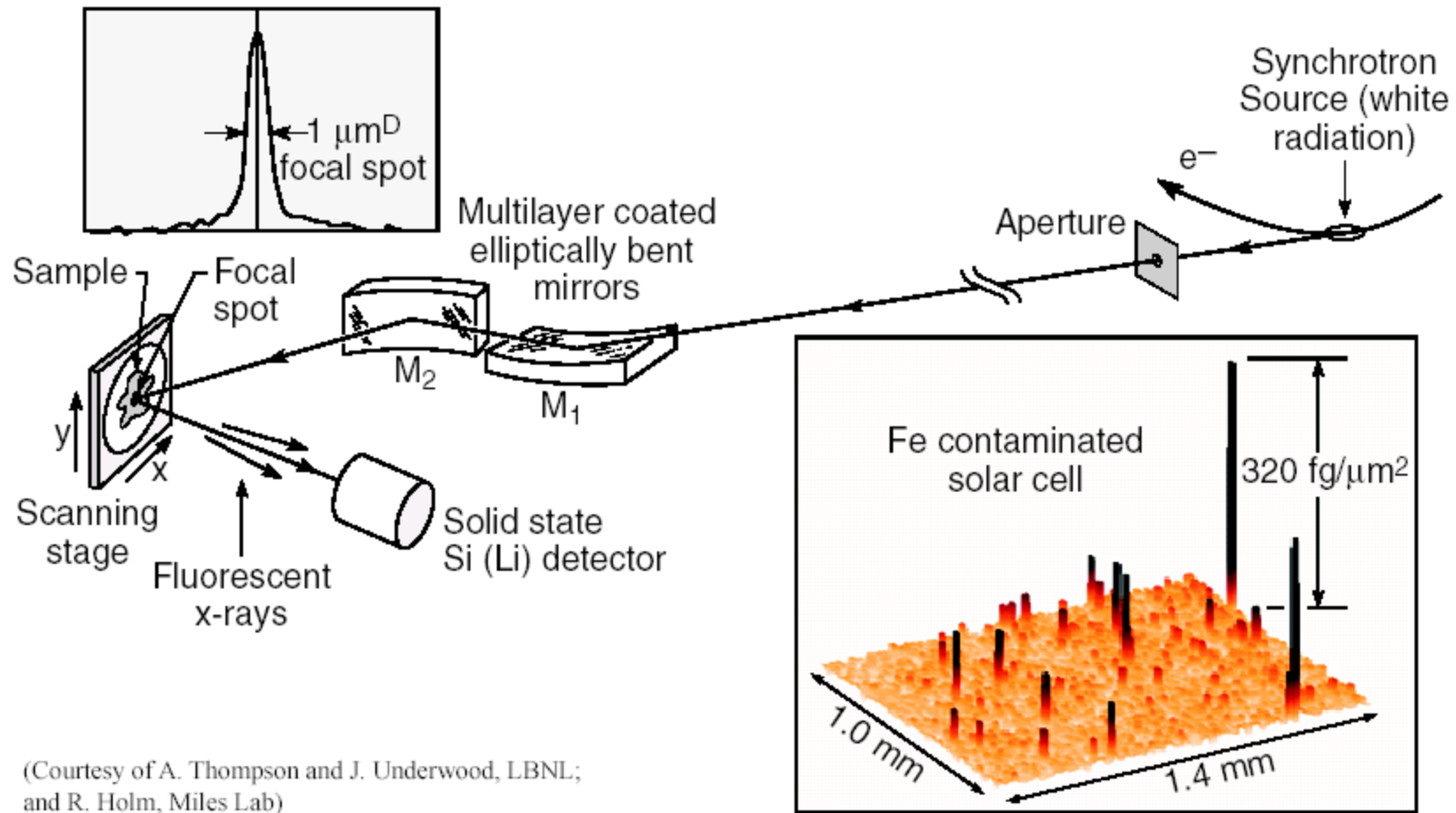
17,1 nm (blue)
19,5 nm (green)
28,4 nm (red)



Soft X-Ray/EUV Emission from a Hot-Dense Plasma

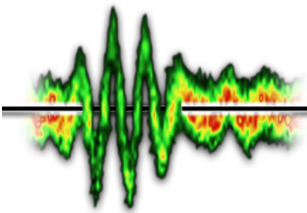


- $kT_e \sim 50 \text{ eV to } 1 \text{ keV}$
- $n_e \sim 10^{20} \text{ to } 10^{22} \text{ e/cm}^3$



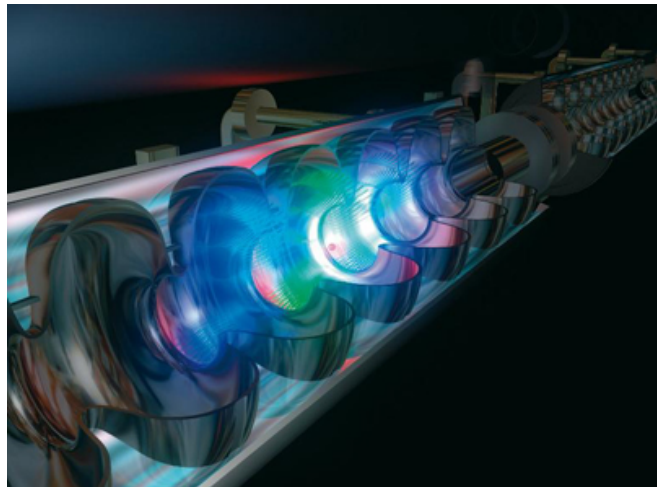
(Courtesy of A. Thompson and J. Underwood, LBNL;
and R. Holm, Miles Lab)

Motivation



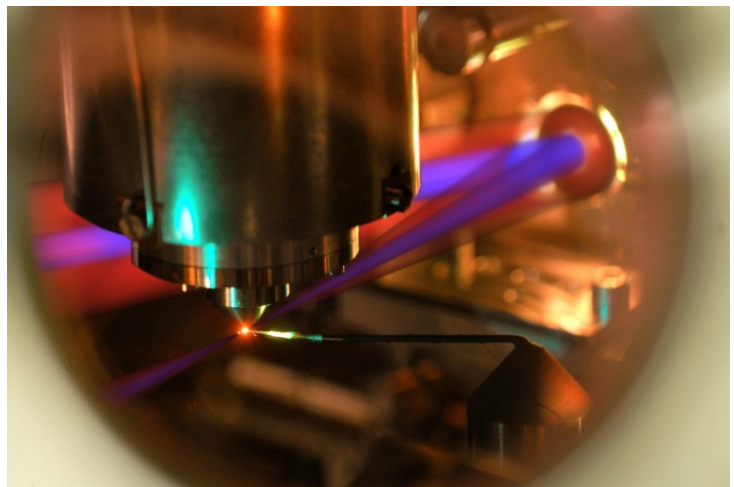
Excellent XUV optics for sources emitting ultrashort pulses:

FEL



(aspiration for sub-) fs pulses
grazing optics due to high intensities

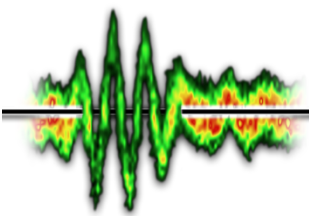
HHG



as pulses (requires large ΔE)
normal incidence optics possible

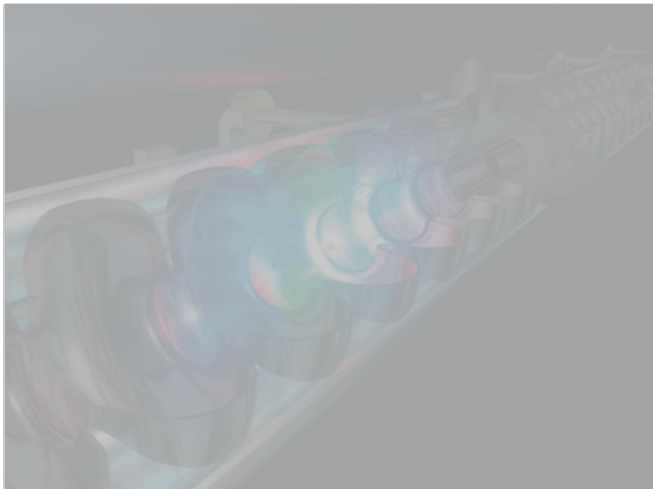
Both require optics for spectral filtering, phase shaping, ...

Motivation



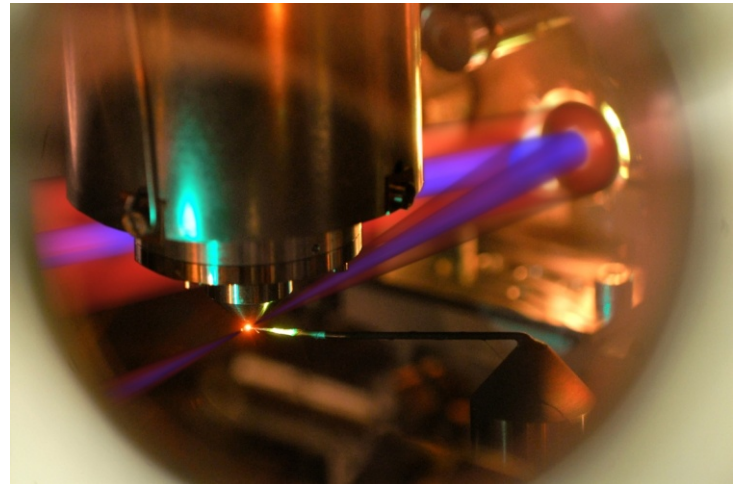
Excellent XUV optics for sources emitting ultrashort pulses:

FEL



(aspiration for sub-) fs pulses
grazing optics due to high intensities

OUR FOCUS: HHG

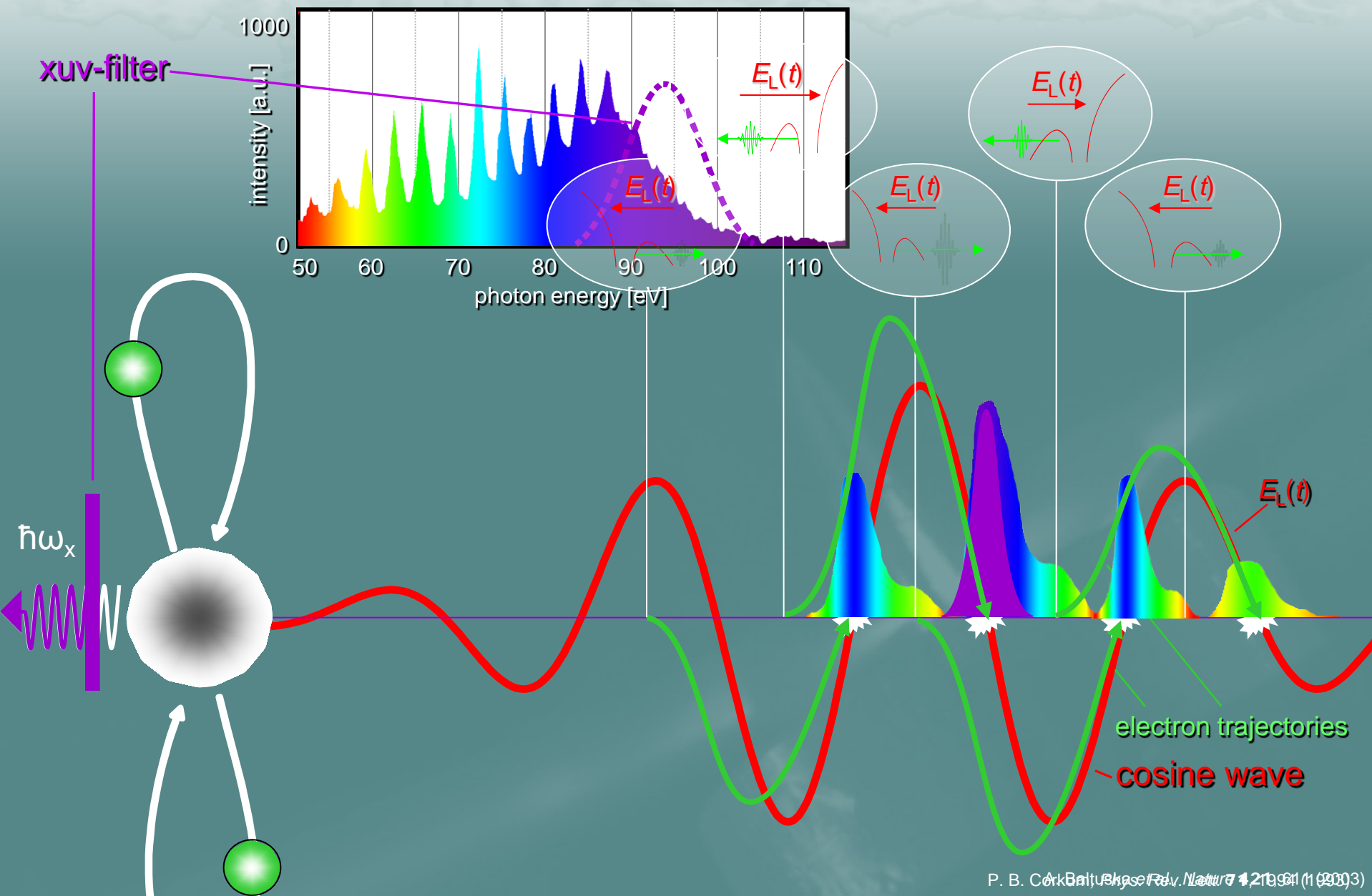


as pulses (requires large ΔE)
normal incidence optics possible

Photon flux essential!

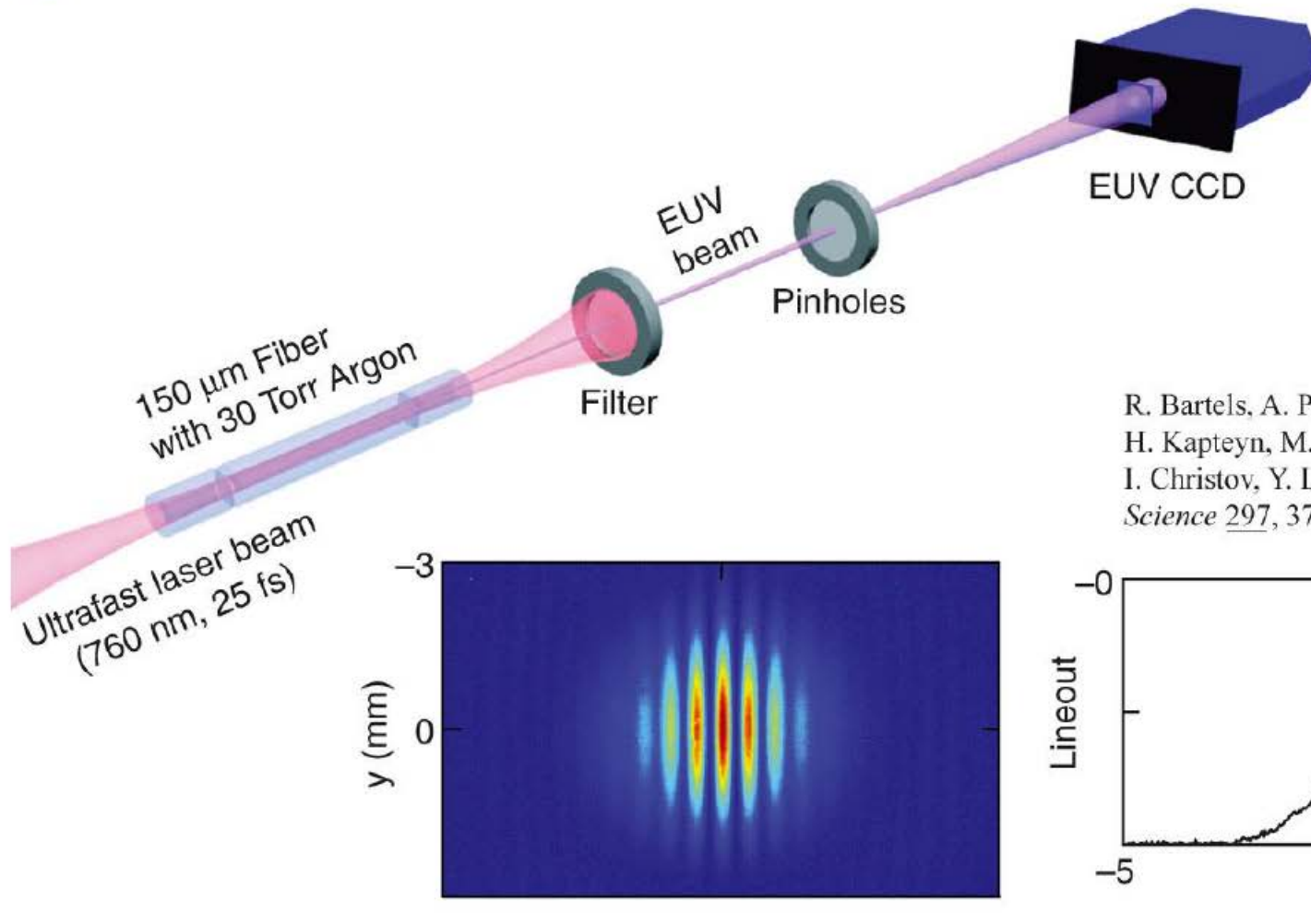
Both require optics for spectral filtering, phase shaping, ...

steering bound electrons with controlled light fields: the birth of an attosecond pulse





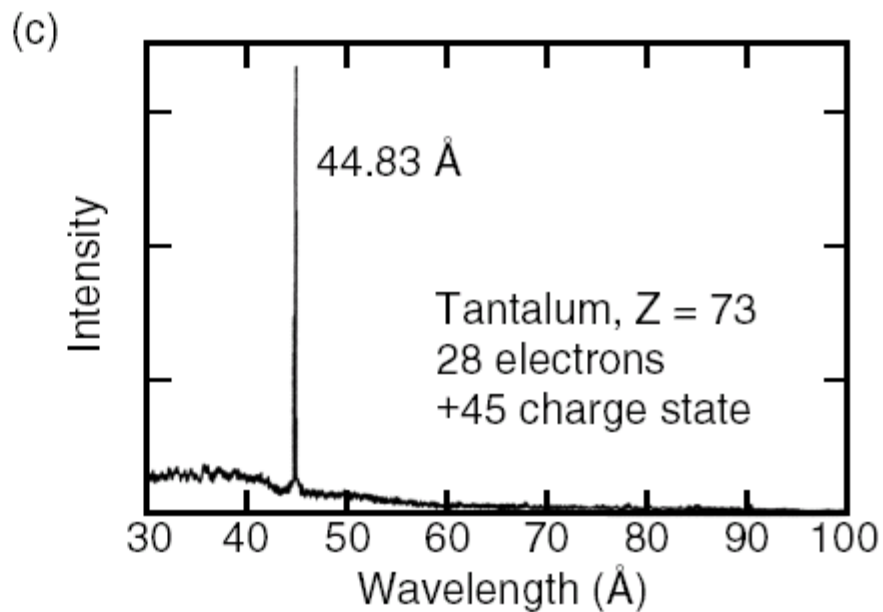
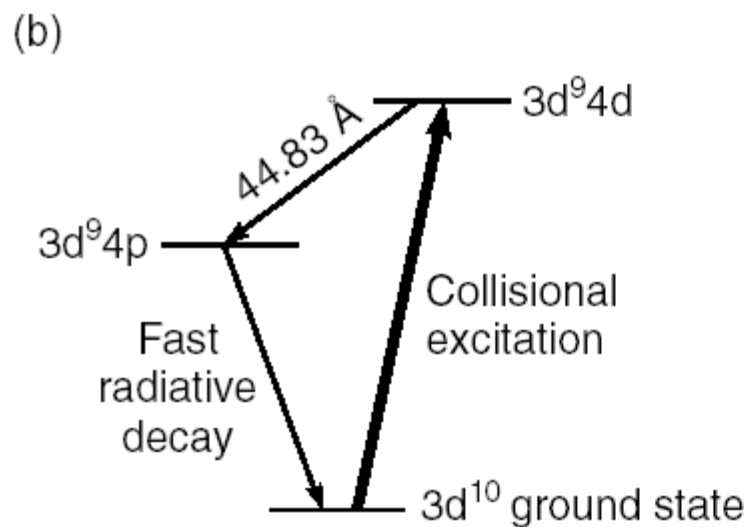
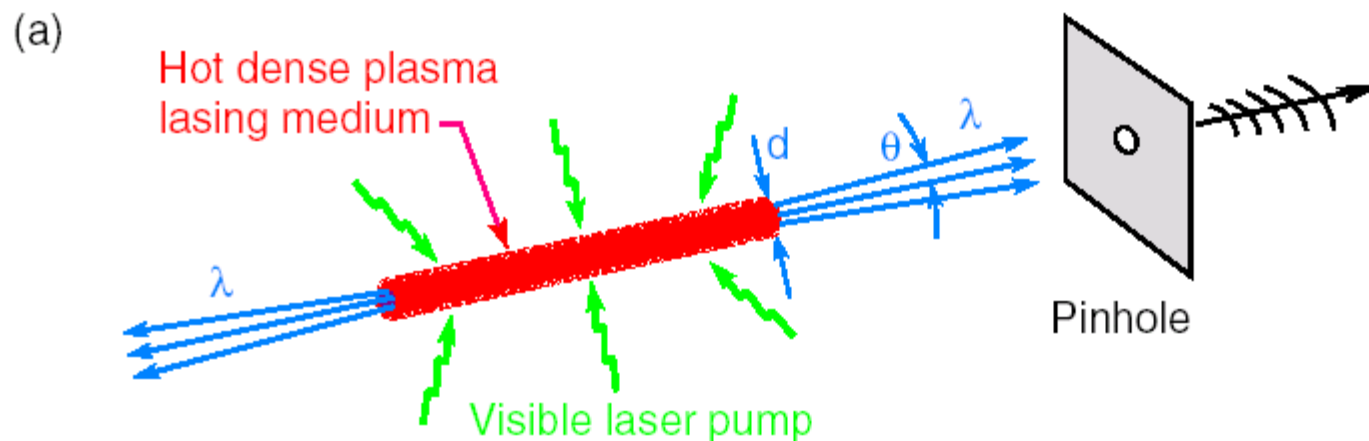
High Harmonic Generation (HHG) Provides Coherent, Femtosecond Pulses



R. Bartels, A. Paul, H. Green,
H. Kapteyn, M. Murnane, S. Backus,
I. Christov, Y. Liu, D. Attwood, C. Jacobsen,
Science **297**, 376 (19 July 2002).

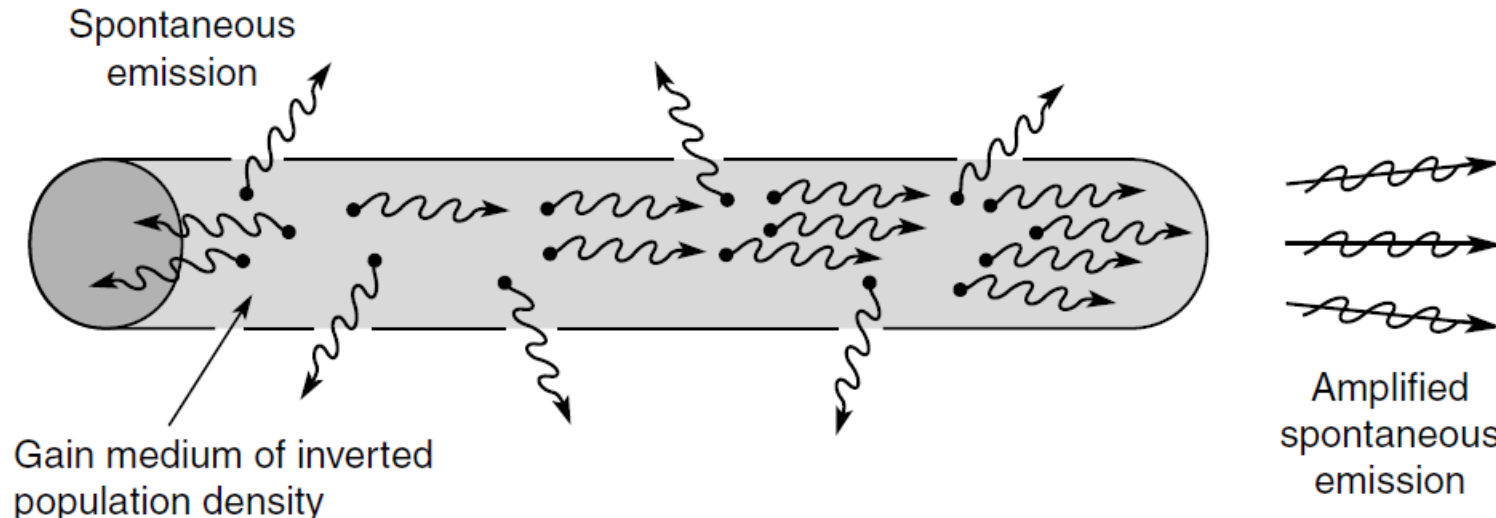
$$P \approx 10 \text{ } \mu\text{W} \rightarrow 2 \times 10^{12} \text{ ph/sec} @ 36 \text{ nm} (n = 21; 34 \text{ eV})$$

Courtesy of Professors Margaret Murnane and Henry Kapteyn, Univ. Colorado

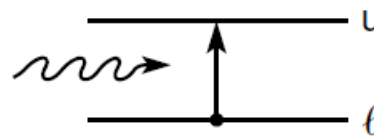




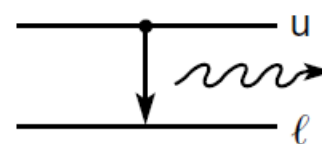
Lasing Begins with Amplified Spontaneous Emission



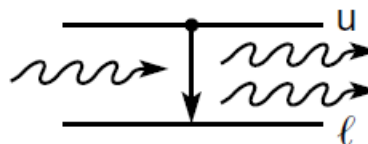
(a) Absorption



(b) Spontaneous emission



(c) Stimulated emission



$$\frac{I}{I_0} = e^{GL} \quad (7.2)$$

$$G = n_u \sigma_{\text{stim}} F \quad (7.4)$$

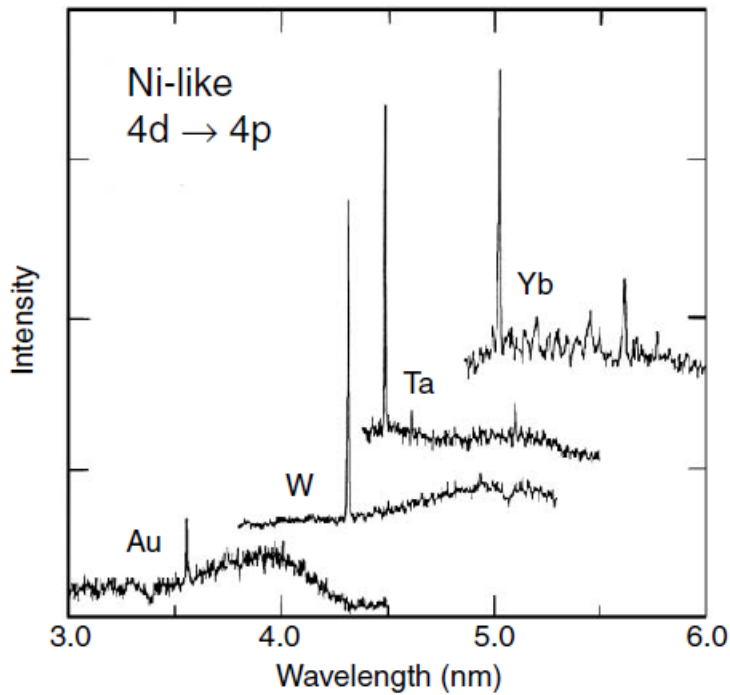
$$\sigma_{\text{stim}} = \frac{\pi \lambda r_e}{(\Delta \lambda / \lambda)} \left(\frac{g_l}{g_u} \right) f_{lu} \quad (7.18)$$

$$\frac{P}{A} = \frac{16\pi^2 c^2 \hbar (\Delta \lambda / \lambda) GL}{\lambda^4} \quad (7.22)$$

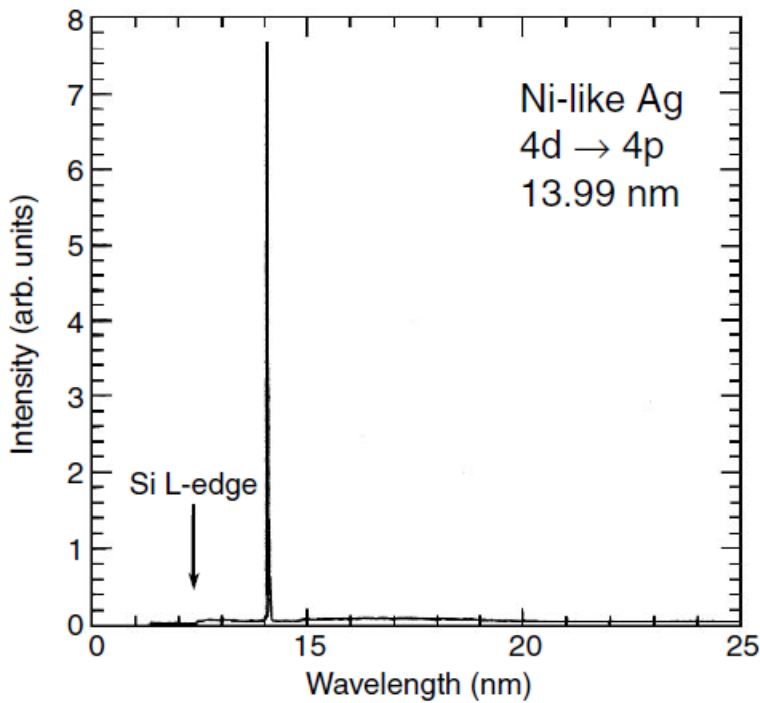


Mirror-less XUV/EUV Lasing (ASE) at Various Labs Around the World

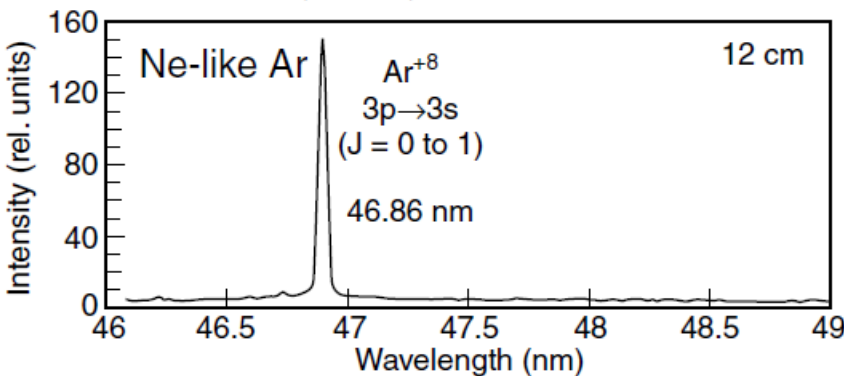
B. MacGowan, et al., Lawrence Livermore Lab



J. Zhang, et al., Rutherford-Appleton



J. Rocca, et al., Colorado State Univ.



S. Suckewer, Princeton Univ.

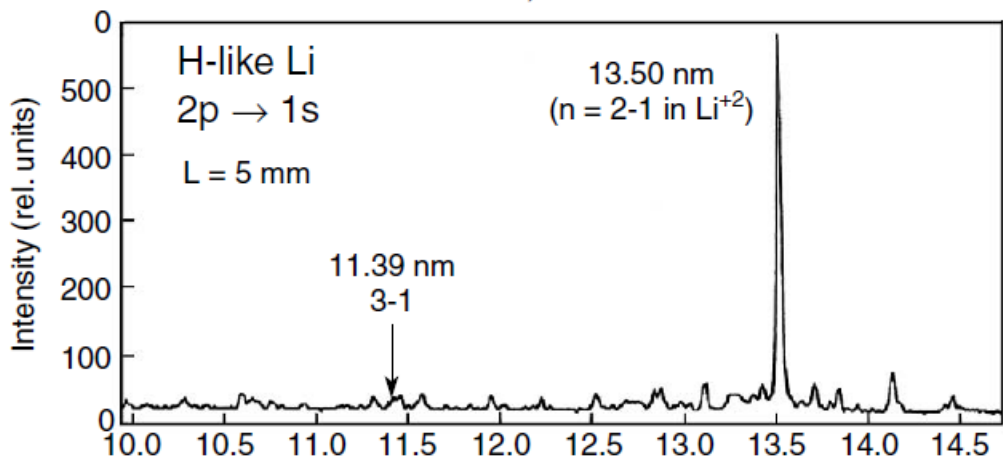
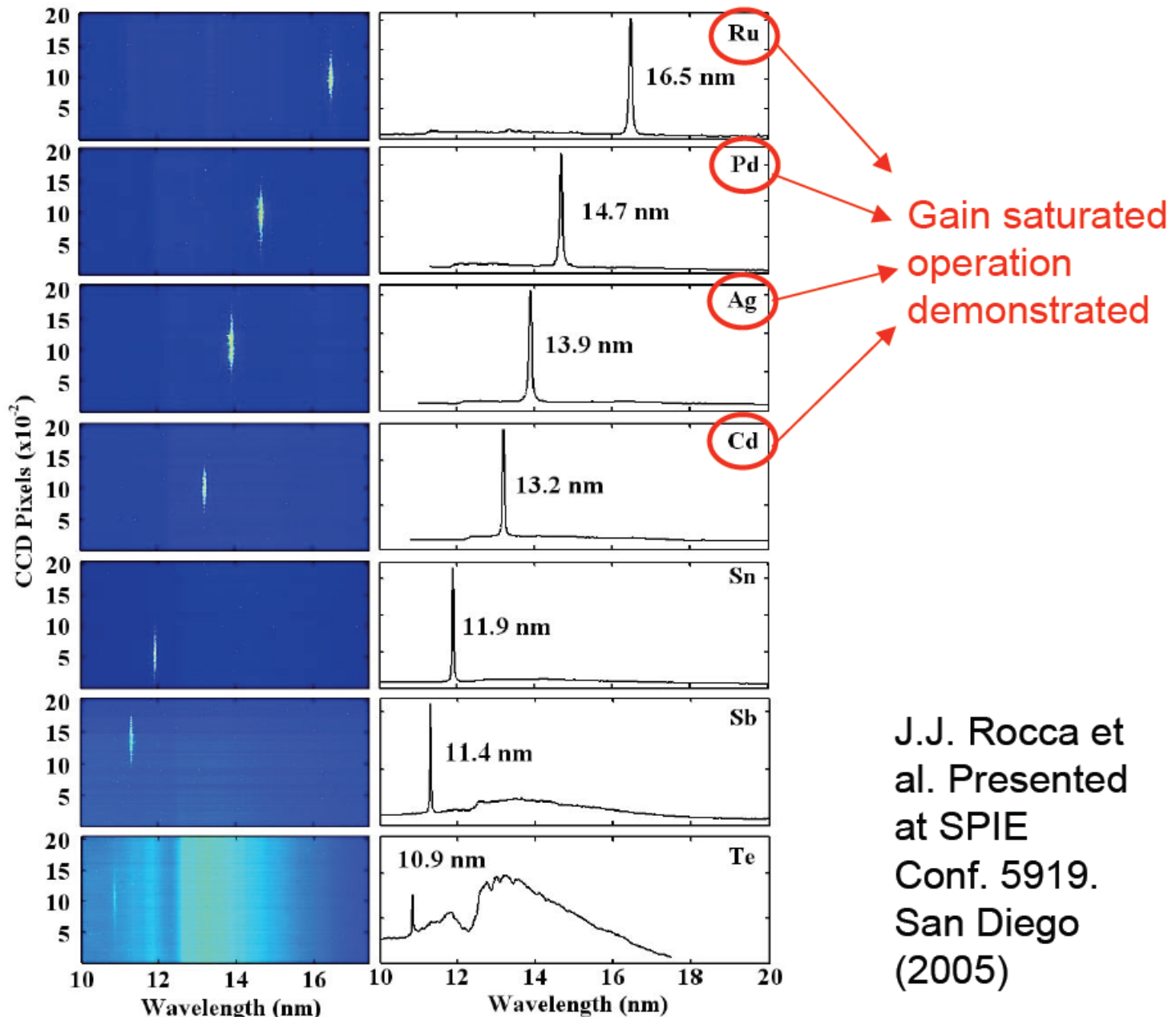
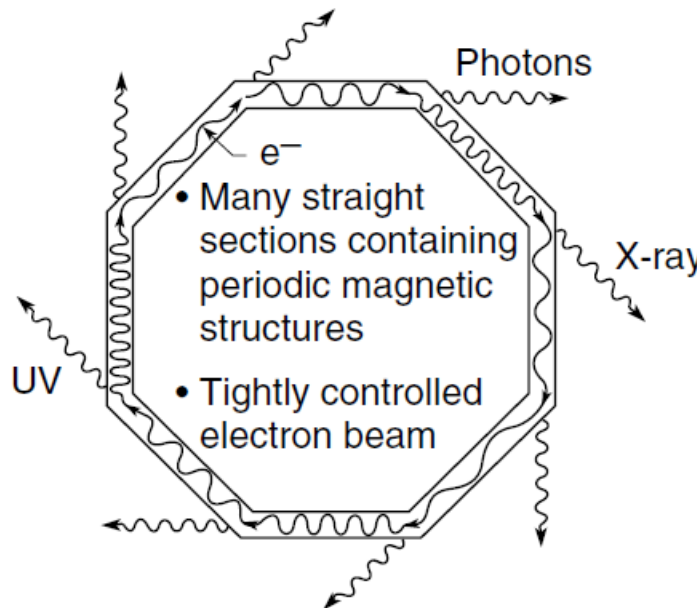


Table-top EUV Lasers





Synchrotron Radiation



Bending Magnet:

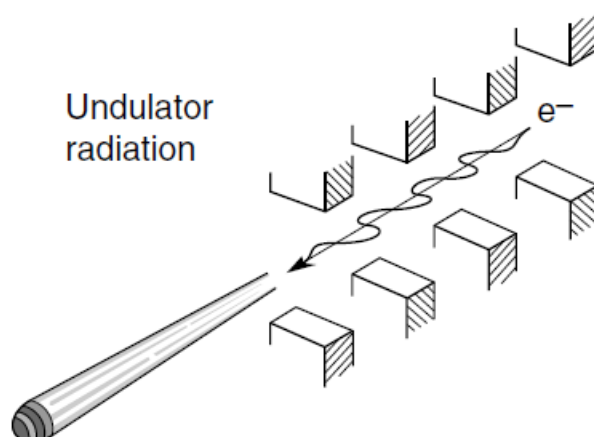
$$\hbar\omega_c = \frac{3e\hbar B\gamma^2}{2m} \quad (5.7)$$

Wiggler:

$$\hbar\omega_c = \frac{3e\hbar B\gamma^2}{2m} \quad (5.80)$$

$$n_c = \frac{3K}{4} \left(1 + \frac{K^2}{2} \right) \quad (5.82)$$

$$P_T = \frac{\pi e K^2 \gamma^2 I N}{3\epsilon_0 \lambda_u} \quad (5.85)$$



Undulator:

$$\lambda = \frac{\lambda_u}{2\gamma^2} \left(1 + \frac{K^2}{2} + \gamma^2 \theta^2 \right) \quad (5.28)$$

$$K = \frac{e B_0 \lambda_u}{2\pi m c} \quad (5.18)$$

$$\theta_{cen} = \frac{1}{\gamma^* \sqrt{N}} \quad (5.15)$$

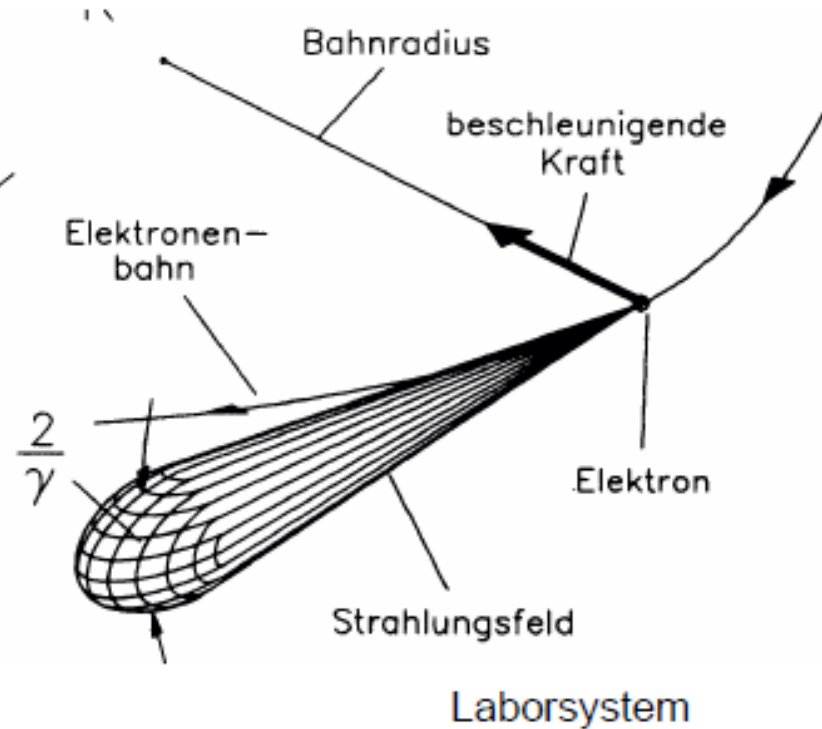
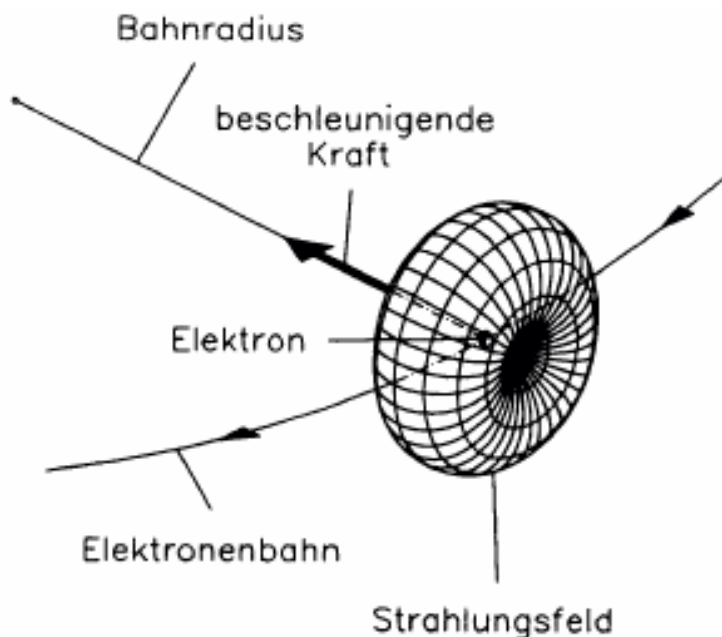
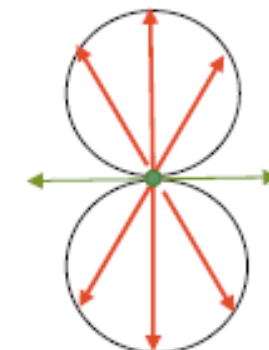
$$\left. \frac{\Delta\lambda}{\lambda} \right|_{cen} = \frac{1}{N} \quad (5.14)$$

$$\bar{P}_{cen} = \frac{\pi e \gamma^2 I}{\epsilon_0 \lambda_u} \frac{K^2}{\left(1 + \frac{K^2}{2} \right)^2} f(K) \quad (5.41)$$

IV.1.2 Synchrotronstrahlungsquellen

Prinzip: **Abstrahlung** elektromagnetischer Wellen
durch **beschleunigte** Ladung
(vgl. oszillierender Dipol)

hier: **Querbeschleunigung** der Ladungen
bei relativistischer Geschwindigkeit



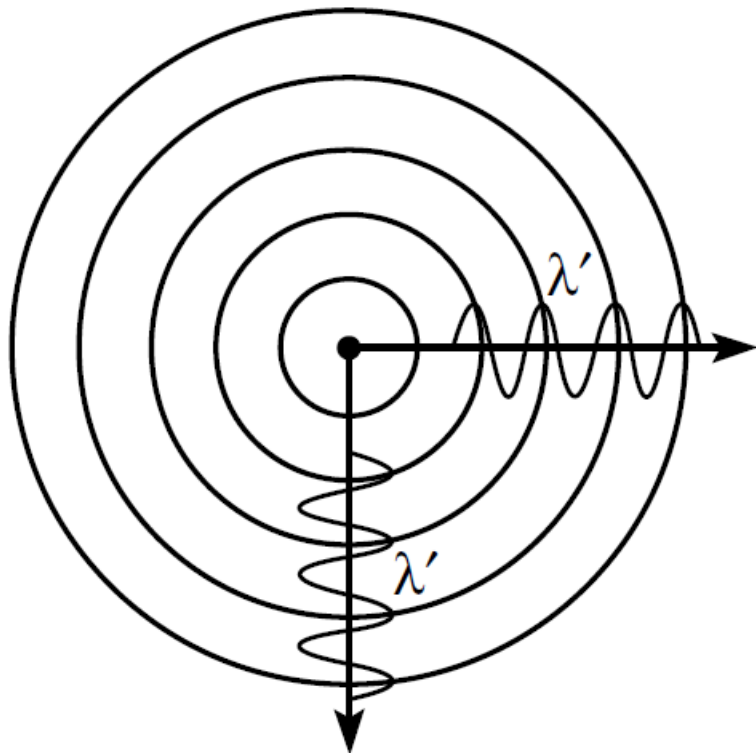
Schwerpunktsystem des Elektrons

Laborsystem

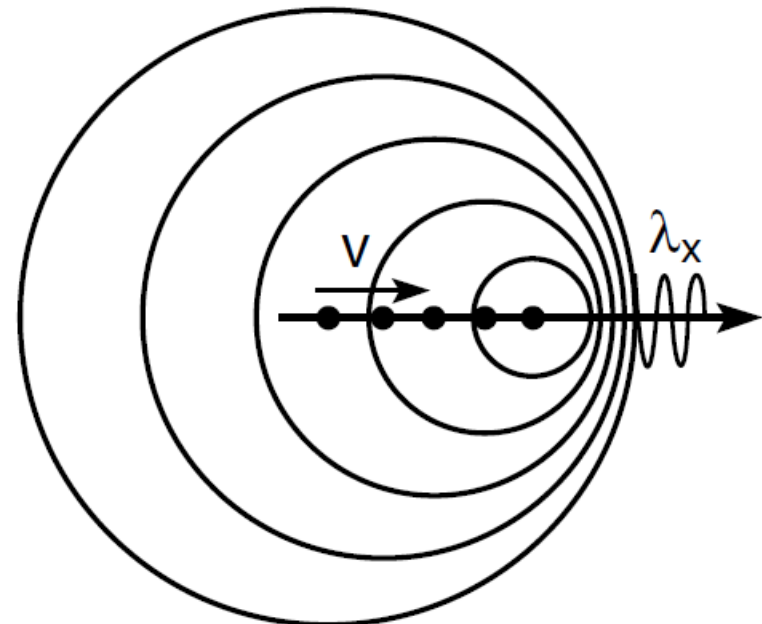


Synchrotron Radiation from Relativistic Electrons

$v \ll c$



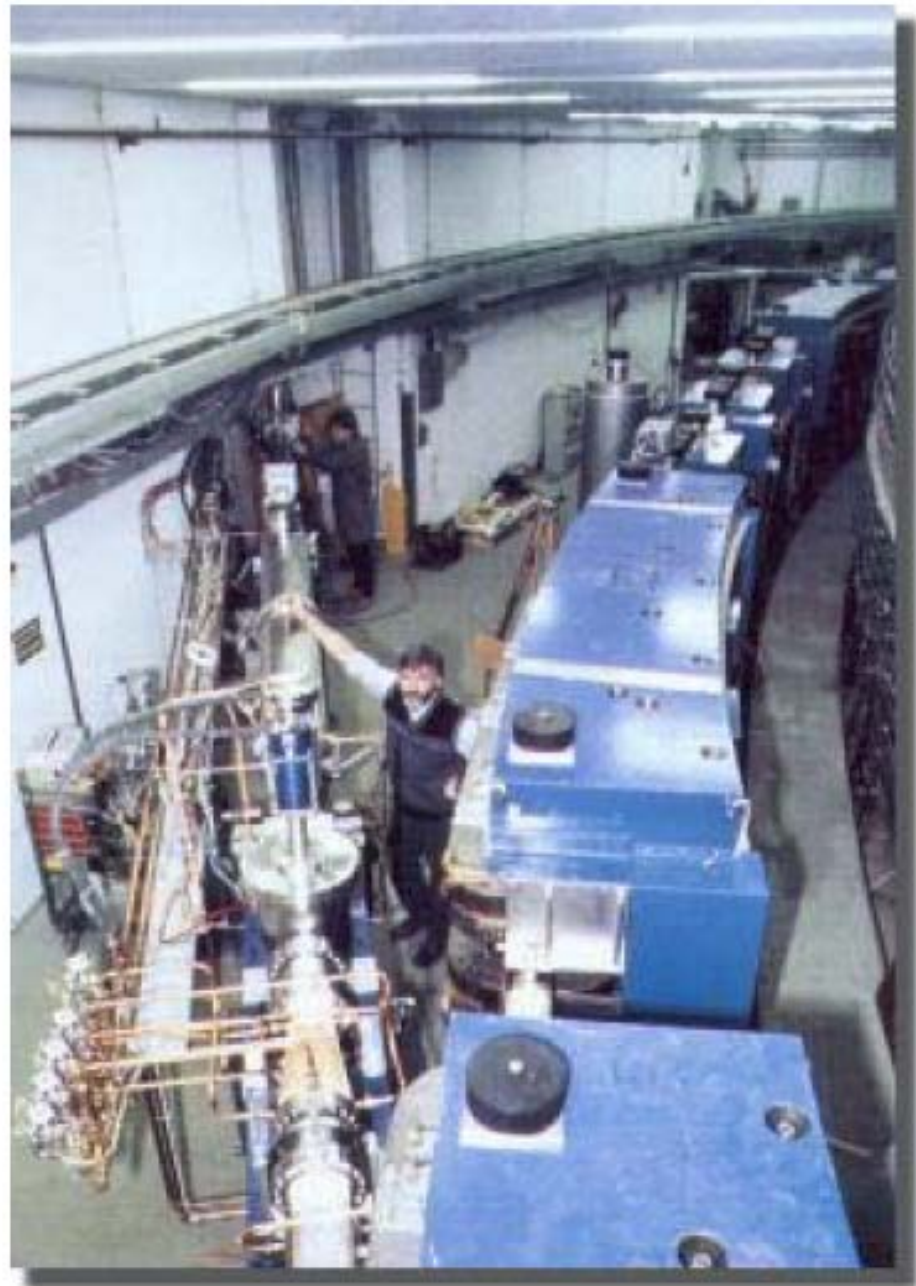
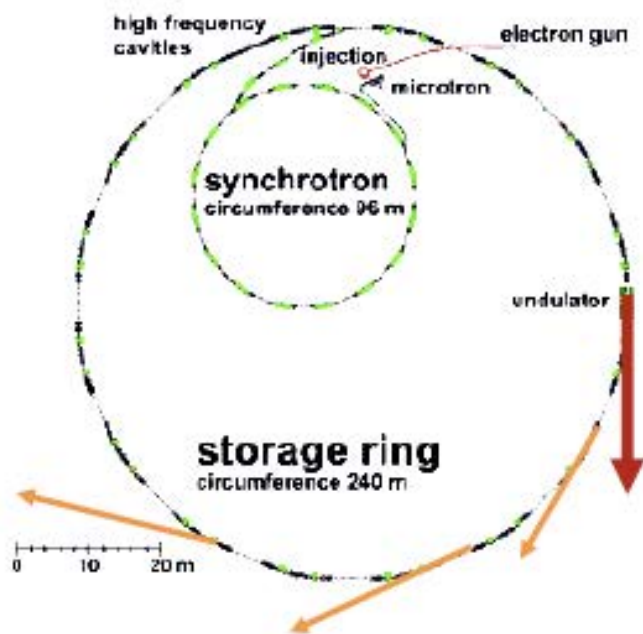
$v \lesssim c$



Note: Angle-dependent doppler shift

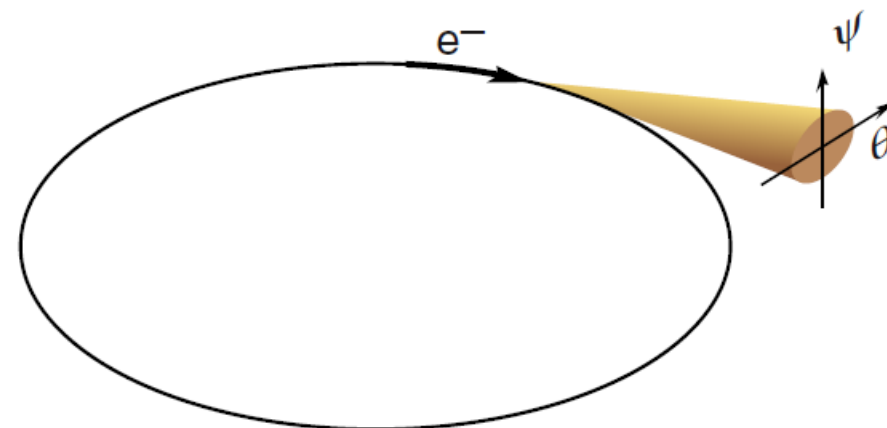
Synchrotronstrahlung

Abstrahlung im Ablenkmagnet





Bending Magnet Photon Flux at the ALS



$$E_c = \hbar\omega_c = \frac{3e\hbar B\gamma^2}{2m} \quad (5.7a)$$

$$E_c(\text{keV}) = 0.6650 E_e^2(\text{GeV}) B(\text{T}) \quad (5.7b)$$

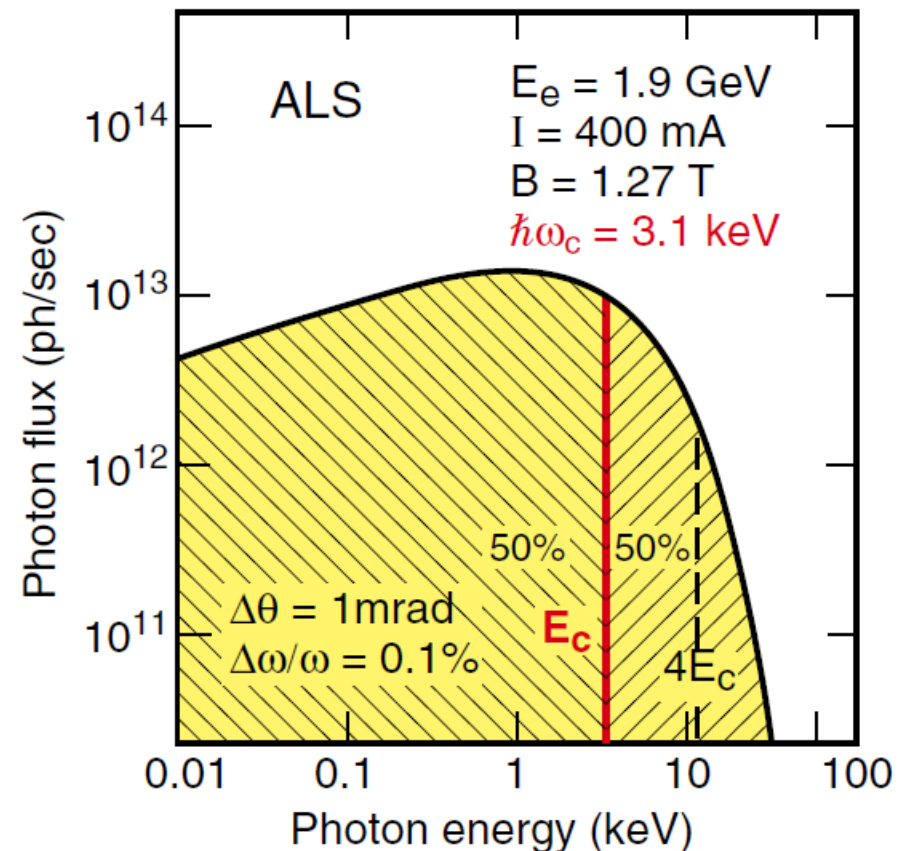
$$\gamma = \frac{E_e}{mc^2} = 1957 E_e(\text{GeV}) \quad (5.5)$$

Advantages: • covers broad spectral range

- least expensive
 • most accessible

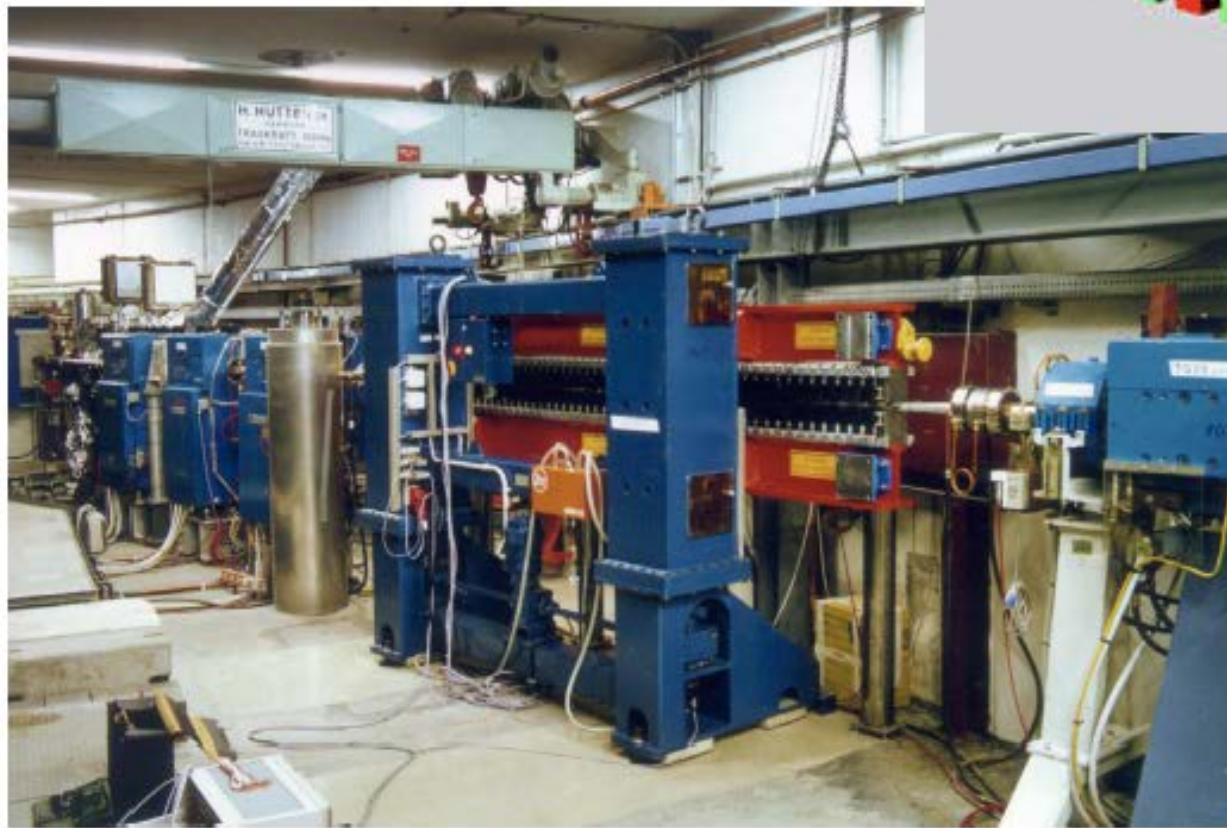
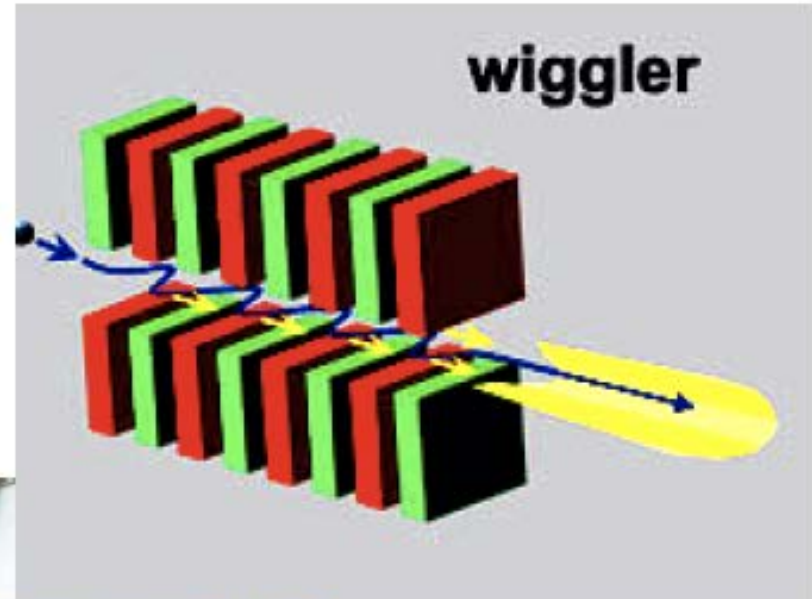
Disadvantages: limited coverage of

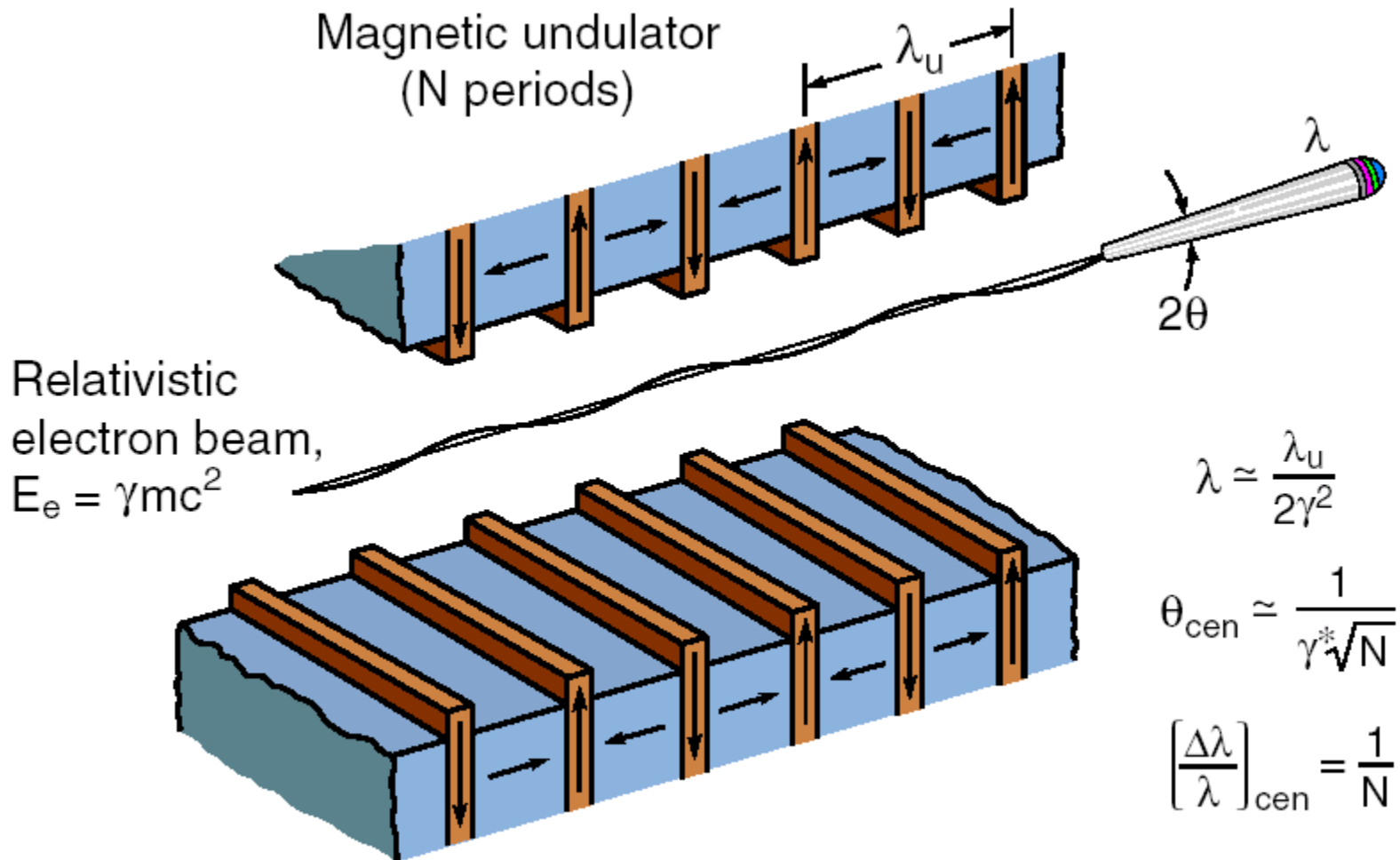
- hard x-rays
 • not as bright as undulator



Synchrotronstrahlung

durch alternierende Magnete:
Überlagerung der Abstrahlprozesse





$$\lambda \simeq \frac{\lambda_u}{2\gamma^2}$$

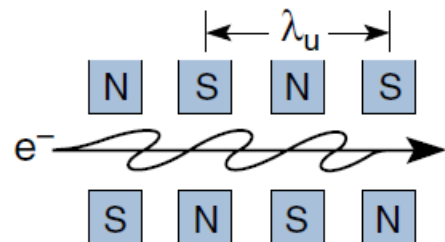
$$\theta_{\text{cen}} \simeq \frac{1}{\gamma^* \sqrt{N}}$$

$$\left[\frac{\Delta\lambda}{\lambda} \right]_{\text{cen}} = \frac{1}{N}$$



Undulator Radiation

Laboratory Frame of Reference



$$E = \gamma mc^2$$

$$\gamma = \frac{1}{\sqrt{1 - \frac{v^2}{c^2}}}$$

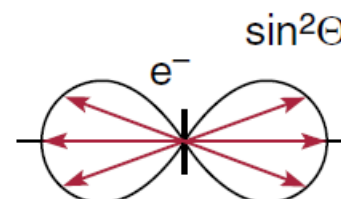
$N = \# \text{ periods}$

$$\lambda' = \frac{\lambda_u}{\gamma}$$

Bandwidth:

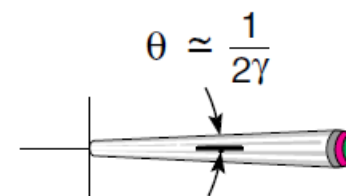
$$\frac{\lambda'}{\Delta\lambda} \simeq N$$

Frame of Moving e^-



e^- radiates at the Lorentz contracted wavelength:

Frame of Observer



Doppler shortened wavelength on axis:

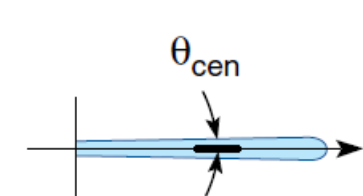
$$\lambda = \lambda' \gamma (1 - \beta \cos \theta)$$

$$\lambda = \frac{\lambda_u}{2\gamma^2} (1 + \gamma^2 \theta^2)$$

Accounting for transverse motion due to the periodic magnetic field:

$$\lambda = \frac{\lambda_u}{2\gamma^2} \left(1 + \frac{K^2}{2} + \gamma^2 \theta^2 \right)$$

Following Monochromator



$$\text{For } \frac{\Delta\lambda}{\lambda} \simeq \frac{1}{N}$$

$$\theta_{\text{cen}} \simeq \frac{1}{\gamma \sqrt{N}}$$

typically

$$\theta_{\text{cen}} \simeq 40 \mu\text{rad}$$

where $K = eB_0\lambda_u / 2\pi mc$

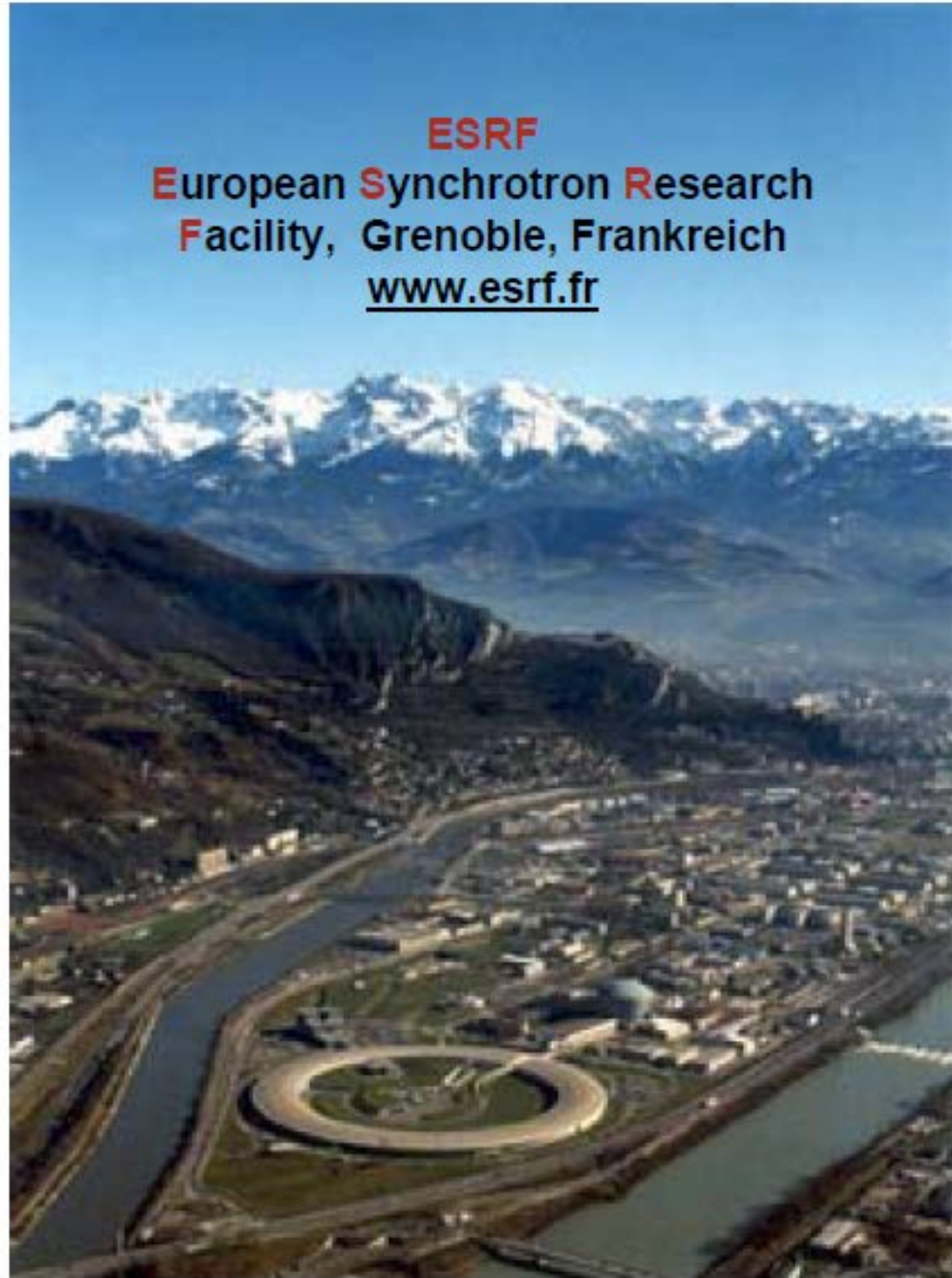
**Info über
Synchrotronstrahlung
im Internet**

DESY
Deutsches Elektronen**synchrotron**
HASYLAB: Hamburger
Synchrotronstrahlungslabor
www-hasylab.desy.de

BESSY
Berliner Elektronen**speicherring** –
Gesellschaft für **Synchrotronstrahlung**
www.bessy.de/guided_tour/

Preis ≥ € 1.000.000.000

ESRF
European **Synchrotron Research Facility**, Grenoble, Frankreich
www.esrf.fr

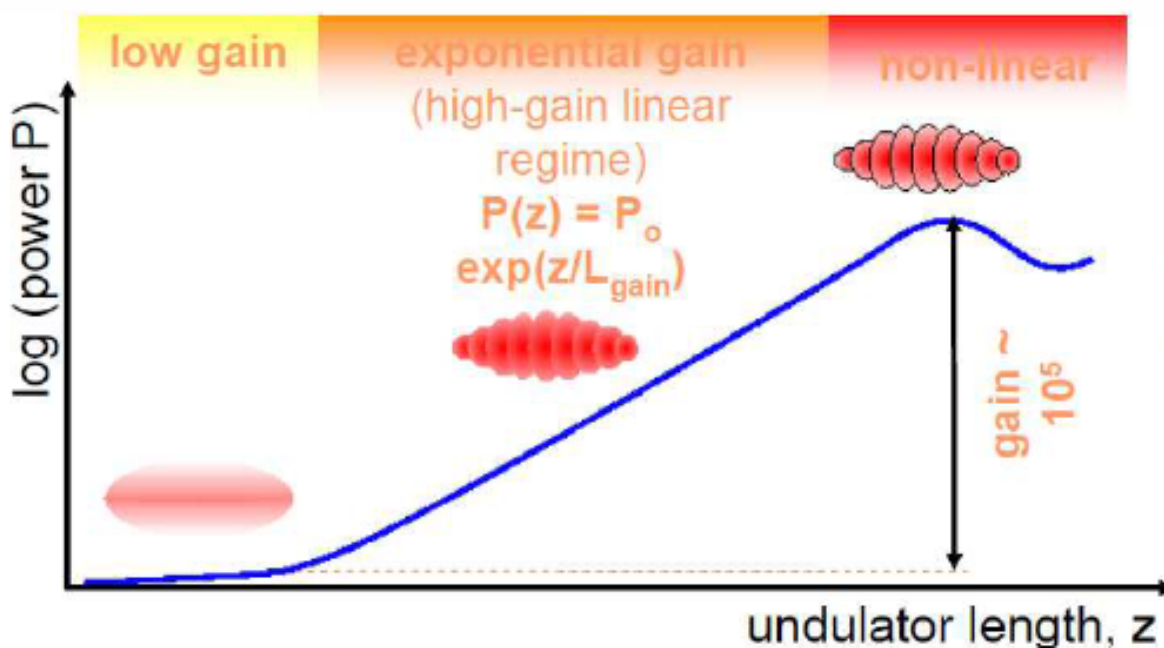
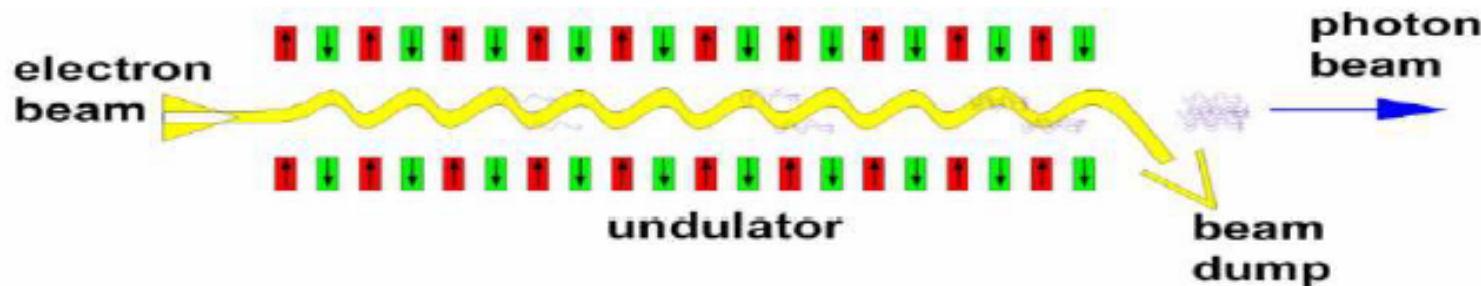


Höchstbrillante Röntgenquelle : Der Freie Elektronenlaser

SASE Prinzip

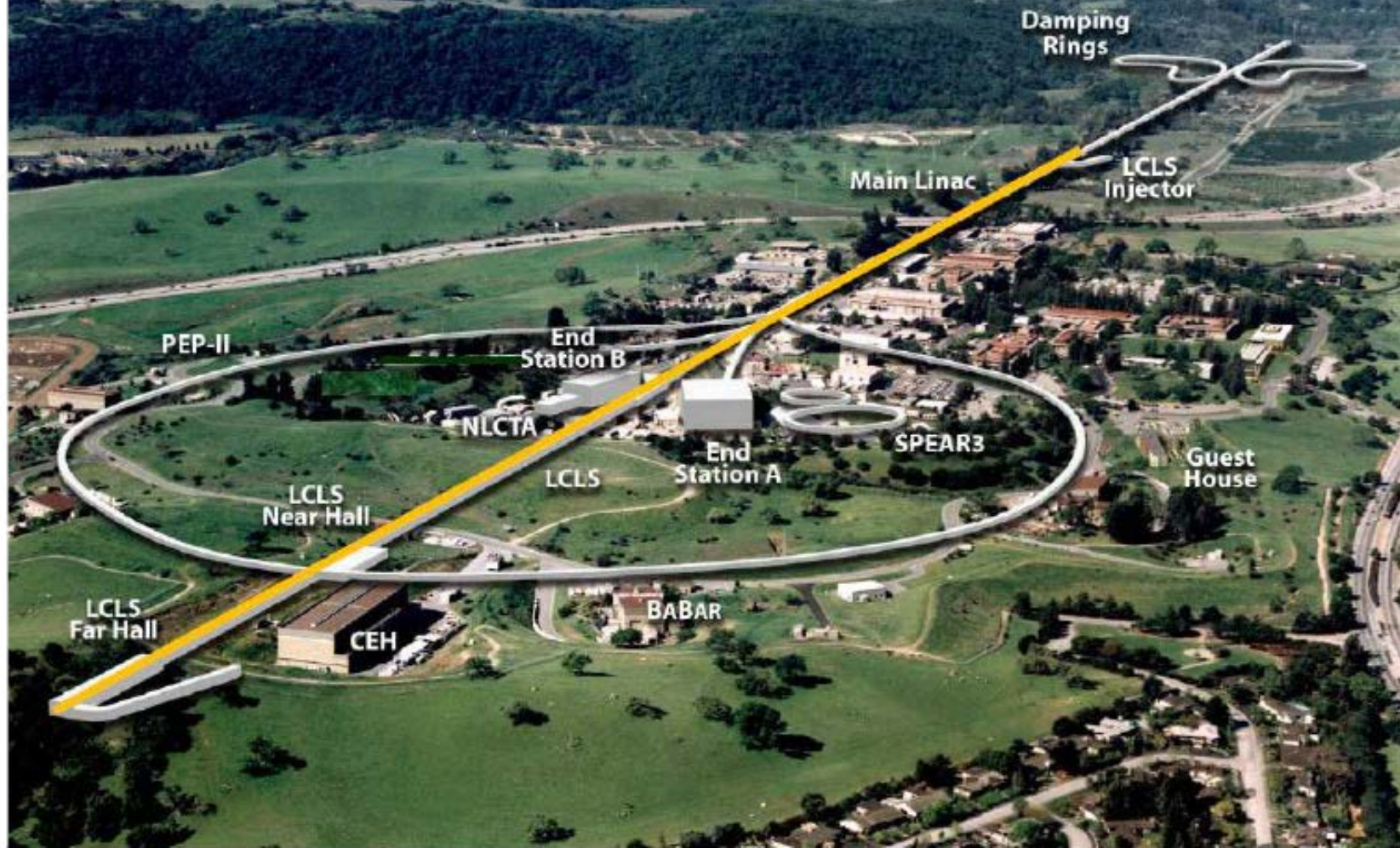
SASE = Self Amplification of Spontaneous Emission

Saldin, Schneidmiller, Yurkov



- Bunch wechselwirkt mit eigenem Photonfeld
 - Mikrobunche entstehen
 - Elektronen strahlen kohärent $\sim N_e^{-2}$ mit $N_e \approx 10^6$
- Verstärkung bis zu N_e !**

SLAC National Accelerator Laboratory



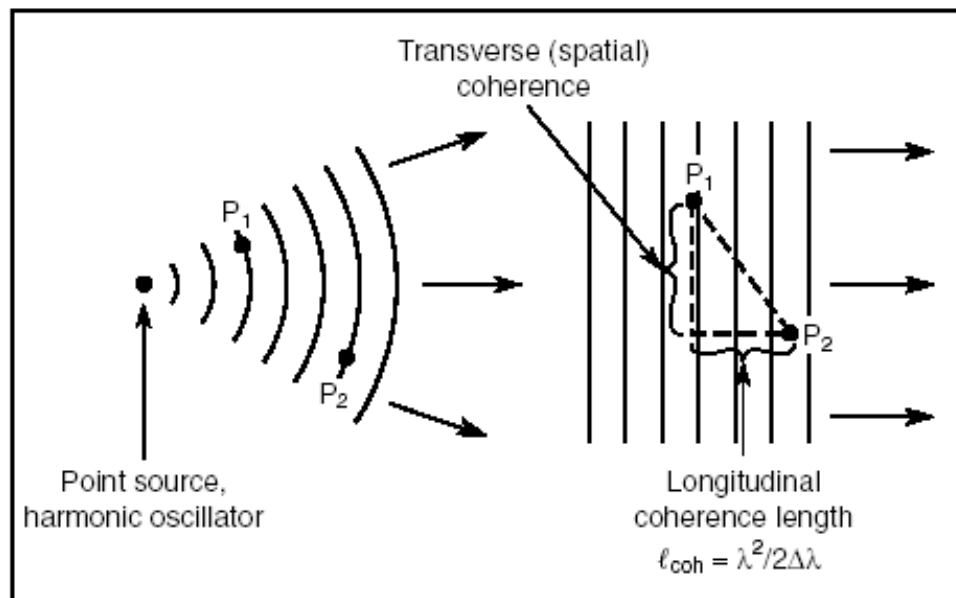
Mutual coherence factor

$$\Gamma_{12}(\tau) \equiv \langle E_1(t + \tau) E_2^*(t) \rangle \quad (8.1)$$

Normalize degree of spatial coherence
(complex coherence factor)

$$\mu_{12} = \frac{\langle E_1(t) E_2^*(t) \rangle}{\sqrt{\langle |E_1|^2 \rangle} \sqrt{\langle |E_2|^2 \rangle}} \quad (8.12)$$

A high degree of coherence ($\mu \rightarrow 1$) implies an ability to form a high contrast interference (fringe) pattern. A low degree of coherence ($\mu \rightarrow 0$) implies an absence of interference, except with great care. In general radiation is partially coherent.

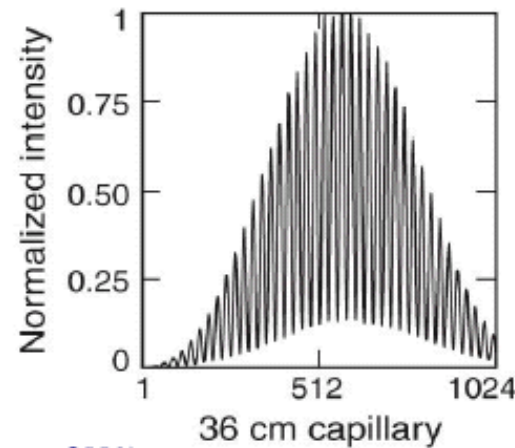
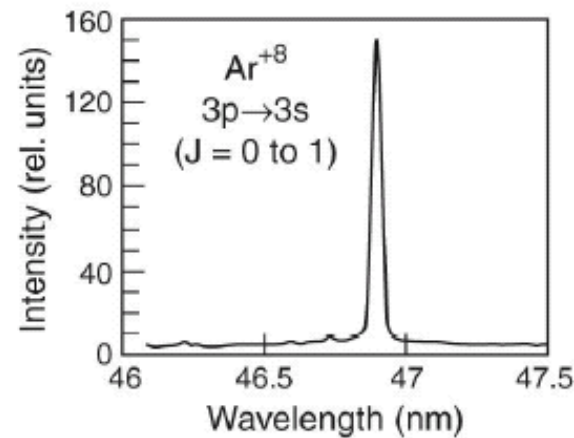
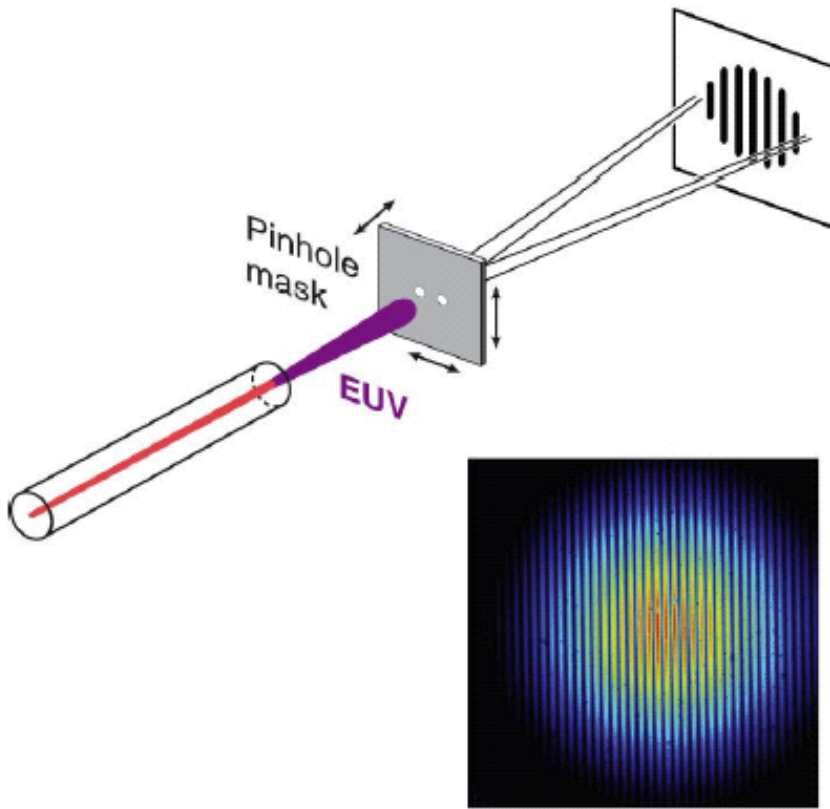


Longitudinal (temporal) coherence length

$$\ell_{coh} = \frac{\lambda^2}{2 \Delta \lambda} \quad (8.3)$$

Full spatial (transverse) coherence

$$d \cdot \theta = \lambda / 2\pi \quad (8.5)$$

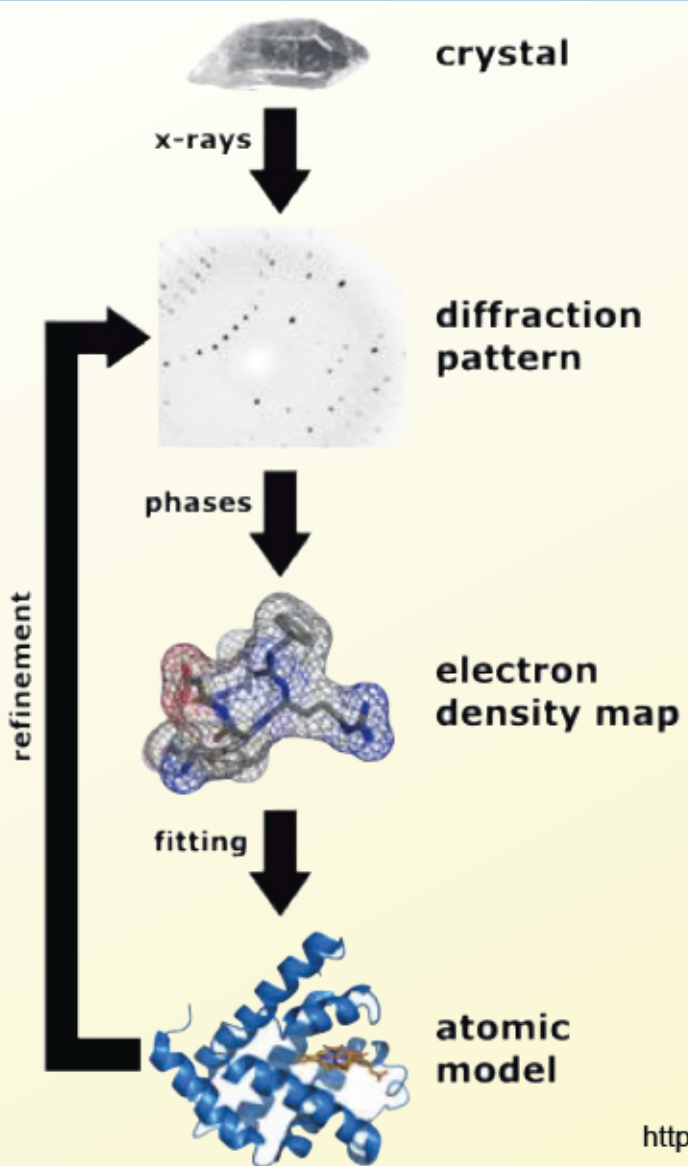


Y.Liu, et al., *Phys. Rev. A* (5 February 2001)

$$P_{\text{coh}} = 3 \text{ mW} \rightarrow 7 \times 10^{14} \text{ ph/sec} @ 46.9 \text{ nm}$$

Courtesy of Prof. Jorge Rocca, Colorado State Univ.

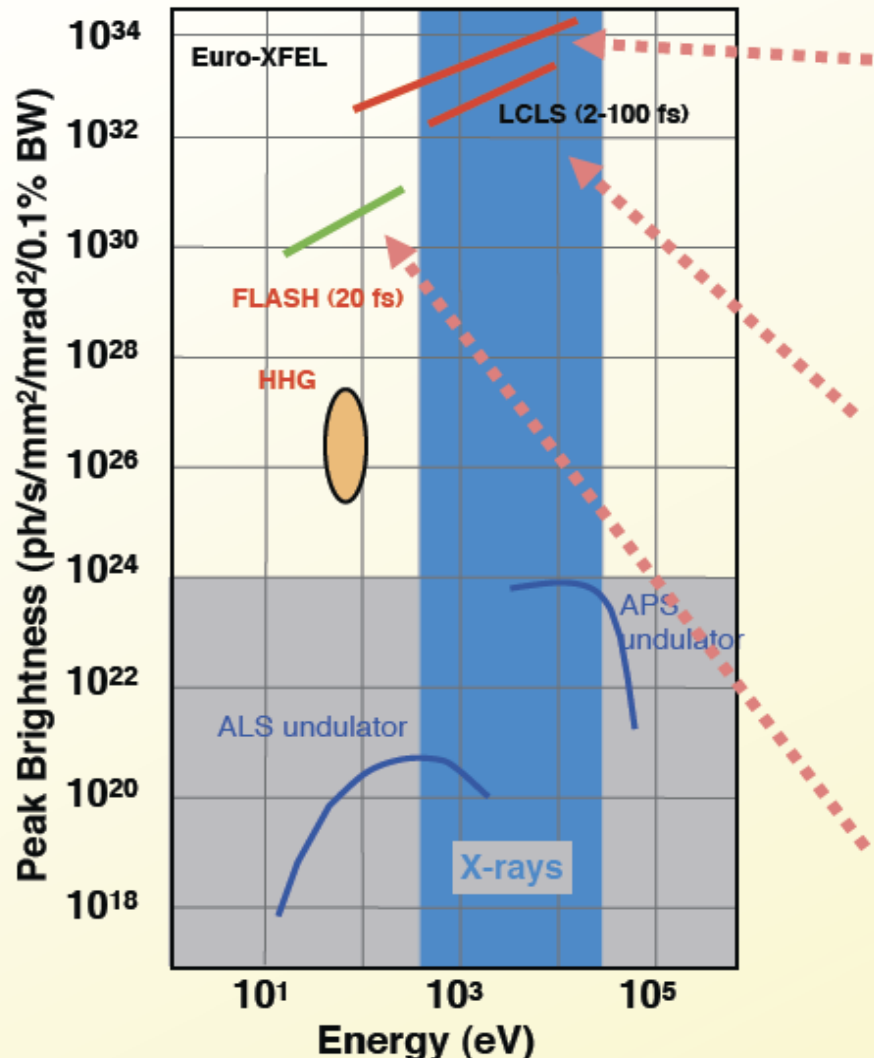
Crystallography overcomes radiation damage and optics limitations, but requires crystals



- ★ Radiation damage is spread out over 10^{10} identical unit cells
- ★ Diffraction from unit cells adds up coherently to form strong Bragg peaks
- ★ ~ 60,000 structures solved (in protein data bank), but ~15,000 distinct structures
 - The bottleneck is in growing crystals

http://en.wikipedia.org/wiki/File:X_ray_diffraction.png

X-ray free-electron lasers provide pulses that are intense, short duration, short wavelength, and coherent



operational 2013

12 keV, 50 fs, 10^{13} photons

European X-ray FEL,
DESY, Hamburg



operational now

800 eV to 2 keV in 2009
8 keV, 100 fs, 10^{12} photons

Linac Coherent Light Source,
SLAC, Stanford



operational now

200 eV, 25 fs, 10^{12} photons
upgrade to 300 eV, 400 fs

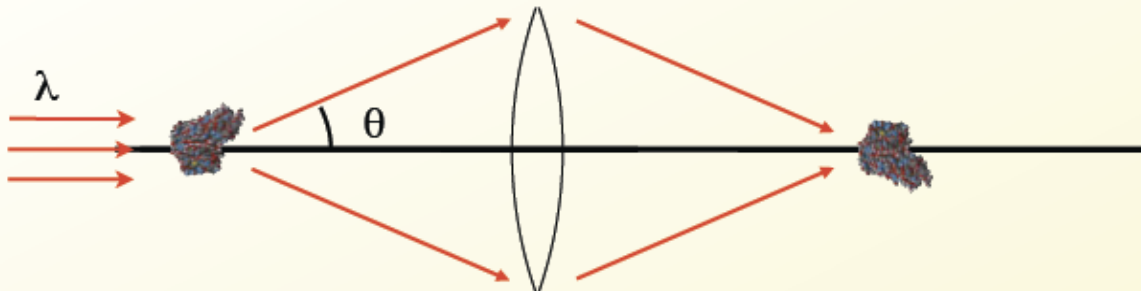
FLASH
DESY, Hamburg

APS=Advanced Photon Source (ANL)

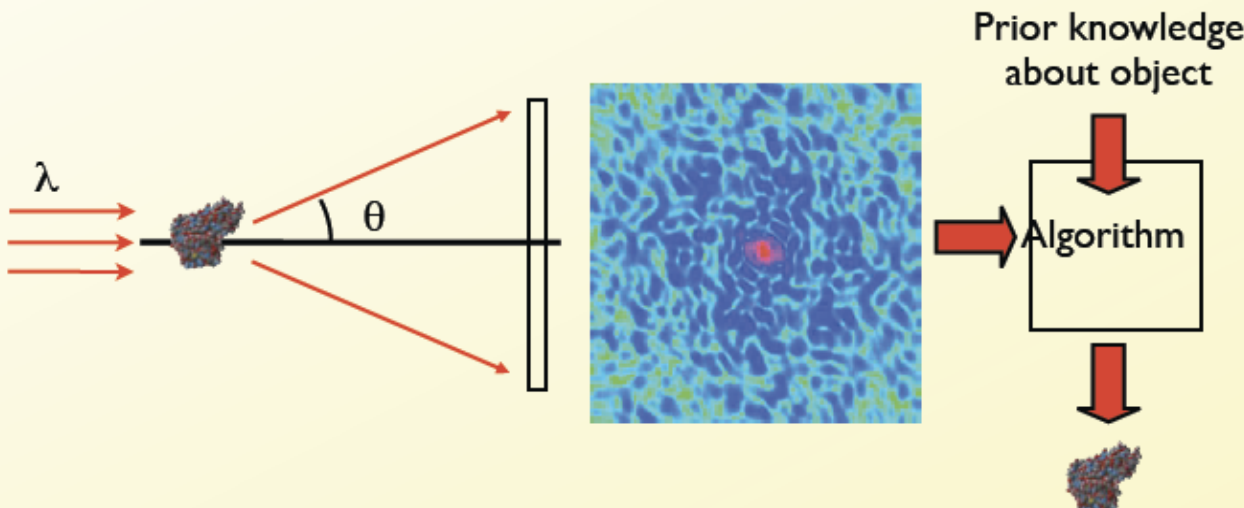
ALS=Advanced Light Source (LBNL)

Coherent diffractive imaging is lensless

Use a computer to phase the scattered light, rather than a lens



A lens recombines the scattered rays with correct phases to give the image



An algorithm finds the phases that are consistent with measurements and prior knowledge

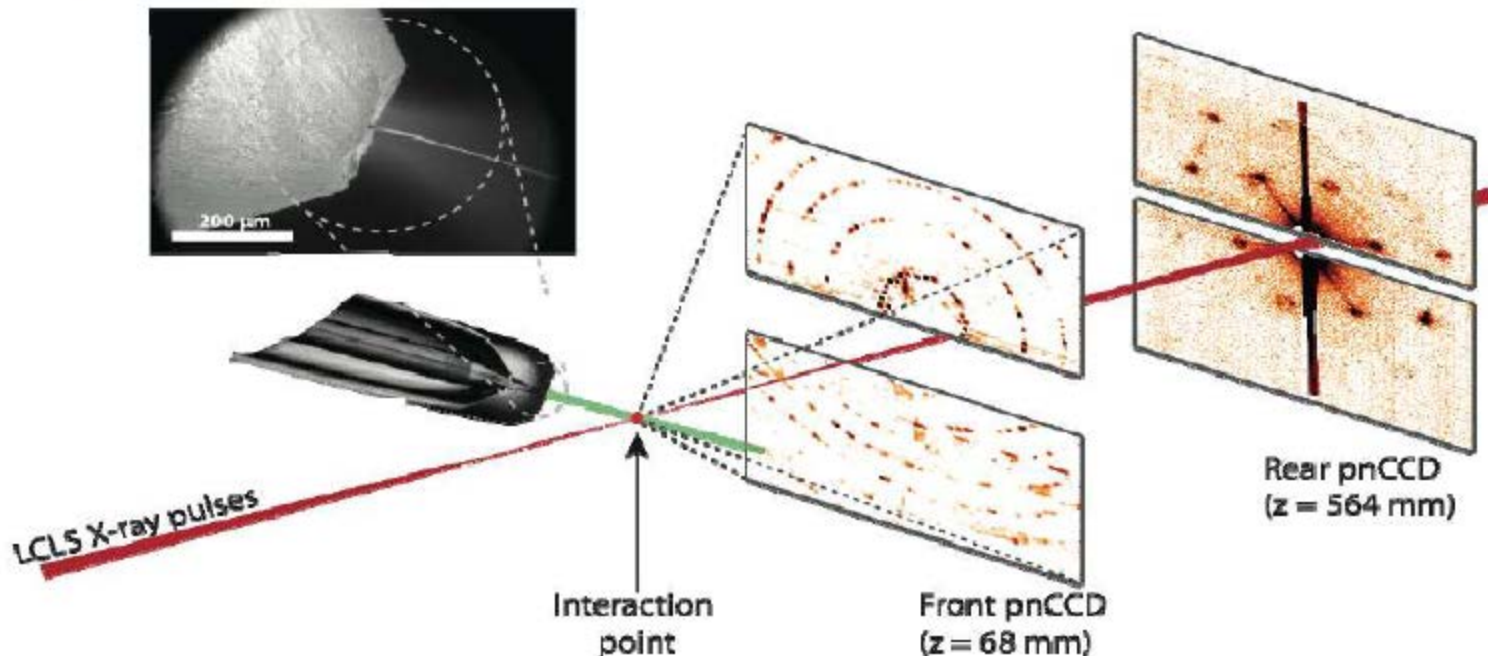
$$\text{Resolution: } \delta = \lambda / \sin \theta$$

J. Fienup, Appl. Opt. **21** 2758 (1987)

J. Miao et al, Nature **400** 342 (1999)

Nanocrystallography carried out in a flowing water microjet

- Single pulse diffraction from Photosystem 1 nanocrystals at LCLS
- $E = 1.8 \text{ keV}$
- $<10, 60, 200 \text{ fs pulse}$
- 2 mJ pulse energy
- patterns collected at 30 Hz
- hit rate >50%
- 5 Tb data in one night!



Chapter One :

- **Basic Absorption and Emission Processes**
- **Atomic Energy Levels and Allowed Transistions**
- **Scattering, Diffraction and Refraction**



Photon Energy, Wavelength, Power

$$\hbar\omega \cdot \lambda = hc = 1239.842 \text{ eV nm} \quad (1.1)$$

$$1 \text{ joule} \Rightarrow 5.034 \times 10^{15} \lambda[\text{nm}] \text{ photons} \quad (1.2a)$$

$$1 \text{ watt} \Rightarrow 5.034 \times 10^{15} \lambda[\text{nm}] \frac{\text{photons}}{\text{s}} \quad (1.2b)$$



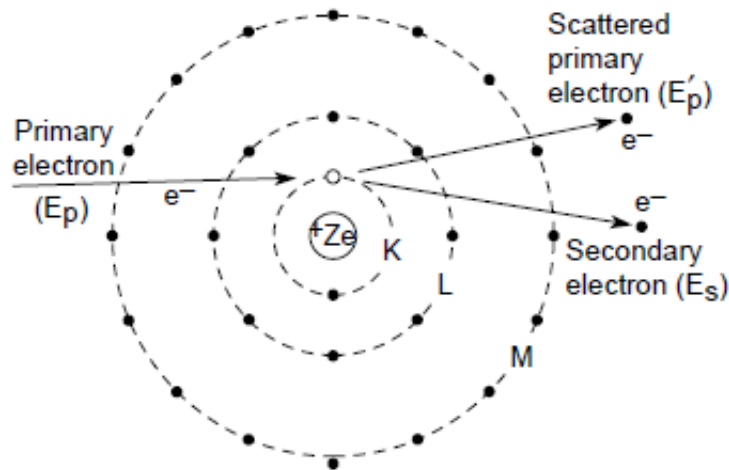
K and L₃-Absorption Edges for Selected Elements

Element	Z	K _{abs} -edge (eV)	L _{abs} -edge (eV)	$\lambda_{\text{K-abs}}$ (nm)	$\lambda_{\text{L-abs}}$ (nm)	I_{abs}	
						100 eV (nm)	1 keV (μm)
Be	4	112	—	11.1	—	730	9.0
C	6	284	—	4.36	—	190	2.1
N	7	410	—	3.02	—	—	—
O	8	543	—	2.28	—	—	—
H ₂ O						160	2.3
Al	13	1,560	73	0.795	17.1	34	3.1
Si	14	1,839	99	0.674	12.5	63	2.7
S	16	2,472	163	0.502	7.63	330	1.9
Ca	20	4,039	346	0.307	3.58	290	1.3
Ti	22	4,966	454	0.250	2.73	65	0.38
V	23	5,465	512	0.227	2.42	46	0.26
Cr	24	5,989	574	0.207	2.16	31	0.19
Fe	26	7,112	707	0.174	1.75	22	0.14
Ni	28	8,333	853	0.149	1.45	16	0.11
Cu	29	8,979	933	0.138	1.33	18	0.10
Se	34	12,658	1,434	0.0979	0.865	63	0.96
Mo	42	20,000	2,520	0.0620	0.492	200	0.19
Sn	50	29,200	3,929	0.0425	0.316	17	0.17
Xe	54	34,561	4,782	0.0359	0.259	—	—
W	74	69,525	10,207	0.0178	0.121	28	0.13
Au	79	80,725	11,919	0.0154	0.104	28	0.10

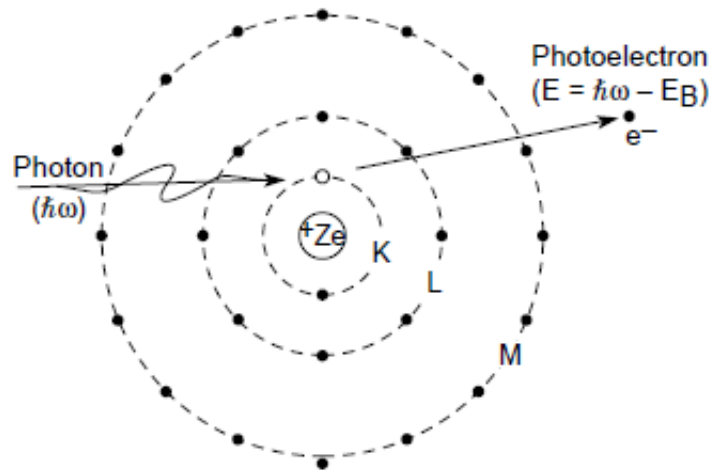


Basic Ionization and Emission Processes in Isolated Atoms

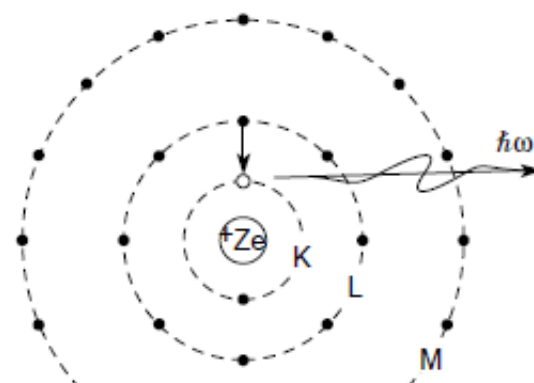
(a) Electron collision induced ionization



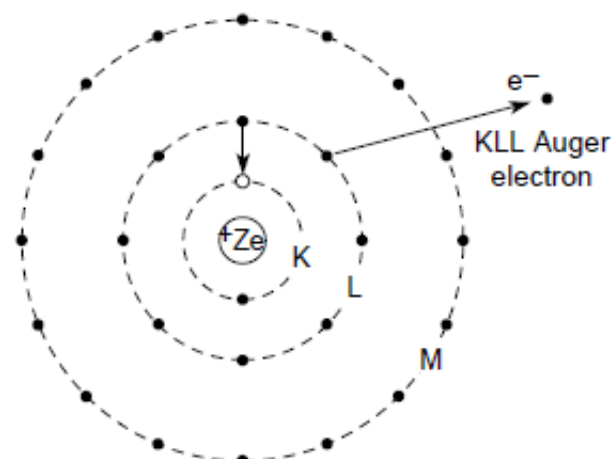
(b) Photoionization



(c) Fluorescent emission of characteristic radiation

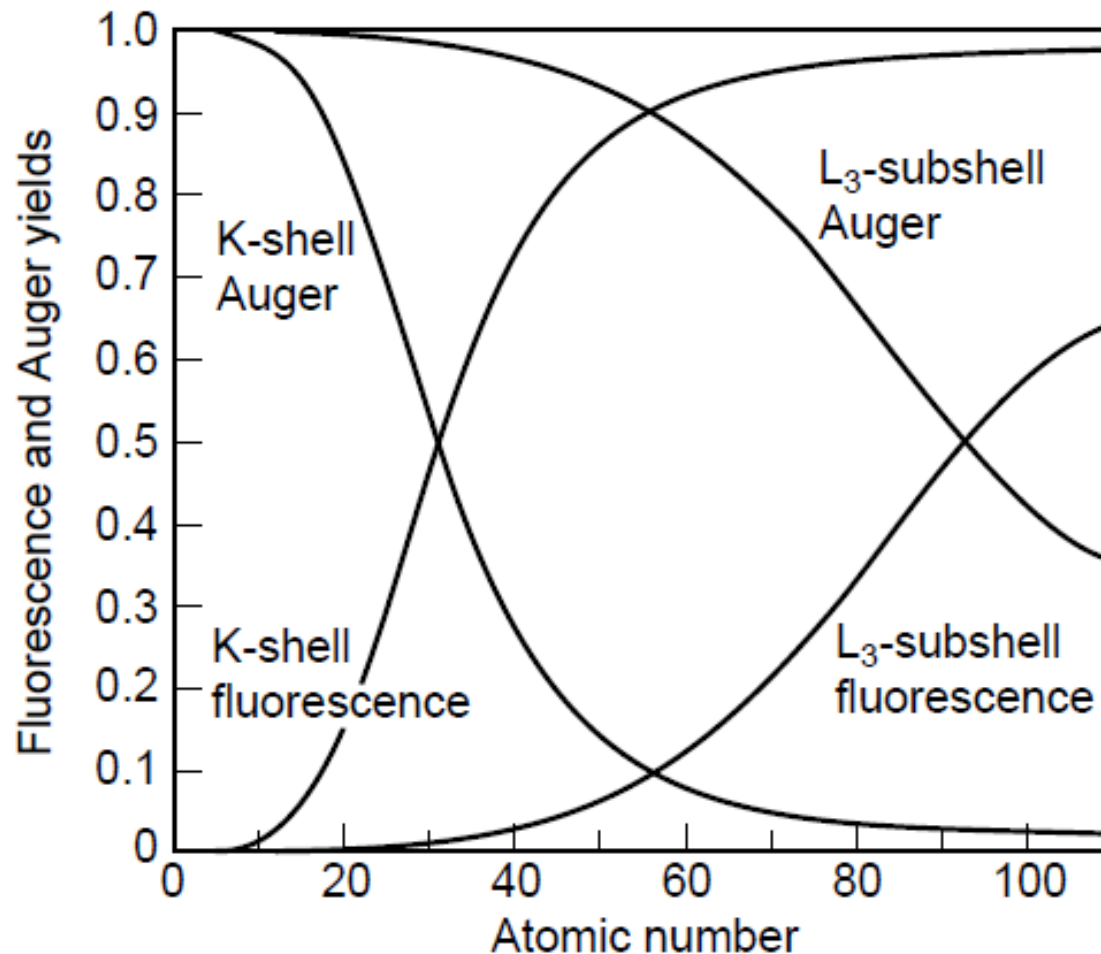


(d) Non-radiative Auger process





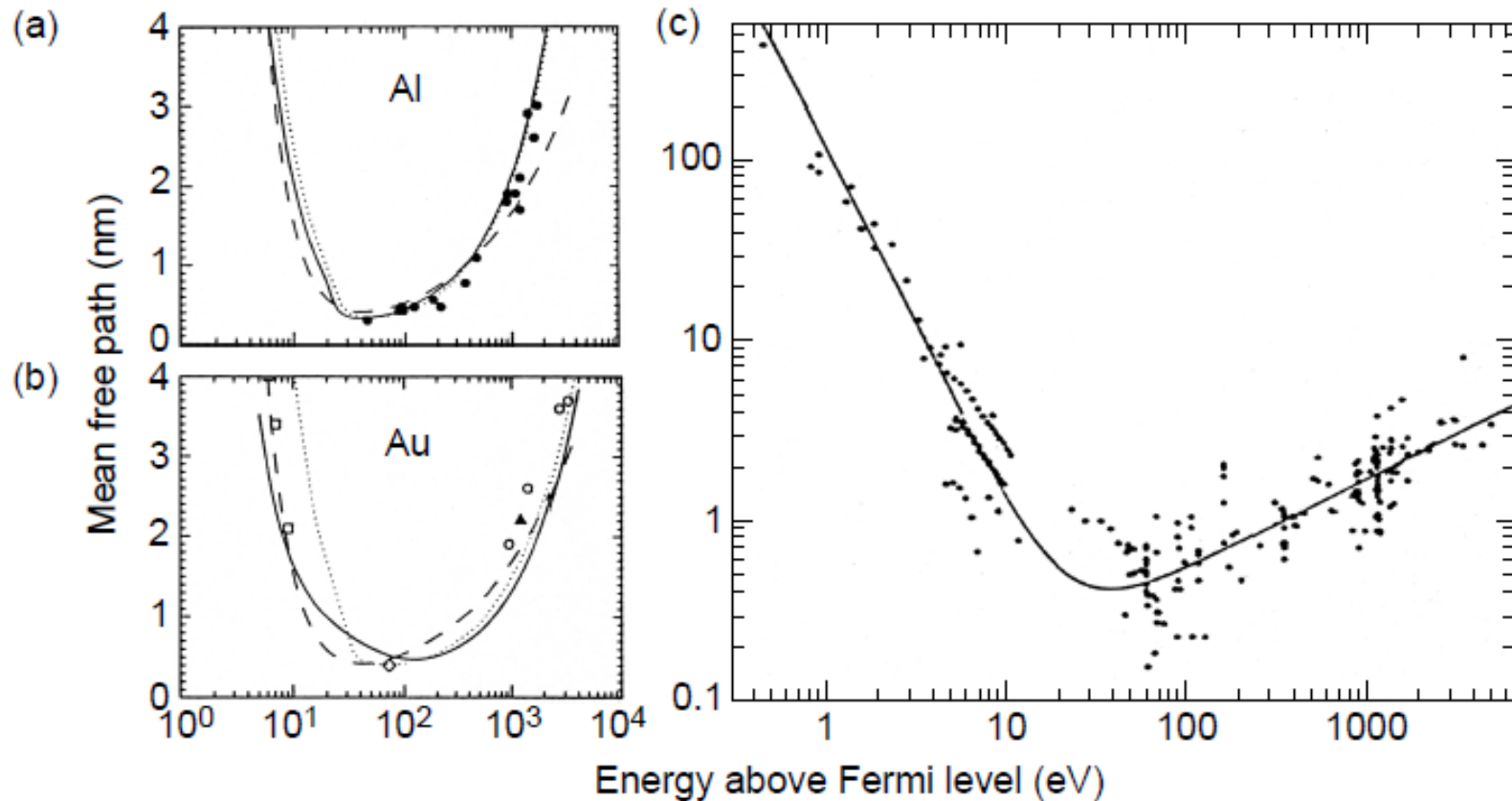
Fluorescence and Auger Emission Yields



(Courtesy of M. Krause, Oak Ridge)



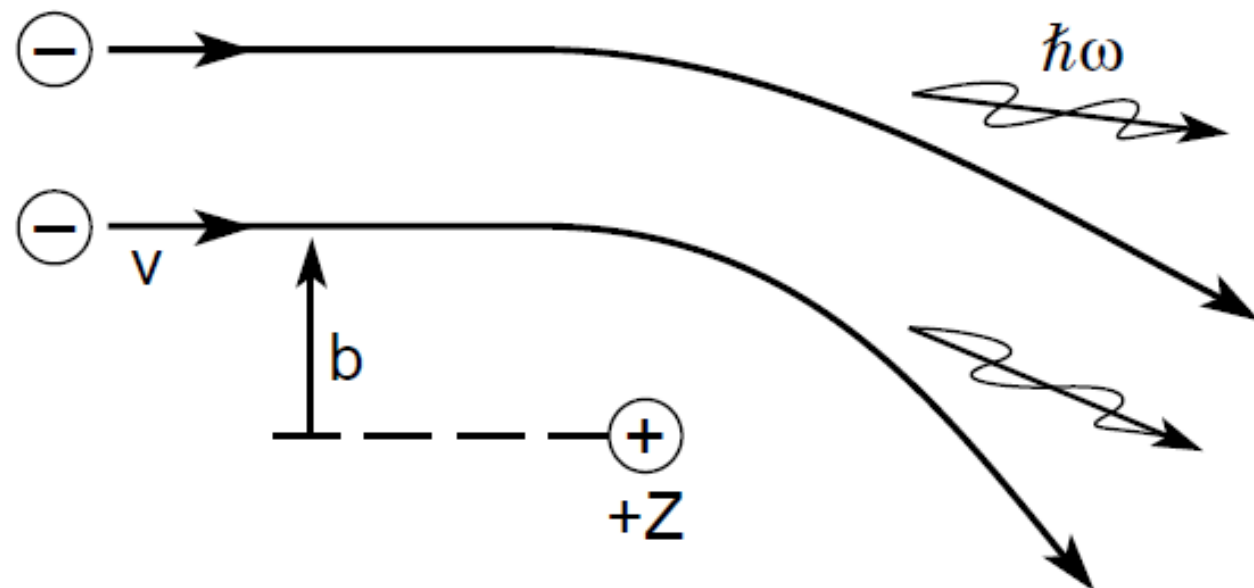
Electron Mean Free Paths As a Function of Energy



Courtesy of: Penn (a & b), Seah and Dench (c)

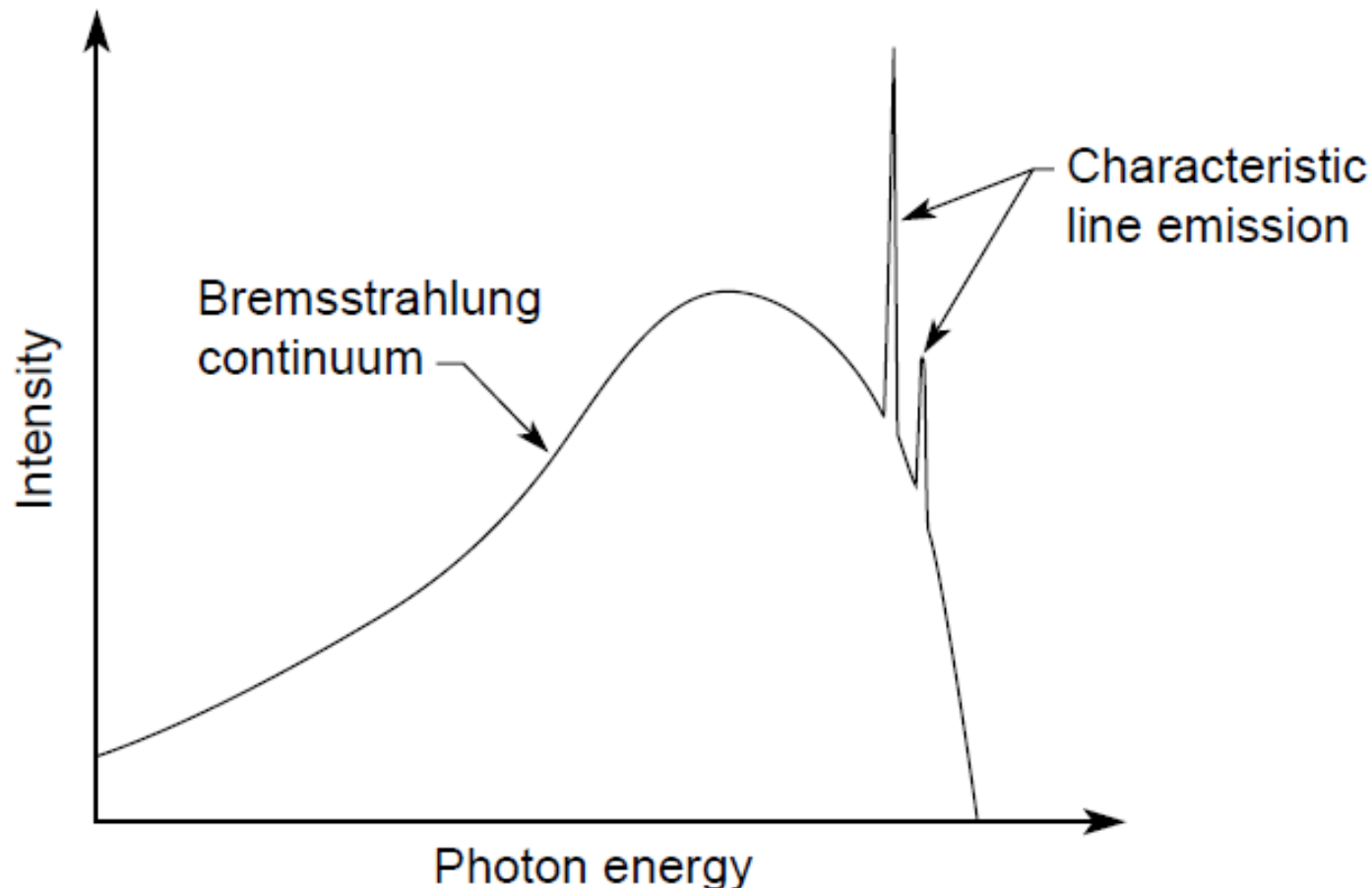


Bremsstrahlung Radiation: Braking Radiation from an Accelerated Charge



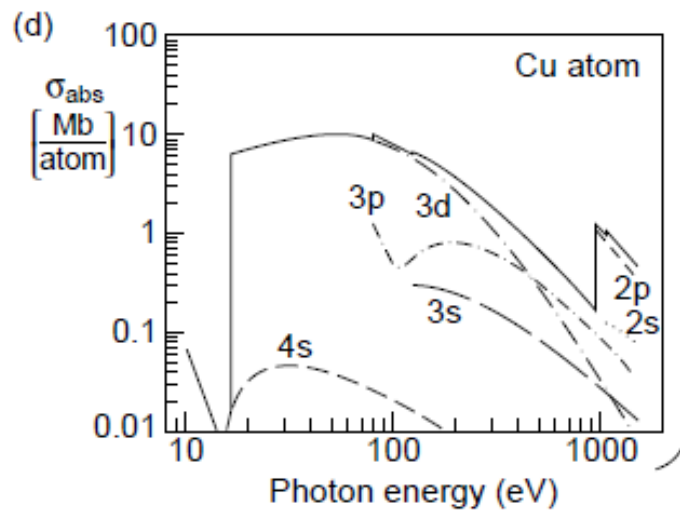
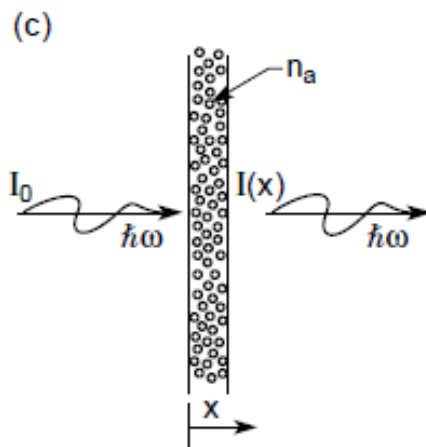
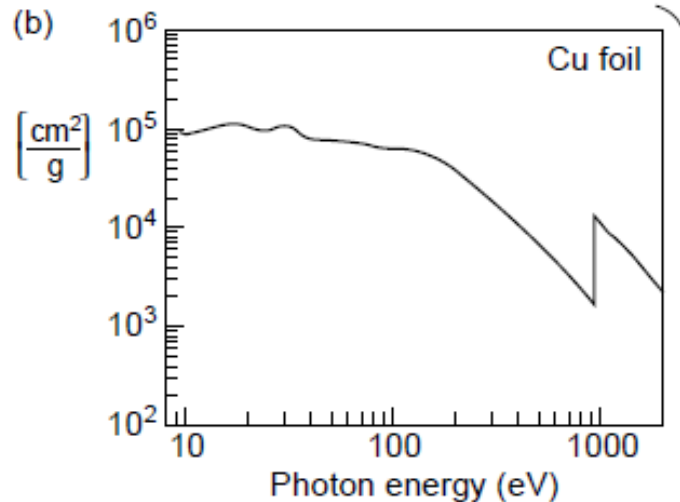
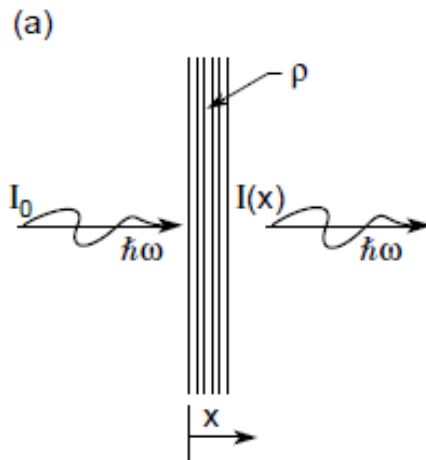


Continuum Bremsstrahlung Radiation and Narrow Characteristic Line Emission from a Solid Target with Electron Bombardment

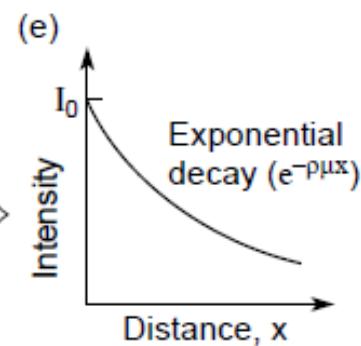




Photoabsorption by Thin Foils and Isolated Atoms



$$\frac{I}{I_0} = e^{-\rho \mu x}$$



$$\frac{I}{I_0} = e^{-n_a \sigma_{\text{abs}} x}$$



Atomic Energy Levels and Allowed Transitions in the Bohr Atom

Equate Coulomb Force $Ze^2/4\pi\epsilon_0 r^2$ to the centripetal force mv^2/r :

$$E_n = \frac{mZ^2e^4}{32\pi^2\epsilon_0^2\hbar^2} \frac{1}{n^2} \quad (1.4)$$

$$r_n = \frac{4\pi\epsilon_0\hbar^2}{me^2Z} \cdot n^2 \quad (1.5)$$

$$\hbar\omega = E_i - E_f = \underbrace{\frac{me^4}{32\pi^2\epsilon_0^2\hbar^2} \left[\frac{1}{n_f^2} - \frac{1}{n_i^2} \right]}_{13.6 \text{ eV}} Z^2 \quad (1.6)$$

$$r_n = \frac{a_0 n^2}{Z} ; \quad a_0 = 0.529 \text{ \AA} \quad (1.9)$$



Quantum Mechanics Based on a Probabilistic Wave Function, $\Psi(\mathbf{r}, t)$

$$-\frac{\hbar^2}{2m} \nabla^2 \Psi(\mathbf{r}, t) + V(\mathbf{r}, t) \Psi(\mathbf{r}, t) = i\hbar \frac{\partial \Psi(\mathbf{r}, t)}{\partial t} \quad (1.10)$$

$$P(\mathbf{r}, t) d\mathbf{r} = \Psi^*(\mathbf{r}, t) \Psi(\mathbf{r}, t) d\mathbf{r} \quad (1.13)$$

$$\bar{\mathbf{r}} = \iiint \mathbf{r} P(\mathbf{r}, t) d\mathbf{r} = \iiint \Psi^*(\mathbf{r}, t) \mathbf{r} \Psi(\mathbf{r}, t) d\mathbf{r} \quad (1.15)$$

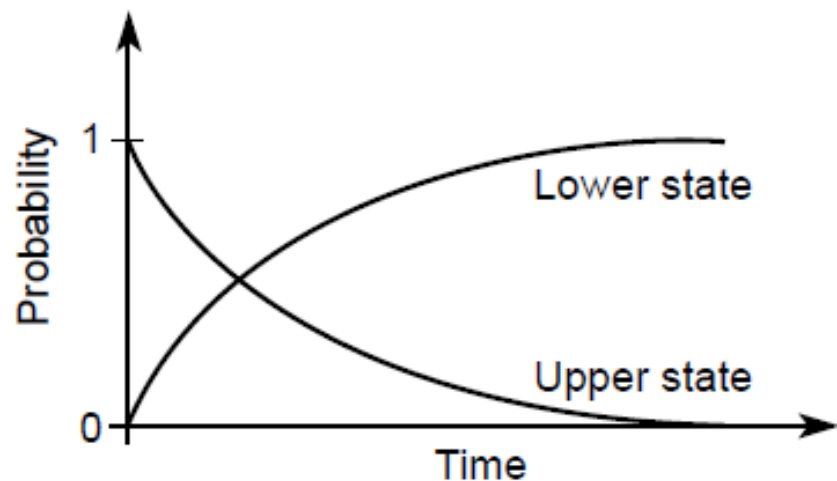
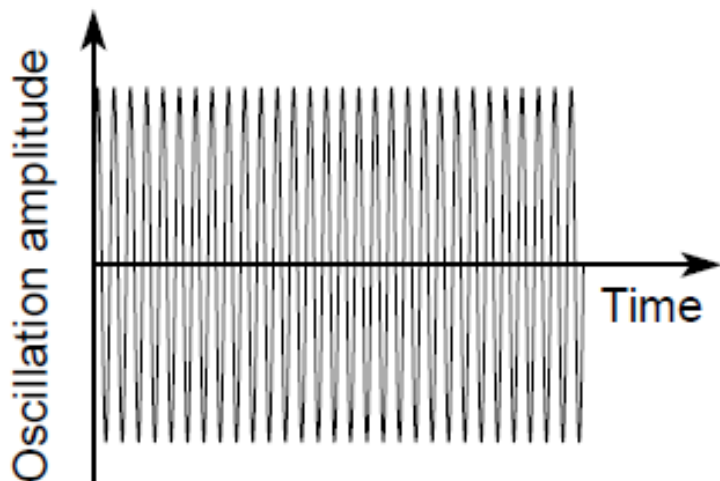
quantum numbers: n , ℓ , m_ℓ , m_s

selection rules for allowed transitions: $\Delta\ell = \pm 1$

$$\Delta j = 0, \pm 1$$

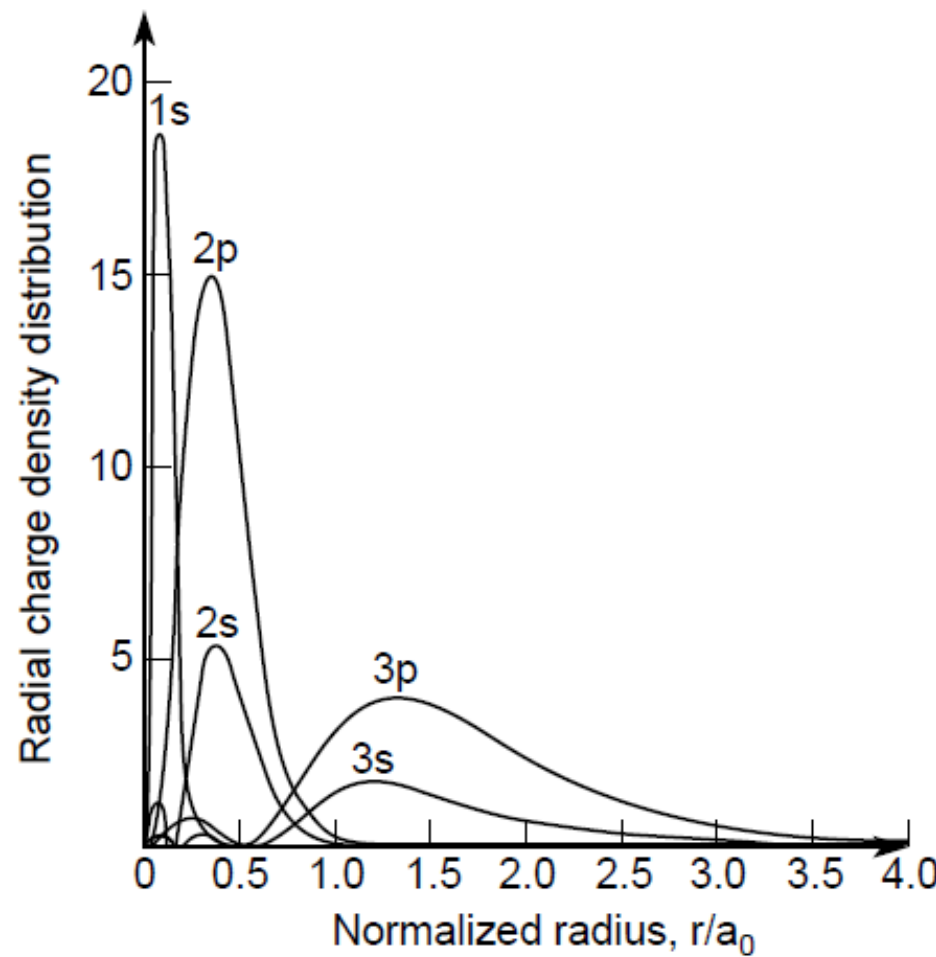


Radiative Decay Involves An Atom Oscillating Between Two Stationary States at the Frequency $\omega_{\text{if}} = (E_i - E_f) / \hbar$





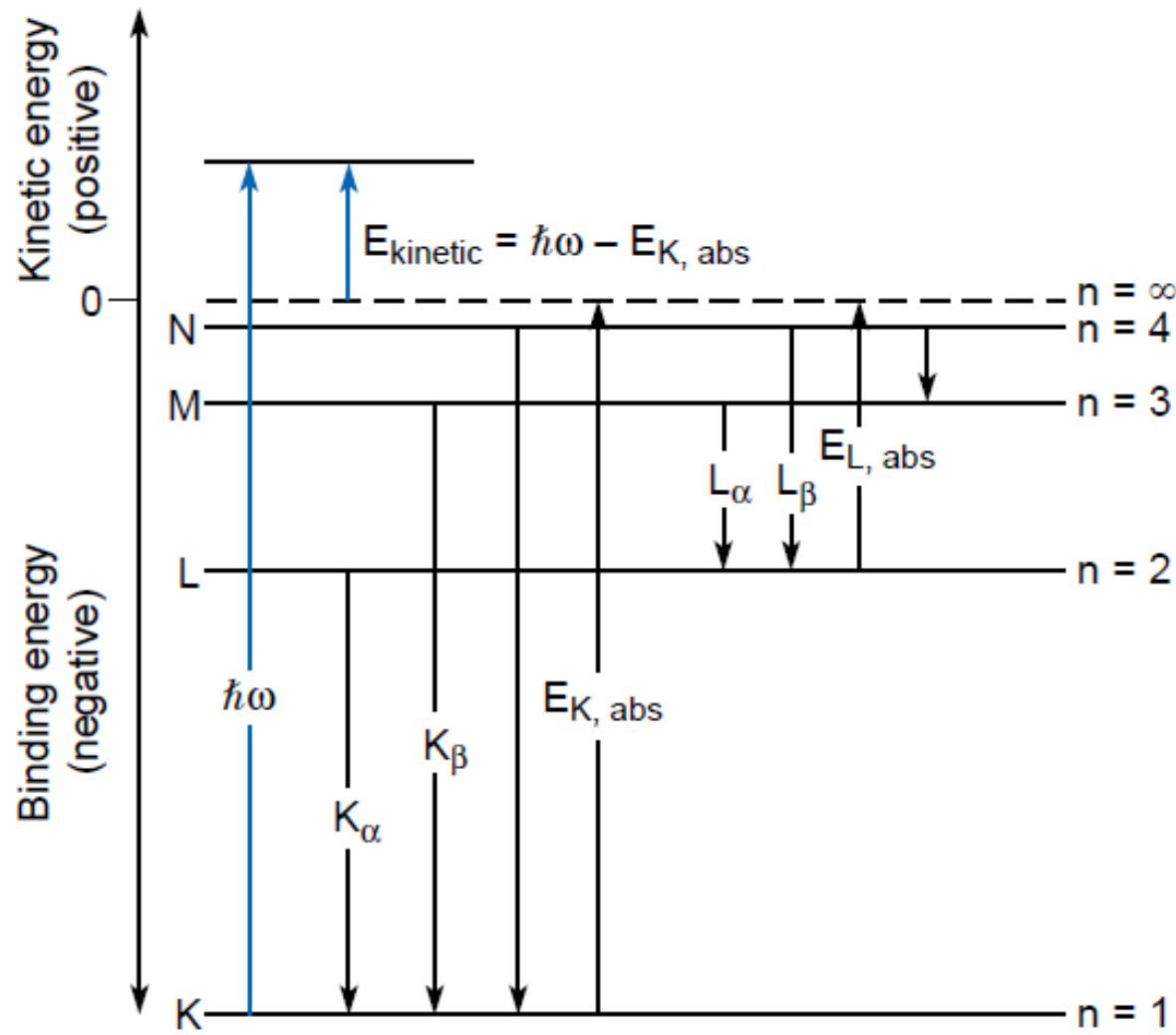
Probabilistic Radial Charge Distribution ($e/\text{\AA}$) in the Argon Atom



Courtesy of Eisberg and Resnick, *Quantum Physics of Atoms, Molecules, Solids, Nuclei, and Particles*.



Energy Levels, Absorption Edges, and Characteristic Line Emissions for a Multi-Electron Atom





Energy Levels, Quantum Numbers, and Allowed Transitions for the Copper Atom

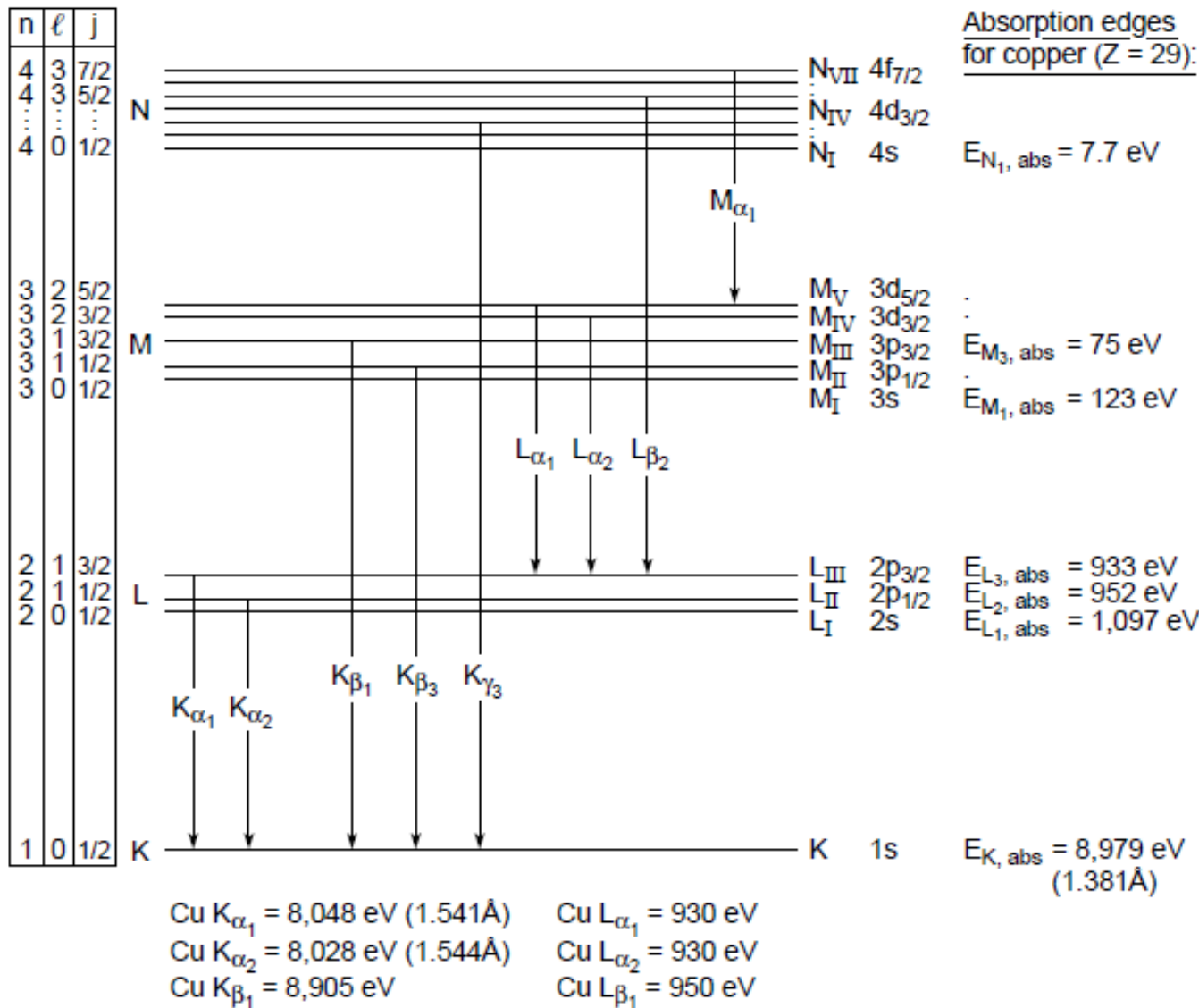




TABLE B.1. Electron binding energies in electron volts for the elements in their natural forms.^a

Element	K 1s	L ₁ 2s	L ₂ 2p _{1/2}	L ₃ 2p _{3/2}	M ₁ 3s	M ₂ 3p _{1/2}	M ₃ 3p _{3/2}	M ₄ 3d _{3/2}	M ₅ 3d _{5/2}	N ₁ 4s	N ₂ 4p _{1/2}	N ₃ 4p _{3/2}
1 H	13.6											
2 He	24.6 ^b											
3 Li	54.7 ^b											
4 Be	111.5 ^b											
5 B	188 ^b											
6 C	284.2 ^b											
7 N	409.9 ^b	37.3 ^b										
8 O	543.1 ^b	41.6 ^b										
9 F	696.7 ^b											
10 Ne	870.2 ^b	48.5 ^b	21.7 ^b	21.6 ^b								
11 Na	1070.8 ^c	63.5 ^c	30.4 ^c	30.5 ^b								
12 Mg	1303.0 ^c	88.6 ^b	49.6 ^c	49.2 ^c								
13 Al	1559.6	117.8 ^b	72.9 ^b	72.5 ^b								
14 Si	1838.9	149.7 ^b	99.8 ^b	99.2 ^b								
15 P	2145.5	189 ^b	136 ^b	135 ^b								
16 S	2472	230.9 ^b	163.6 ^b	162.5 ^b								
17 Cl	2822.4	270.2 ^b	202 ^b	200 ^b								
18 Ar	3205.9 ^b	326.3 ^b	250.6 ^b	248.4 ^b	29.3 ^b	15.9 ^b	15.7 ^b					
19 K	3608.4 ^b	378.6 ^b	297.3 ^b	294.6 ^b	34.8 ^b	18.3 ^b	18.3 ^b					
20 Ca	4038.5 ^b	438.4 ^c	349.7 ^c	346.2 ^c	44.3 ^c	25.4 ^c	25.4 ^c					
21 Sc	4492.8	498.0 ^b	403.6 ^b	398.7 ^b	51.1 ^b	28.3 ^b	28.3 ^b					
22 Ti	4966.4	560.9 ^c	461.2 ^c	453.8 ^c	58.7 ^c	32.6 ^c	32.6 ^c					
23 V	5465.1	626.7 ^c	519.8 ^c	512.1 ^c	66.3 ^c	37.2 ^c	37.2 ^c					
24 Cr	5989.2	695.7 ^c	583.8 ^c	574.1 ^c	74.1 ^c	42.2 ^c	42.2 ^c					
25 Mn	6539.0	769.1 ^c	649.9 ^c	638.7 ^c	82.3 ^c	47.2 ^c	47.2 ^c					
26 Fe	7112.0	844.6 ^c	719.9 ^c	706.8 ^c	91.3 ^c	52.7 ^c	52.7 ^c					
27 Co	7708.9	925.1 ^c	793.3 ^c	778.1 ^c	101.0 ^c	58.9 ^c	58.9 ^c					
28 Ni	8332.8	1008.6 ^c	870.0 ^c	852.7 ^c	110.8 ^c	68.0 ^c	66.2 ^c					
29 Cu	8978.9	1096.7 ^c	952.3 ^c	932.5 ^c	122.5 ^c	77.3 ^c	75.1 ^c					
30 Zn	9658.6	1196.2 ^b	1044.9 ^b	1021.8 ^b	139.8 ^b	91.4 ^b	88.6 ^b	10.2 ^b	10.1 ^b			



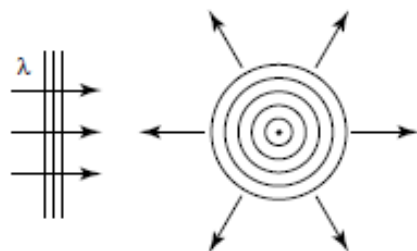
TABLE B.2. Photon energies, in electron volts, of principal K and L shell emission lines.^a

Element	K α_1	K α_2	K β_1	L α_1	L α_2	L β_1	L β_2	L γ_1
3 Li	54.3							
4 Be	108.5							
5 B	183.3							
6 C	277							
7 N	392.4							
8 O	524.9							
9 F	676.8							
10 Ne	848.6	848.6						
11 Na	1,040.98	1,040.98	1,071.1					
12 Mg	1,253.60	1,253.60	1,302.2					
13 Al	1,486.70	1,486.27	1,557.45					
14 Si	1,739.98	1,739.38	1,835.94					
15 P	2,013.7	2,012.7	2,139.1					
16 S	2,307.84	2,306.64	2,464.04					
17 Cl	2,622.39	2,620.78	2,815.6					
18 Ar	2,957.70	2,955.63	3,190.5					
19 K	3,313.8	3,311.1	3,589.6					
20 Ca	3,691.68	3,688.09	4,012.7	341.3	341.3	344.9		
21 Sc	4,090.6	4,086.1	4,460.5	395.4	395.4	399.6		
22 Ti	4,510.84	4,504.86	4,931.81	452.2	452.2	458.4		
23 V	4,952.20	4,944.64	5,427.29	511.3	511.3	519.2		
24 Cr	5,414.72	5,405.509	5,946.71	572.8	572.8	582.8		
25 Mn	5,898.75	5,887.65	6,490.45	637.4	637.4	648.8		
26 Fe	6,403.84	6,390.84	7,057.98	705.0	705.0	718.5		
27 Co	6,930.32	6,915.30	7,649.43	776.2	776.2	791.4		
28 Ni	7,478.15	7,460.89	8,264.66	851.5	851.5	868.8		
29 Cu	8,047.78	8,027.83	8,905.29	929.7	929.7	949.8		
30 Zn	8,638.86	8,615.78	9,572.0	1,011.7	1,011.7	1,034.7		

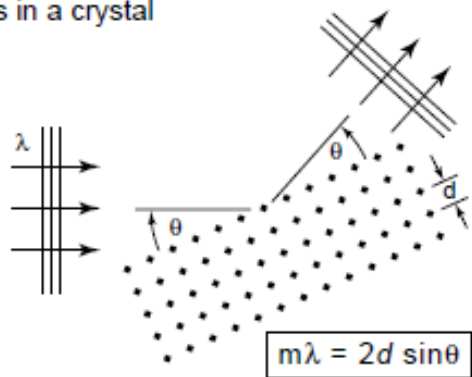


Scattering, Diffraction, and Refraction

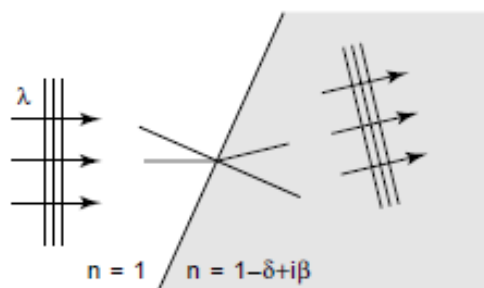
(a) Isotropic scattering from a point object



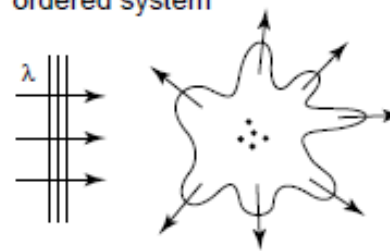
(c) Diffraction by an ordered array of atoms, as in a crystal



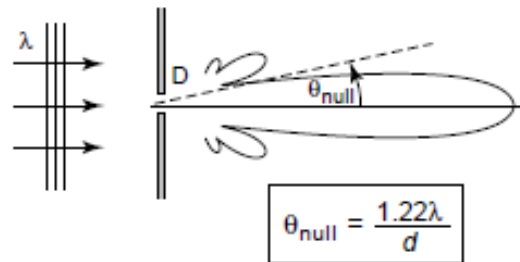
(e) Refraction at an interface



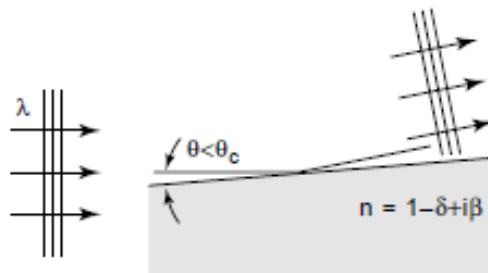
(b) Non-isotropic scattering from a partially ordered system



(d) Diffraction from a well-defined geometric structure, such as a pinhole



(f) Total external reflection



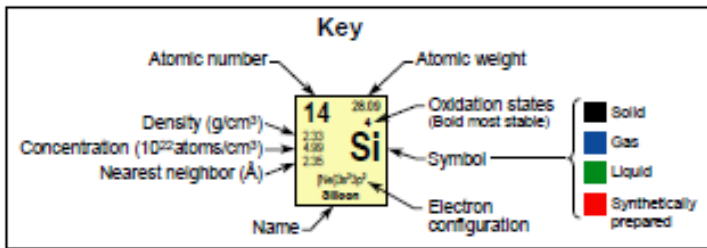


Periodic Table of the Elements



Group
IA

1	1.0079 H Hydrogen	IIA
3	6.941 Li Lithium	4 Be Boron
11	22.990 Na Sodium	12 Mg Magnesium
19	39.068 K Potassium	20 Ca Calcium



	III A	IV A	V A	VIA	VII A	VIIIA	IB	IIB	
21	44.96 Sc Scandium	22 47.88 Ti Titanium	23 50.94 V Vanadium	24 52.00 Cr Chromium	25 54.94 Mn Manganese	26 55.85 Fe Iron	27 56.93 Co Cobalt	28 58.88 Ni Nickel	29 61.55 Cu Copper
37	85.47 Rb Rubidium	38 87.63 Sr Strontium	39 88.91 Y Yttrium	40 91.22 Zr Zirconium	41 92.91 Nb Niobium	42 95.94 Mo Molybdenum	43 98.98 Tc Technetium	44 101.1 Ru Ruthenium	45 102.91 Rh Rhodium
55	131.91 Cs Cesium	56 137.33 Ba Barium	57 138.91 La Lanthanum	72 178.49 Hf Hafnium	73 180.95 Ta Tantalum	74 183.85 W Tungsten	75 186.21 Re Rhenium	76 190.2 Os Osmium	77 192.2 Ir Iridium
87	223.0 Fr Francium	88 (226) Ra Radium	89 (227) Ac Actinium	104 (261) Rf Rutherfordium	105 (262) Db Dubnium	106 (266) Sg Seaborgium	107 (264) Bh Bohrium	108 (277) Hs Hassium	109 (288) Mt Meitnerium

Lanthanide series

58	140.12 Ce Cerium	59	140.91 Pr Praseodymium	60	144.24 Nd Neodymium	61	(145) Pm Promethium	62	150.86 Sm Samarium	63	152.0 Eu Europium	64	157.25 Gd Gadolinium	65	158.93 Tb Terbium	66	162.50 Dy Dysprosium	67	164.93 Ho Holmium	68	167.26 Er Erbium	69	168.93 Tm Thulium	70	173.04 Yb Ytterbium	71	174.97 Lu Lutetium
90	232.05 Th Thorium	91	231.04 Pa Protactinium	92	238.03 U Uranium	93	237.64 Np Neptunium	94	240.0 Pu Plutonium	95	243.0 Cm Americium	96	247.0 Bk Berkelium	97	247.0 Cf Californium	98	251.0 Es Einsteinium	99	252.0 Fm Fermium	100	257.0 Md Mendelevium	101	258.0 No Nobelium	102	259.0 Lr Lawrencium		

Actinide series